

Supporting Information

Correlating NMR H/D Exchange Kinetics with IR Red Shifts: Towards a Comprehensive Scale for Intermolecular Hydrogen Bond Strength

*Supravat Roy, Sourav Mandal, and Alope Das**

Department of Chemistry, Indian Institute of Science Education and Research Pune, Dr.
Homi Bhabha Road, Pashan, Pune-411008, India.

*Corresponding Author: a.das@iiserpune.ac.in

Sr. No	Content	Page No
1.	Methodology of experimental and computational studies	S7-S12
2.	FTIR spectra of indole, 7-azaindole, substituted indoles, and phenol in the presence of hydrogen-bond acceptors	S13-S20
2.1.	Figure S1. Concentration-dependent FTIR spectra of indole in CHCl ₃ showing monomer and emerging dimer N–H peaks.	S13
2.2.	Figure S2: Concentration-dependent FTIR spectra of (a) phenol (Phe) and (b) 7-azaindole (7AI) in CHCl ₃ showing monomer and emerging dimer O-H and N-H peaks, respectively.	S14
2.3.	Figure S3. FTIR spectra measured in the N–H stretching region of (a) indole (Ind), (b) Ind···BP (1), (c) Ind···AP (2), (d) NMF, (e) Ind···NMF (4), (f) Ind···NDMF (5), (g) NMA, and (h) Ind···NMA (7) in CHCl ₃ .	S15
2.4.	Figure S4. FTIR spectra measured in the N–H stretching region of (a) indole (Ind), (b) Ind···THF (12), (c) Ind···THP (13), (d) imidazole (Im), (e) Ind···Im (16), and (f) Ind···Py (17) in CHCl ₃ .	S16
2.5.	Figure S5: FTIR spectra measured in the N–H stretching region of (a) 5-methylindole (5MI), (b) 5MI···AM (9), (c) 5-chloroindole (5CI), and (d) 5CI···AM (10) in CHCl ₃ .	S17
2.6.	Figure S6. FTIR spectra measured in the N–H stretching region of (a) 7-azaindole (7AI), (b) 7AI···THF (14), (c) 7AI···THP (15), (d) imidazole (Im), (e) 7AI···Im (18), and (f) 7AI···Py (19) in CHCl ₃ .	S18
2.7.	Figure S7: FTIR spectra measured in the O–H stretching region of (a) phenol monomer (Phe), (b) Phe···FM (22), (c) Phe···BP (20), (d) Phe···AP (21), (e) Phe···NMA (24), (f) Phe···AM (23), and (g) Phe···NDMA (25) in CHCl ₃ .	S19
2.8.	Figure S8: FTIR spectra measured in the O–H stretching region of (a) phenol (Phe), (b) Phe···THF (26), (c) Phe···THP (27), (d) imidazole (Im), (e) Phe···Im (28), and (f) Phe···Py (29) in CHCl ₃ .	S20
3.	Optimized structures of the series of hydrogen-bonded complexes, highlighting their key interaction features	S21-S26

3.1.	Figure S9: Optimized structures of the series of N–H···O=C hydrogen-bonded complexes (1–11), highlighting their key interaction features.	S21
3.2.	Figure S10: Optimized structures of the series of N–H···O hydrogen-bonded complexes (12–15), highlighting their key interaction features.	S22
3.3.	Figure S11: Optimized structures of the series of N–H···N hydrogen-bonded complexes (16–19), highlighting their key interaction features.	S23
3.4.	Figure S12: Optimized structures of the series of O–H···O=C hydrogen-bonded complexes (20–25), highlighting their key interaction features.	S24
3.5.	Figure S13: Optimized structures of the series of O–H···O hydrogen-bonded complexes (26–27), highlighting their key interaction features.	S25
3.6.	Figure S14: Optimized structures of the series of O–H···N hydrogen-bonded complexes (28–29), highlighting their key interaction features.	S26
4.	¹H NMR studies of indole, substituted indoles, 7-azindole, and phenol in the presence of hydrogen-bond acceptors	S27–S37
4.1.	Figure S15: Concentration-dependent ¹ H NMR shifts of the N–H proton of indole in CDCl ₃ .	S27
4.2.	Figure S16: Concentration-dependent ¹ H NMR chemical-shift changes of the N–H proton of 7-azaindole (7AI) in CDCl ₃ .	S28
4.3.	Figure S17: Concentration-dependent ¹ H NMR chemical-shift changes of the O–H proton of phenol (Phe) in CDCl ₃ .	S29
4.4.	Figure S18: ¹ H NMR spectra of (a) indole (Ind) monomer, (b) Ind···FM (3), (c) Ind···NMF (4), and (d) Ind···NDMF (3) in CDCl ₃ .	S30
4.5.	Figure S19: ¹ H NMR spectra of (a) indole (Ind) monomer and (b) Ind···THF (12), (c) Ind···THP (13), (d) Ind···Im (16), and (e) Ind···Py (17) in CDCl ₃ .	S31
4.6.	Figure S20: ¹ H NMR spectra of (a) 7-azaindole (7AI) monomer, (b) 7AI···THF (14), (c) 7AI···THP (15), (d) 7AI···Im (18), and (e) 7AI···Py (19) in CDCl ₃ .	S32

4.7.	Figure S21: ^1H NMR spectra of (a) 5-methylindole (5MI), (b) 5MI \cdots AM (9), (c) 5-chloroindole (5CI), (d) 5CI \cdots AM (10), (e) 5-nitroindole (5NI), and (f) 5NI \cdots AM (11) in CDCl_3 .	S33
4.8.	Figure S22: ^1H NMR spectra of (a) phenol (Phe) monomer (Phe) and (b) Phe \cdots BP (20), (c) Phe \cdots AP (21), (d) Phe \cdots FM (22), (e) Phe \cdots NMA (24), (f) Phe \cdots AM (23), and (g) Phe \cdots NDMA (25) in CDCl_3 .	S34
4.9.	Figure S23: ^1H NMR spectra of (a) phenol monomer (Phe), (b) Phe \cdots THF (26), (c) Phe \cdots THP (27), (d) Phe \cdots Im (28), and (e) Phe \cdots Py (29) in CDCl_3 .	S35
4.10.	Figure S24: Variable-temperature (VT) ^1H NMR spectra of the $\text{Ind}_{\text{N-H}}$ and $\text{AM}_{\text{N-H}}$ protons of the Ind \cdots AM complex recorded over 278–318 K in CDCl_3 . The ^1H NMR spectra of the indole and acetamide monomers are shown at the top for comparison.	S36
4.11.	Figure S25: ^1H NMR spectra of (a) indole and (b–i) the Ind \cdots AM complex recorded with increasing acetamide concentrations.	S37
5.	H/D exchange kinetics investigated through D_2O addition and monitored by ^1H NMR spectroscopy	S38-S42
5.1.	Figure S26: (a) Time-dependent decrease of the $\text{Ind}_{\text{N-H}}$ ($\delta \approx 8.2$ ppm) and $\text{AM}_{\text{N-H}}$ ($\delta \approx 5.4$ ppm) of Ind \cdots AM complex following D_2O addition at 20 mM acetamide concentration. (b) Time evolution of the integrated $\text{AM}_{\text{N-H}}$ ^1H NMR signal of the Ind \cdots AM complex in CDCl_3 after D_2O -induced H/D exchange.	S38
5.2.	Figure S27: Time-dependent decrease in the $\text{Ind}_{\text{N-H}}$ signal intensity of the Ind \cdots AM complex after D_2O addition at (a) 5 mM, (b) 20 mM, and (c) 100 mM acetamide concentrations. (d) Integrated $\text{Ind}_{\text{N-H}}$ ^1H NMR signal for the Ind \cdots AM complex at different acetamide concentrations in CDCl_3 as a function of time following D_2O addition.	S39
5.3.	Figure 28-53. Determination of the average H/D exchange rate constant value from repeat measurements and errors from the individual rate constant measurements for each of the complexes	S40-S65
5.4.	Figure S54: Kinetic profiles showing the time-dependent decrease in the N-H ^1H NMR signal for N-H \cdots O=C hydrogen bond type complexes with various hydrogen-bond acceptors in CDCl_3 upon D_2O -induced H/D exchange.	S66
5.5.	Figure S55: Kinetic profiles showing the time-dependent	S67

	decrease in the N-H ¹ H NMR signal for N-H···O and N-H···N hydrogen bond type complexes with various hydrogen-bond acceptors in CDCl ₃ upon D ₂ O-induced H/D exchange.	
5.6.	Figure S56: Kinetic profiles showing the time-dependent decrease in the O-H ¹ H NMR signal for O-H···O=C, O-H···O and O-H···N hydrogen bond type complexes with various hydrogen-bond acceptors in CDCl ₃ upon D ₂ O-induced H/D exchange.	S68
6.	Figure S57. Correlation between the H/D exchange rate constants ($k_{ex}^{H/D}$) and the IR red shift ($\Delta\nu$) for all 29 complexes with the exponential fit ($R^2 = 0.993$). The shaded grey area shows the 95% confidence band. This band represents the region where we are 95% certain the "true" underlying model curve resides.	S69
7.	Table S1: Comparison of experimental and theoretical FTIR spectra (gas phase and solution phase) in the N–H and O–H stretching regions for indole, 7-azaindole, substituted indole, and phenol complexes with hydrogen-bond acceptors in CHCl ₃	S70-S71
8.	Table S2: Observed change in chemical shift in ¹ H NMR for the N-H and O-H protons in all 29 complexes	S72
9.	Table S3: Comparison of experimentally observed IR red shifts ($\Delta\nu$) (cm ⁻¹) and H/D exchange rates ((min ⁻¹) in the N–H and O–H stretching regions for indole, substituted indoles, and phenol–acceptor complexes in chloroform	S73-S74
10.	References	S75-S76
11.	Cartesian co-ordinate of optimized structures of the series of hydrogen-bonded complexes.	S77-S98
11.1.	Cartesian co-ordinate of optimized structures of the series of N–H···O=C hydrogen-bonded complexes (1-11).	S77-S84
11.2.	Cartesian co-ordinate of optimized structures of the series of N–H···O hydrogen-bonded complexes (12–15).	S85-S87
11.3.	Cartesian co-ordinate of optimized structures of the series of N–H···N hydrogen-bonded complexes (16–19).	S88-S90
11.4.	Cartesian co-ordinate of optimized structures of the series of O–H···O=C hydrogen-bonded complexes (20-25).	S91-S94

- 11.5. Cartesian co-ordinate of optimized structures of the series of O–H \cdots O hydrogen-bonded complexes (26-27). S95-S96
- 11.6. Cartesian co-ordinate of optimized structures of the series of O–H \cdots N hydrogen-bonded complexes (28-29). S97-S98

1. Methodology of experimental and computational studies

A. FTIR Spectroscopy

The FTIR spectra of all the monomers and complexes were measured at 293 K using a Fourier-Transform IR (FTIR) spectrometer (Bruker Vertex 70). To record the IR spectra, the compounds were dissolved in CHCl_3 solvent, and the concentration of the solutions was maintained at 20 mM for all cases except for acetamide (100 mM) and phenol (5 mM). The sample solutions were placed in a cell with a 1 mm path length, consisting of CaF_2 windows, separated by a mylar spacer of 56 μm thickness. For recording each spectrum, 48 scans were collected at 1 cm^{-1} resolution, though the instrument had a maximum resolution of 0.4 cm^{-1} .

B. NMR Spectroscopy: Chemical shift measurement and error analysis

The ^1H NMR spectra were recorded at 298 K using a Bruker Ascend Evo 400 MHz spectrometer operating at a magnetic field strength of 9.4 T in CDCl_3 . Proton chemical shifts are reported in ppm (δ) relative to the internal standard tetramethylsilane (TMS, $\delta = 0.0$ ppm), or referenced to the residual solvent signal (CDCl_3 , $\delta = 7.27$ ppm) relative to TMS. All spectra were processed using TopSpin (v4.0), with phase and baseline corrections applied to ensure optimal signal clarity and accurate integration. For all investigated complexes, ^1H NMR spectra were recorded at solution concentrations of approximately 20 mM, prepared in 500 μL of CDCl_3 .

To estimate the uncertainty in the experimental data, all potential sources of systematic error (e.g., weighing and volume measurements) were first identified and minimized to negligible levels. The remaining uncertainties are therefore random in nature and can be assessed by repeated measurements and evaluation of the standard error (SE). For example, the chemical shift of the N–H proton in the ind \cdots AM complex was measured five times, each using a freshly prepared solution containing 20 mM indole (ind) and 20 mM acetamide (AM). The observations are reported such that i denotes the measurement number, and x represents the corresponding chemical shift value of indole in the ind \cdots AM complex.

No of Readings (i)	Value (x)
1	8.227
2	8.225
3	8.227
4	8.228

Reasonably, our best estimate would be to calculate the standard error (SE).

Now,

$$SE = \frac{\text{standard deviation (SD)}}{\sqrt{N}} \quad \text{Where } N = \text{No. of measurements}$$

Again,

$$SD (\sigma_x) = \sqrt{\frac{1}{N-1} \sum_{i=1}^N (d_i)^2} \quad \text{Where } d_i = \text{deviation}$$

Now,

$$d_i = x_i - \bar{x} \quad \text{Where } \bar{x} = \text{average or mean}$$

We find the SD

$$\sigma_x \approx 0.0013$$

Thus, the standard error or the average uncertainty in the chemical shift measurement of Ind···AM complex is approximately 0.0007. We have measured the standard error (SE) in the chemical shift for all other complexes in a similar manner.

C. NMR H/D exchange experiments and error analysis

We carried out deuterium exchange ^1H NMR studies to determine the intermolecular H-bond strength in the complexes. Initially, an NMR spectrum was measured with 500 μL solution of the dimeric complex (20 mM) in CDCl_3 . Subsequently, D_2O (2% v/v) was added to the solution, defining time zero, to give a final D_2O concentration of 1.1 M, thereby ensuring pseudo-first-order kinetics. ^1H NMR spectra were then acquired at different time intervals. In a typical experiment, spectra were collected every 5 minutes initially, followed by measurements at regular intervals of 15–20 minutes over a total duration of 350 minutes. The integrals of the indole, 7-azaindole N–H, and phenol O–H resonances were calculated relative to an aromatic C–H signal of CDCl_3 as a function of time after D_2O addition. Integration ranges for the exchanging protons were user-defined but kept consistent within each experiment. Rate constants were determined from the slope of a nonlinear least squares fit to the graph of $A_t = A_0 \exp(-k_{\text{ex}}^{\text{H/D}} \times t)$. The y-intercept is taken as the calculated value at time zero, and this value is used to normalize the final data to a scale of 100-0% hydrogen remaining.

Error analysis in the measurement of integrated ^1H signals: The experiments were repeated three times on different days. Standard errors (SE) were determined from the standard deviation of the integrated ^1H signals corresponding to the N–H and O–H protons at a given time point. As an example, we have measured the H/D exchange kinetics of the solution mixture of indole (20 mM) and AM (20 mM) at a similar time interval. The observations after 105 minutes are as follows:

No of Readings (i)	Percentage Hydrogen (x)
1	63
2	59
3	65

Now,

$$SE = \frac{\text{standard deviation (SD)}}{\sqrt{N}} \quad \text{Where } N = \text{No. of measurements}$$

Again,

$$SD (\sigma_x) = \sqrt{\frac{1}{N-1} \sum_{i=1}^N (d_i)^2} \quad \text{Where } d_i = \text{deviation}$$

Now,

$$d_i = x_i - \bar{x} \quad \text{Where } \bar{x} = \text{average or mean}$$

We find the SD

$$\sigma_x \approx 2.59$$

Thus, the standard error (SE) or the average uncertainty in the percentage hydrogen measurement is approximately 1.16 for Ind \cdots AM complex after 105 minutes of D₂O addition. Similarly, SE values in the percentage hydrogen measurement for all other time intervals were determined for the Ind \cdots AM complex. Afterwards, SE values in the percentage hydrogen measurement at different time intervals for all other complexes are determined in a similar manner.

Error analysis in the measurement of H/D exchange rate constants ($k_{\text{ex}}^{\text{H/D}}$): H/D exchange rate constant for each complex was determined by least-squares fitting of the time-dependent decay of the integrated ^1H NMR signals using a first-order rate equation. Exponential fitting was performed in OriginPro using the Levenberg-Marquardt (L-M) algorithm, and the

uncertainty in the determined rate constant values was obtained from the variance-covariance matrix of the least-squares regression analysis. The H/D exchange kinetic experiments were repeated three times on non-consecutive days. Accordingly, three independent rate constants (k_1, k_2, k_3) and their corresponding uncertainties were obtained for each complex. The average rate constant (k_{ex}^{avg}) was calculated from these three measurements. The standard deviation of the experimental rate constant values was then determined from the multiple trials. It is also possible to determine the propagated uncertainty from the error values obtained from the fitting of the kinetics data from individual rate constant measurements by using the equation: $e_{av} = [(\text{SQRT}(e_1^2 + e_2^2 + e_3^2))]/3$, where the errors e_1, e_2 , and e_3 are obtained from the least squares fitting of the data from individual measurements in multiple trials. However, we estimated the uncertainty in the rate constants for each complex as the standard deviation of the rate constants obtained from repeated measurements. Finally, we have plotted k_{ex}^{avg} for the H/D exchange of the individual complex as a function of IR red-shift ($\Delta\nu$), and shown the standard error in Figure 6 of the manuscript. Fitting of the kinetics data from individual rate constant measurements (k_1, k_2, k_3) for multiple trials of all the complexes is shown on pages S44-S69 of the supporting information. For each complex, individual rate constants are reported with their respective least-squares fitting errors, while the average rate constant (k_{ex}^{avg}) is presented with its standard error. k_{ex}^{avg} is denoted as $k_{ex}^{H/D}$ throughout the manuscript and supporting information.

D. Confidence Interval (CI) for the Fitted Correlation of the $k_{ex}^{H/D}$ versus IR red-shift ($\Delta\nu$)

The 95% confidence interval (CI) for the fitted correlation curve between the $k_{ex}^{H/D}$ and $\Delta\nu$ provided in Figure 6 was calculated as (Reference: Fitting models to biological data using linear and nonlinear regression, 2004, Oxford University Press, Page No.: 103):

$$CI(x) = \hat{y}(x) \pm (t_{critical} \times \sigma_y(x))$$

Where,

$t_{critical} = 2.056$ for 95% Confidence Interval. $t_{critical}$ is calculated based on the Student's t-distribution with degrees of freedom (D), where $D = N - P$, where N is the sample size and P is the number of parameters. Now, the degrees of freedom (D) = $29 - 3 = 26$ for our data set with 29 complexes (N) and 3 (P) parameters (m, c, and n) from the fitting equation $k_{ex}^{H/D} = m \times e^{-\Delta\nu/c} + n$.

$\hat{y}(x)$ stands for $k_{ex}^{H/D}(\Delta\nu)$ for our fitted correlation curve.

The values in a t-table are generated using the Probability Density Function (PDF) of the student's t-distribution.

The t-distribution curve is defined by a complex formula that depends on the degrees of freedom (ν):

$$f(t) = \frac{\Gamma(\frac{D+1}{2})}{\sqrt{(D\pi)}\Gamma(\frac{D}{2})} \left(1 + \frac{t^2}{D}\right)^{-\frac{D+1}{2}} \text{ Where, } \Gamma = \text{Gamma function}$$

$\sigma_y(x)$ = standard deviation of the fit (σ_y) at a specific point x . It can be calculated by the following equation:

$$\sigma_y(x) = \sqrt{J \cdot P_{cov} \cdot J^T}$$

Here,

J = Jacobian vector for any specific x

For our fitting equation, $k_{ex}^{H/D} = m \times e^{-\Delta v/c} + n$; $J = \left[\frac{dy}{dm}, \frac{dy}{dc}, \frac{dy}{dn}\right]$, where m , n , and c are the three parameters.

P_{cov} = Covariance Matrix; when we run the fit, the algorithm calculates the Hessian matrix of the residuals. The inverse of this matrix is the Covariance Matrix, which contains the variance of each parameter and how they relate to each other:

$$P_{cov} = \begin{bmatrix} \sigma_m^2 & \sigma_{m,c} & \sigma_{m,n} \\ \sigma_{c,m} & \sigma_c^2 & \sigma_{c,n} \\ \sigma_{n,m} & \sigma_{n,c} & \sigma_n^2 \end{bmatrix}$$

It includes individual parameter uncertainties and parameter correlations. σ_m , σ_n , and σ_c are the uncertainties of the parameters m , n , and c , respectively, while $\sigma_{m,c}$, $\sigma_{m,n}$, and $\sigma_{c,n}$ are uncertainties of the correlation of the parameters.

J^T = Transpose of the Jacobian matrix.

Now, the uncertainty in the fitted curve was estimated using standard error propagation based on the covariance matrix of the nonlinear least-squares fit. The standard error of the fitted response at each point was calculated. The 95% confidence band was obtained as

$$\hat{y}_{fit} \pm (t_{critical} \times \sigma_y(x)) \text{ where } y = k_{ex}^{H/D} \text{ and } x = \Delta v$$

D. Quantum Chemistry Calculations

The experimental vibrational frequencies of N-H and O-H groups were supported by theoretical calculations performed on optimized complexes. Low-energy conformers were generated using the CREST (Conformer–Rotamer Ensemble Sampling Tool),¹ which efficiently explores conformational space through the GFN2-xTB semi-empirical tight-binding method.² Ten conformers of each pair were then subjected to the MMFF94 (Merck Molecular Force Field)-based calculations³ in Open Babel.⁴ The structures of all the complexes (Figure 1) were optimized using the Gaussian 09 Program package⁵ at the M06-2X/6-311++G(d,p) level of theory.⁶⁻⁷ The atomic coordinates of all the complexes are presented in the Supplementary Information. The number of imaginary frequencies was zero in the individual structures and the interacting pairs. As the shifts in FTIR spectra were monitored in chloroform solution, the optimizations of structures were carried out in a simulated solution using the Polarizable Continuum Model (PCM)⁸ implemented in Gaussian 09. The discussion of vibrations mainly focuses on the purely N-H & O-H stretching vibrations, as visualized in GaussView 6.⁹

2. FTIR spectra of 1:1 complex of indole, 7-azaindole, substituted indoles, and phenol with various hydrogen-bond acceptors:

2.1. FTIR spectra of indole measured at different concentrations:

We have recorded indole FTIR spectra over a concentration range of 10-200 mM of indole in CHCl_3 . We observed a peak at 3481 cm^{-1} , and a new additional N-H stretching band at 3410 cm^{-1} , which appears only at concentrations above 20 mM. The band centred at 3481 cm^{-1} , attributed to the free N-H stretching vibration of indole monomer, while that of 3410 cm^{-1} indicates the formation of indole dimer. The reported values for the N-H stretching frequency measured in the indole monomer and dimer in carbon tetrachloride (CCl_4) solution are 3491 cm^{-1} and 3425 cm^{-1} , respectively.¹⁰

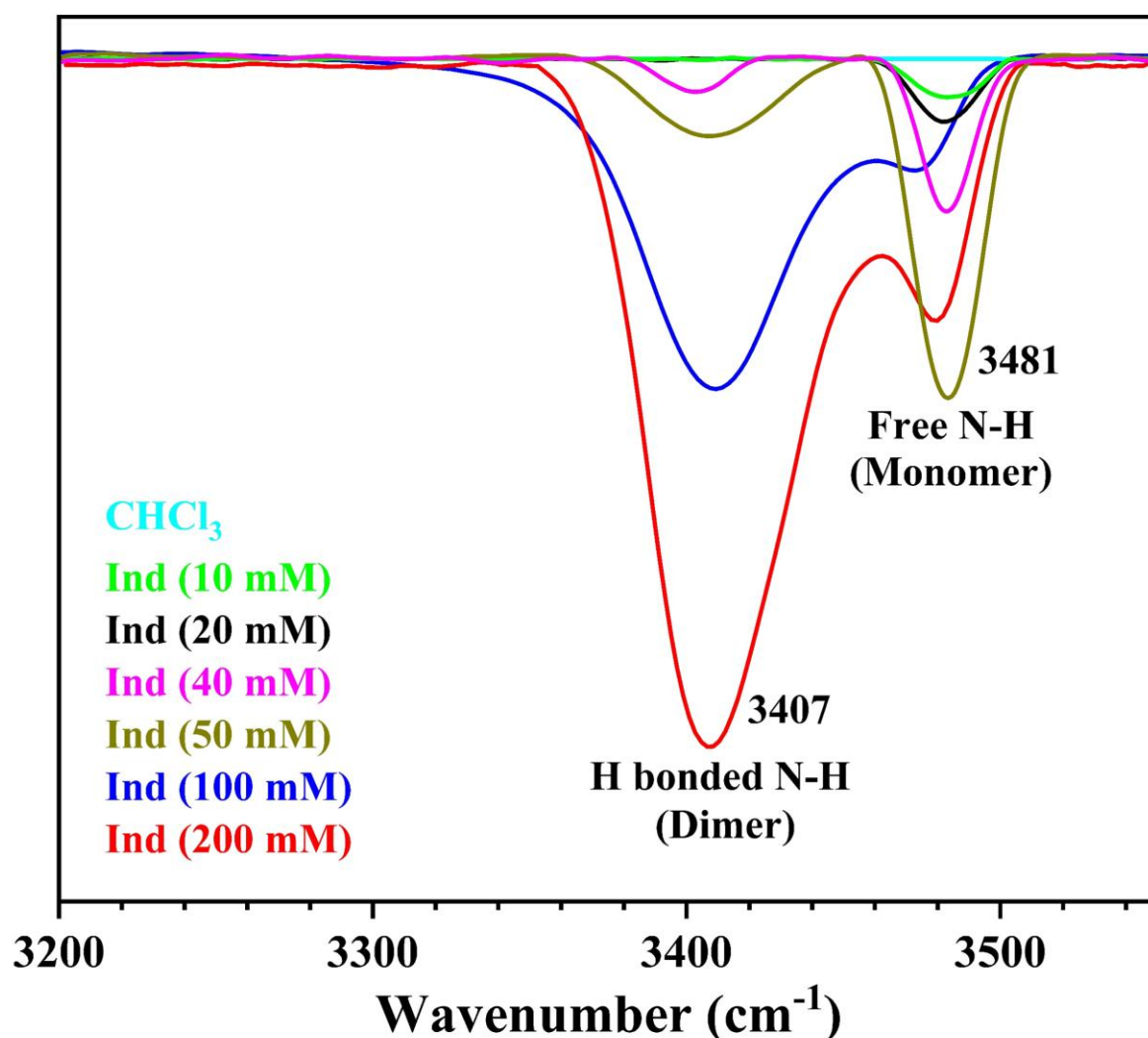


Figure S1. Concentration-dependent FTIR spectra of indole (Ind) measured in CHCl_3 solution showing the N-H bands of the monomer (3481 cm^{-1}) and emerging dimer (3407 cm^{-1}). FTIR spectrum of only the solvent CHCl_3 is also provided in the figure.

2.2. FTIR spectra of phenol and 7-azaindole measured at different concentrations:

We have recorded FTIR spectra of phenol and 7-azaindole over a concentration range of 5-50 mM and 10-100 mM, respectively, in CHCl_3 solution. In Figure S2a, the band observed at 3610 cm^{-1} is attributed to the free O-H stretching vibration of phenol monomer, and a new additional O-H stretching band at 3549 cm^{-1} appearing only at concentrations above 10 mM is assigned as phenol dimer. In the case of 7-azaindole, the monomeric N-H stretching band is observed at 3472 cm^{-1} , while the dimeric N-H band appears as a complex substructure in the $3000\text{-}3250\text{ cm}^{-1}$ region due to Fermi resonance between the N-H stretching fundamental and overtones/combination bands of N-H bend/ring vibrations. The dimeric substructure of 7-azaindole appears only at concentrations above 20 mM. The reported O-H stretching frequencies measured for phenol monomer and dimer in CCl_4 solution are 3612 cm^{-1} and 3490 cm^{-1} , respectively.¹¹ In the case of 7-azaindole measured in CCl_4 , the monomeric N-H stretching frequency is reported at 3480 cm^{-1} , while the vibrational substructure for the dimeric N-H stretching frequency is reported in the $2950\text{-}3300\text{ cm}^{-1}$ region.^{12,13}

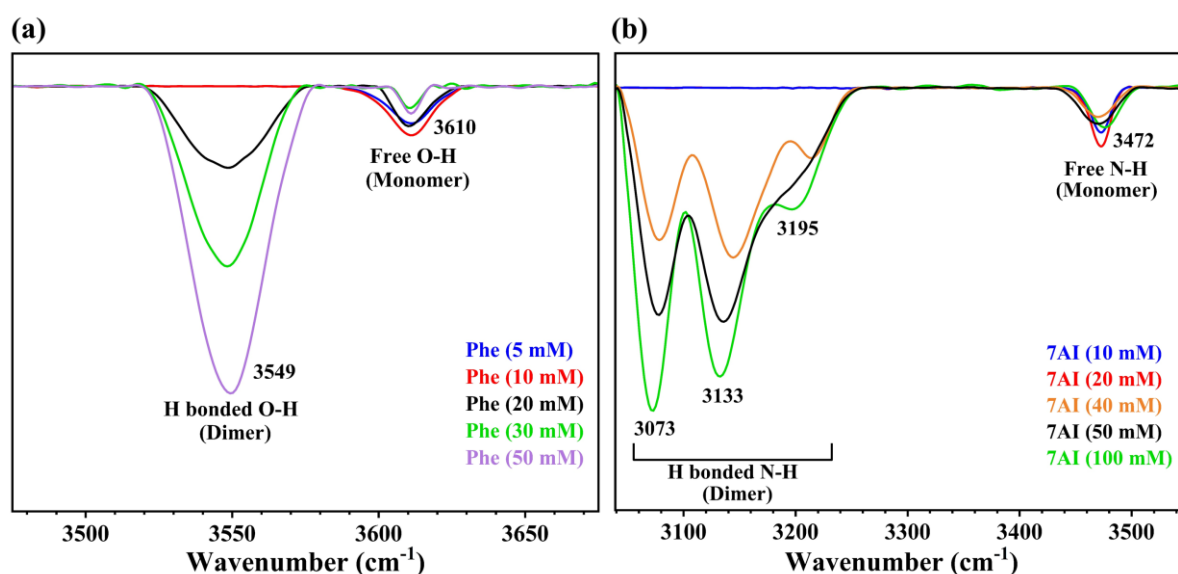


Figure S2. Concentration-dependent FTIR spectra of (a) phenol (Phe) and (b) 7-azaindole (7AI) measured in CHCl_3 solution. Figure S2a shows the O-H band of the monomer (3610 cm^{-1}) and emerging dimer (3549 cm^{-1}) of phenol, while Figure S2b shows the N-H band of the monomer (3472 cm^{-1}) and substructure of dimeric N-H vibration ($3000\text{-}3250\text{ cm}^{-1}$) of 7-azaindole.

2.3. FTIR spectra of the complexes of indole:

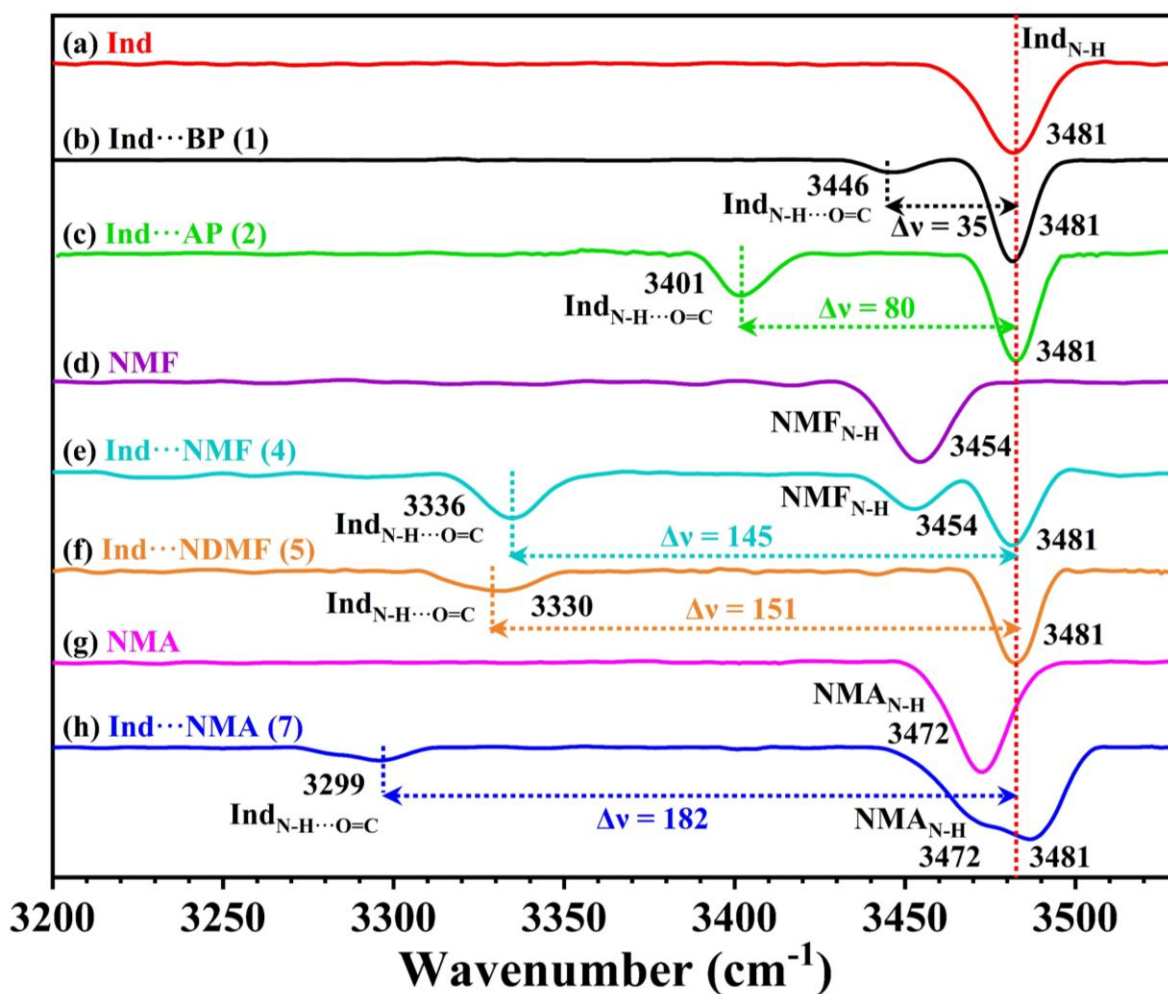


Figure S3. FTIR spectra measured in the N–H stretching region of (a) indole (Ind), (b) Ind \cdots BP (1), (c) Ind \cdots AP (2), (d) NMF, (e) Ind \cdots NMF (4), (f) Ind \cdots NDMF (5), (g) NMA, and (h) Ind \cdots NMA (7) in CHCl_3 . The number provided in the parenthesis next to the description of the complex indicates their identification number mentioned in Figure 1 of the manuscript. The magnitude of the N–H stretching red shift ($\Delta\nu$) in cm^{-1} of the complexes with respect to that in the monomer is indicated with double headed horizontal arrow.

2.4. FTIR spectra of the complexes of indole (continued):

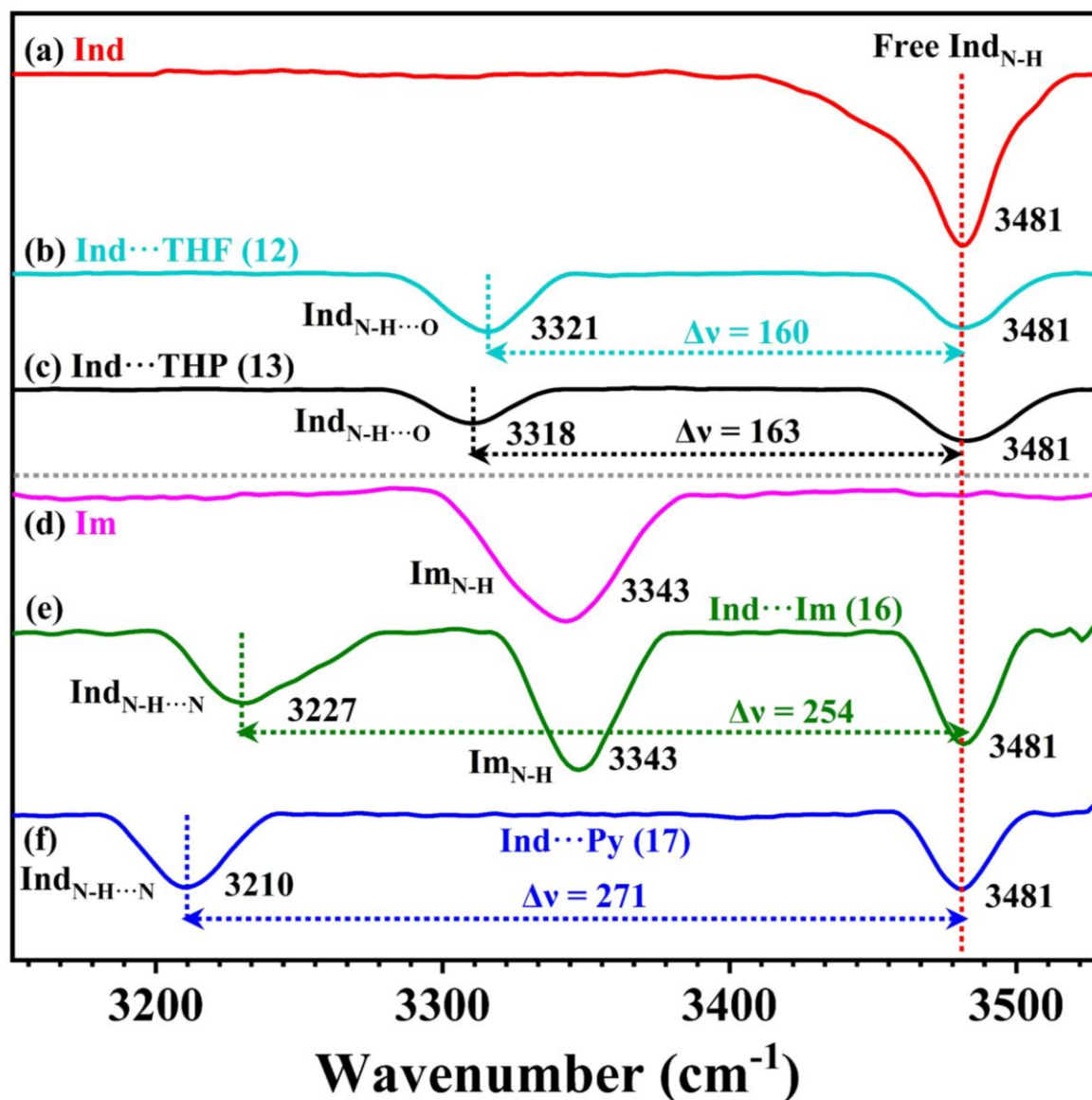


Figure S4. FTIR spectra measured in the N–H stretching region of (a) indole (Ind), (b) Ind···THF (12), (c) Ind···THP (13), (d) imidazole (Im), (e) Ind···Im (16), and (f) Ind···Py (17) in CHCl_3 . In number provided in the parenthesis next to the description of the complex indicates their identification number mentioned in Figure 1 of the manuscript. The magnitude of the N–H stretching red shift ($\Delta\nu$) in cm^{-1} of the complexes with respect to that in the monomer is indicated with double headed horizontal arrow.

2.5. FTIR spectra of the complexes of substituted indoles:

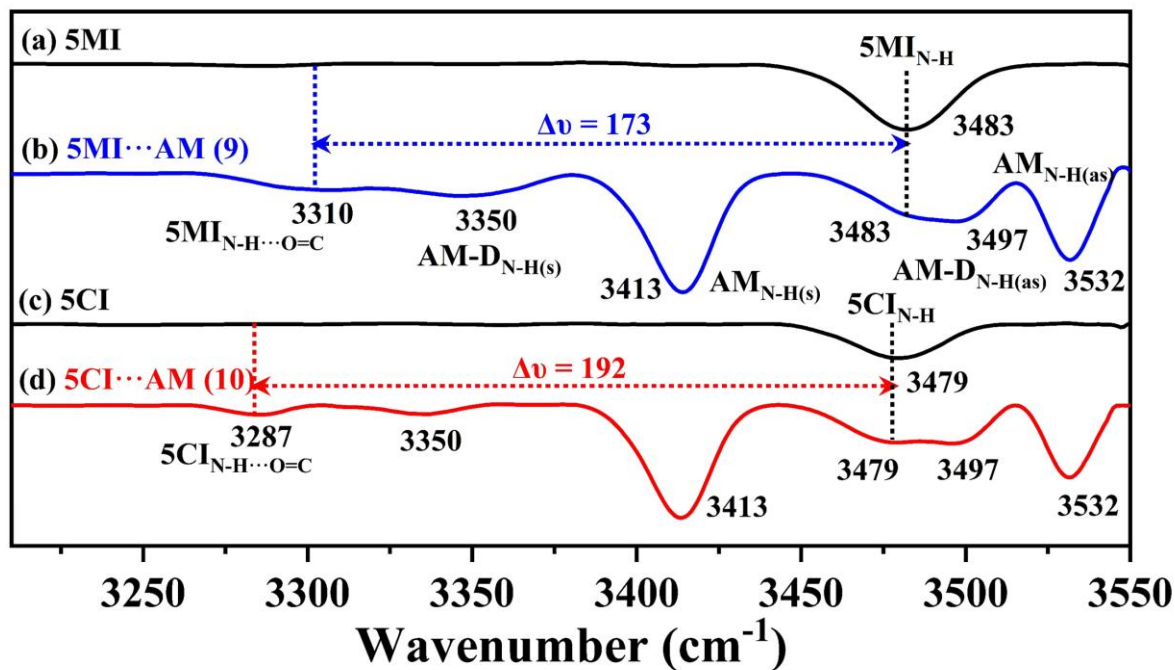


Figure S5. FTIR spectra measured in the N–H stretching region of (a) 5-methylindole (5MI), (b) 5MI...AM (9), (c) 5-chloroindole (5CI), and (d) 5CI...AM (10) in CHCl₃. The number provided in the parenthesis next to the description of the complex indicates their identification number mentioned in Figure 1 of the manuscript. The magnitude of the N–H stretching red shift ($\Delta\nu$) in cm⁻¹ of the complexes with respect to that in the monomer is indicated with double headed horizontal arrow.

2.6. FTIR spectra of the complexes of 7-azaindole (7AI):

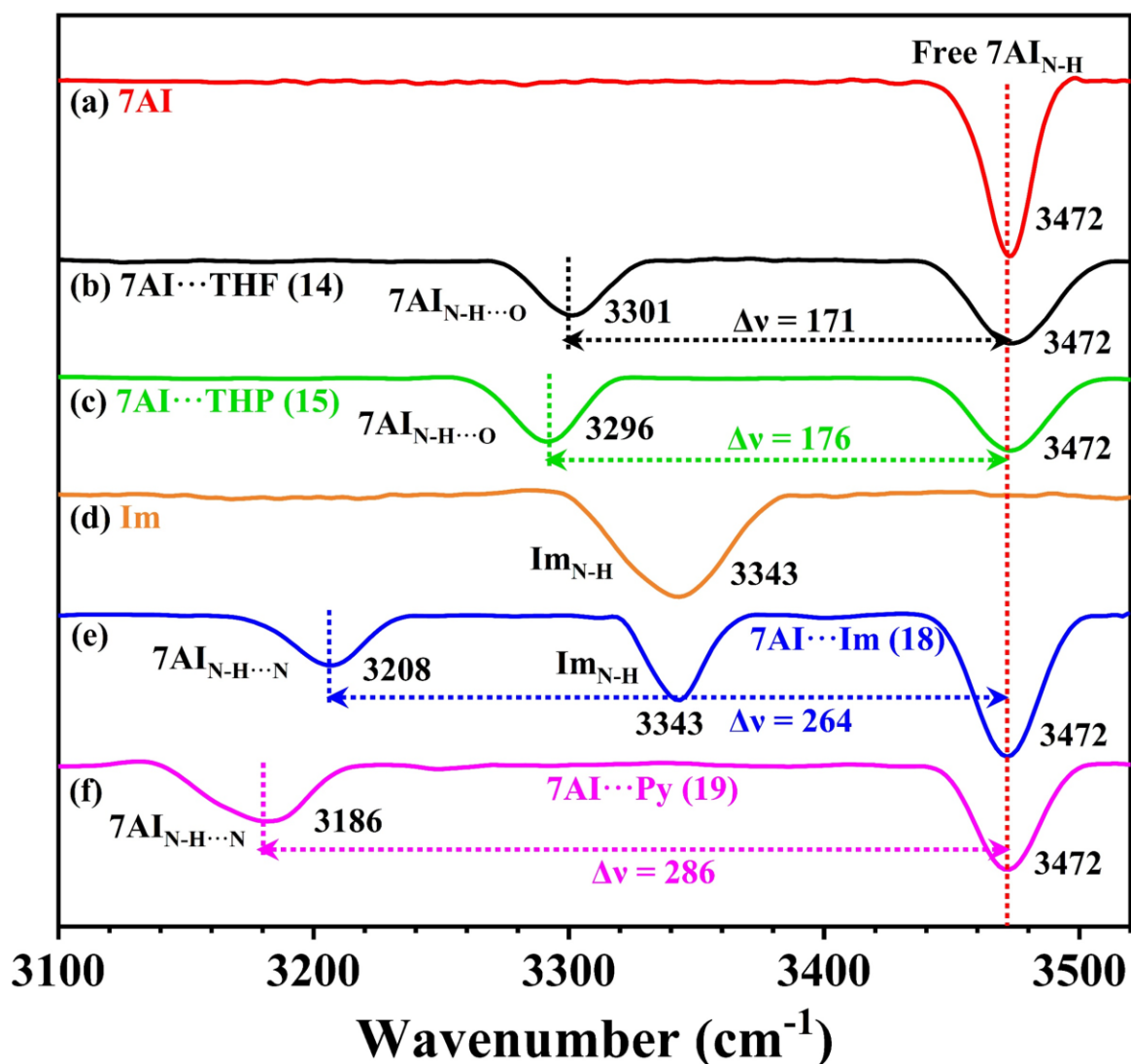


Figure S6. FTIR spectra measured in the N–H stretching region of (a) 7-azaindole (7AI), (b) 7AI···THF (14), (c) 7AI···THP (15), (d) imidazole (Im), (e) 7AI···Im (18), and (f) 7AI···Py (19) in CHCl₃. The number provided in the parenthesis next to the description of the complex indicates their identification number mentioned in Figure 1 of the manuscript. The magnitude of the N–H stretching red shift ($\Delta\nu$) in cm⁻¹ of the complexes with respect to that in the monomer is indicated with double headed horizontal arrow.

2.7. FTIR spectra of the complexes of phenol (Phe):

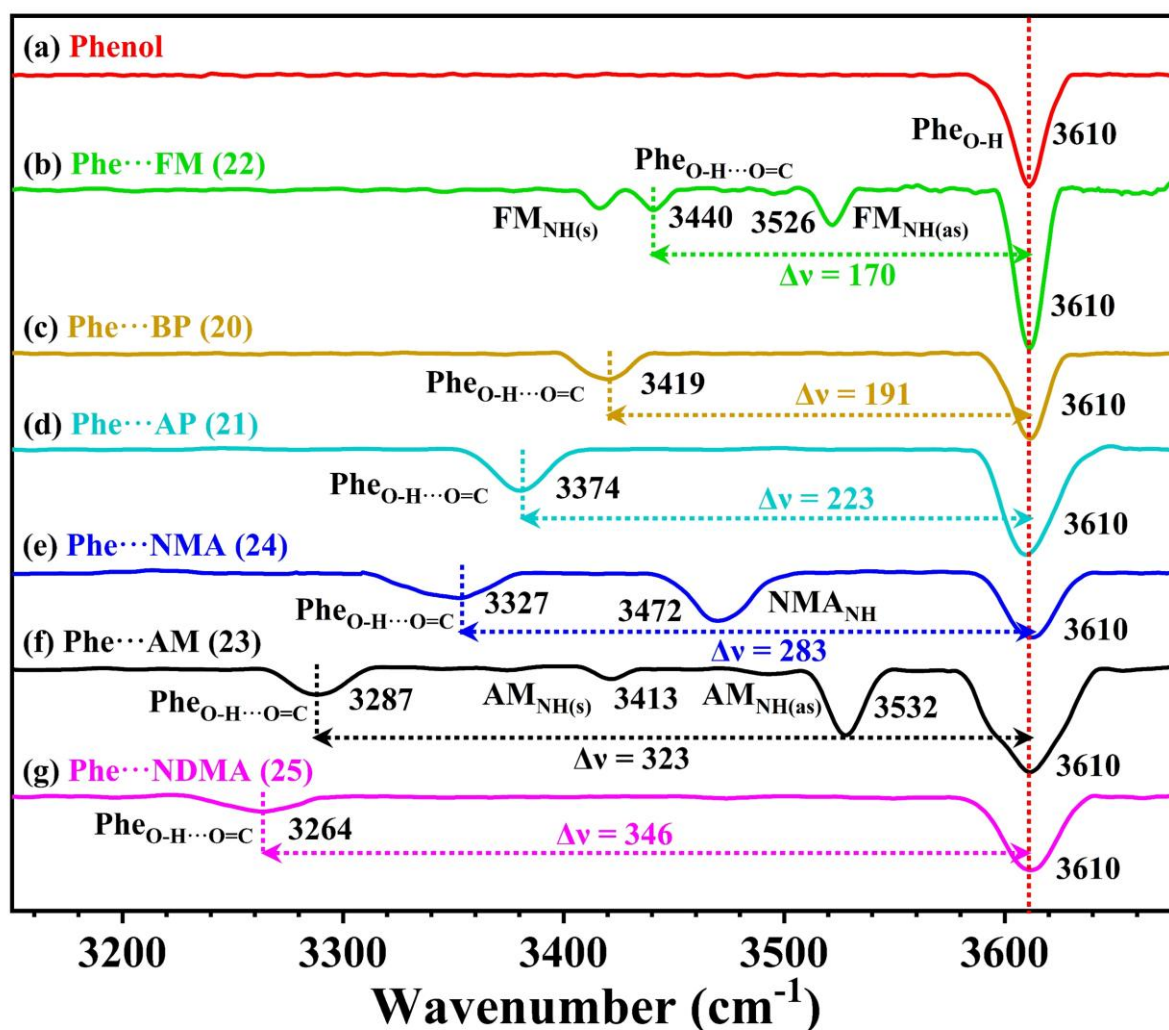


Figure S7. FTIR spectra measured in the O–H stretching region of (a) phenol monomer (Phe), (b) Phe···FM (22), (c) Phe···BP (20), (d) Phe···AP (21), (e) Phe···NMA (24), (f) Phe···AM (23), and (g) Phe···NDMA (25) in CHCl₃. The number provided in the parenthesis next to the description of the complex indicates their identification number mentioned in Figure 1 of the manuscript. The magnitude of the N–H stretching red shift ($\Delta\nu$) in cm⁻¹ of the complexes with respect to that in the monomer is indicated with double headed horizontal arrow.

2.8. FTIR spectra of the complexes of phenol (continued):

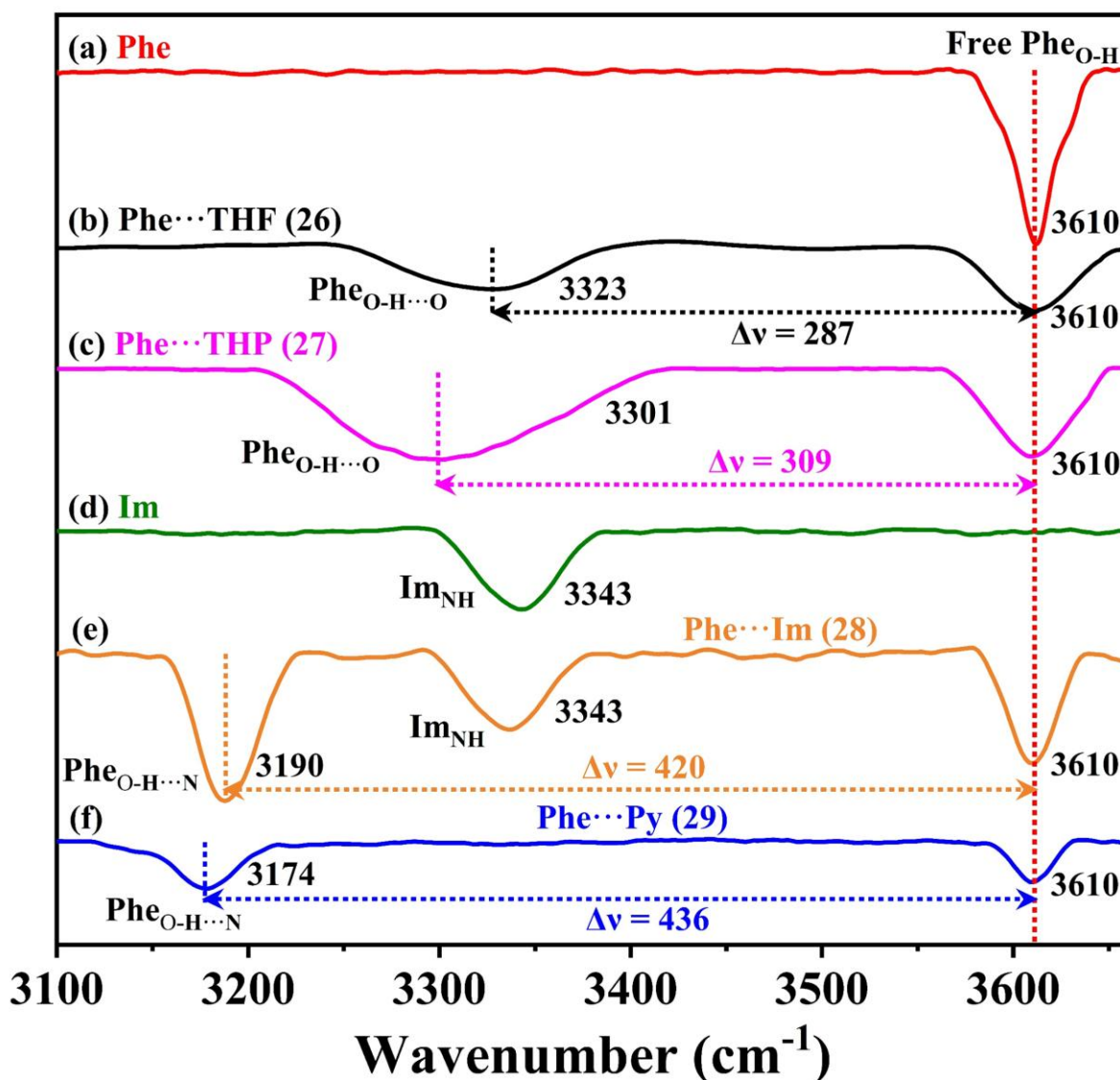


Figure S8. FTIR spectra measured in the O–H stretching region of (a) phenol (Phe), (b) (Phe···THF (26), (c) Phe···THP (27), (d) imidazole (Im), (e) Phe···Im (28), and (f) Phe···Py (29) in CHCl₃. The number provided in the parenthesis next to the description of the complex indicates their identification number mentioned in Figure 1 of the manuscript. The magnitude of the N–H stretching red shift ($\Delta\nu$) in cm⁻¹ of the complexes with respect to that in the monomer is indicated with double headed horizontal arrow.

3. Optimized structures of the complexes:

3.1. Optimized structures of the N–H···O=C hydrogen bonded complexes:

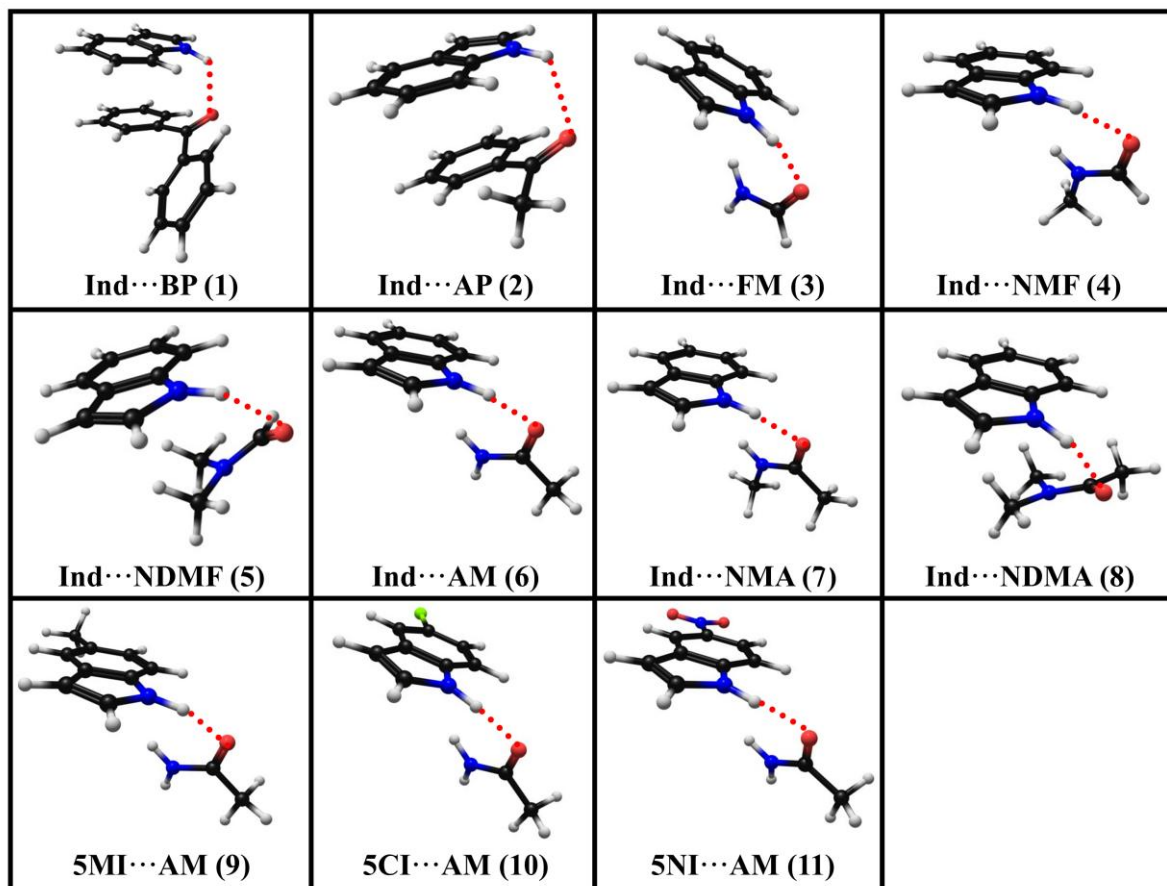


Figure S9. Structures of the N–H···O=C hydrogen bonded complexes optimized at the M06-2X/6-311++G(d,p) level. The number provided in the parenthesis next to the description of the complex indicates their identification number mentioned in Figure 1 of the manuscript.

3.2. Optimized structures of the N–H···O hydrogen bonded complexes:

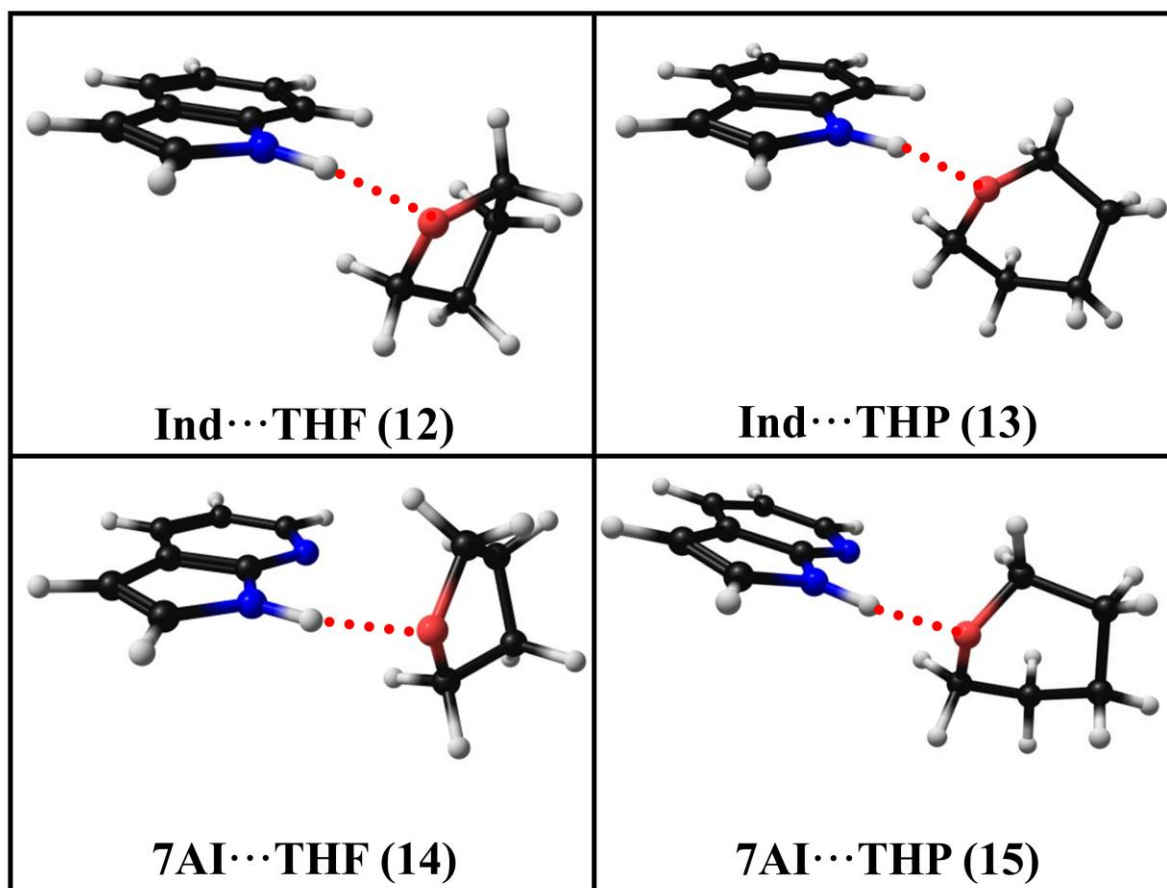


Figure S10. Structures of the N–H···O hydrogen bonded complexes optimized at the M06-2X/6-311++G(d,p) level. The number provided in the parenthesis next to the description of the complex indicates their identification number mentioned in Figure 1 of the manuscript.

3.3. Optimized structures of the N–H···N hydrogen bonded complexes:

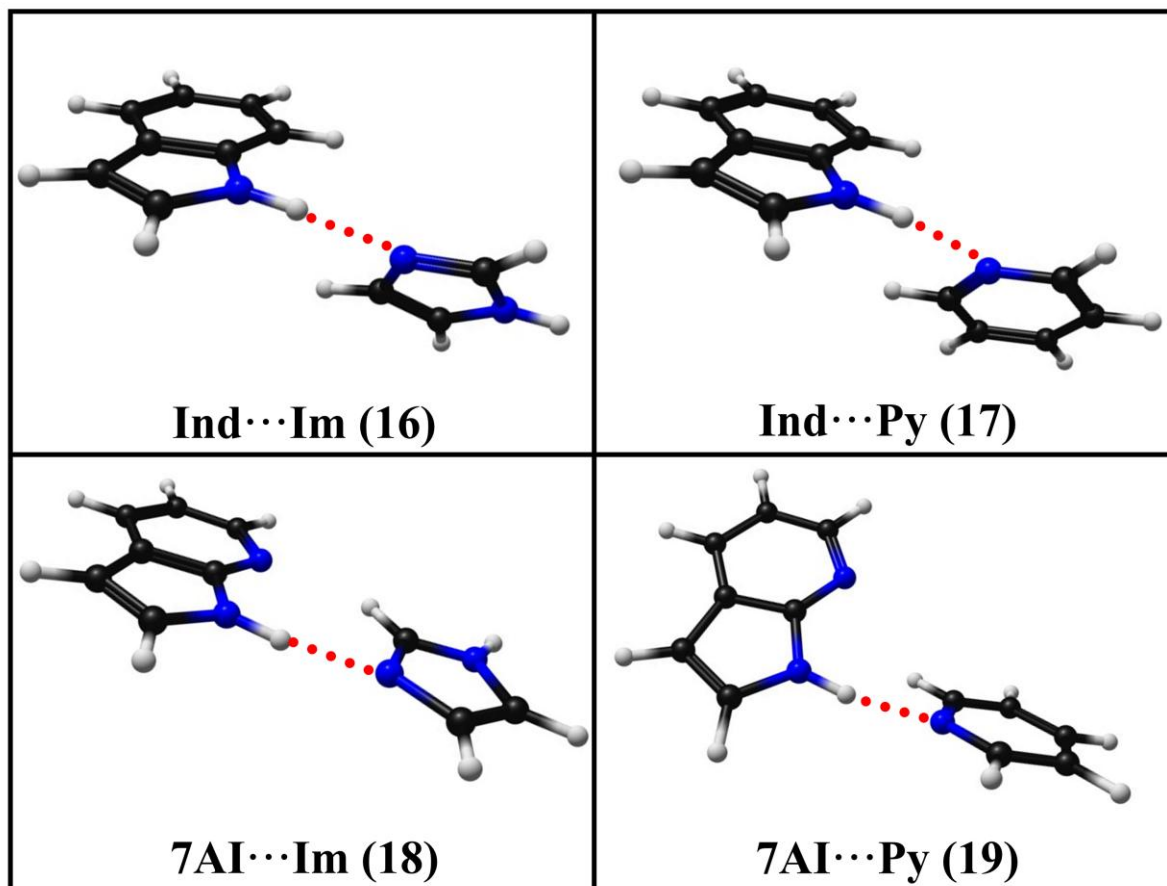


Figure S11. Structures of the N–H···N hydrogen bonded complexes optimized at the M06-2X/6-311++G(d,p) level. The number provided in the parenthesis next to the description of the complex indicates their identification number mentioned in Figure 1 of the manuscript.

3.4. Optimized structures of the O–H···O=C hydrogen bonded complexes:

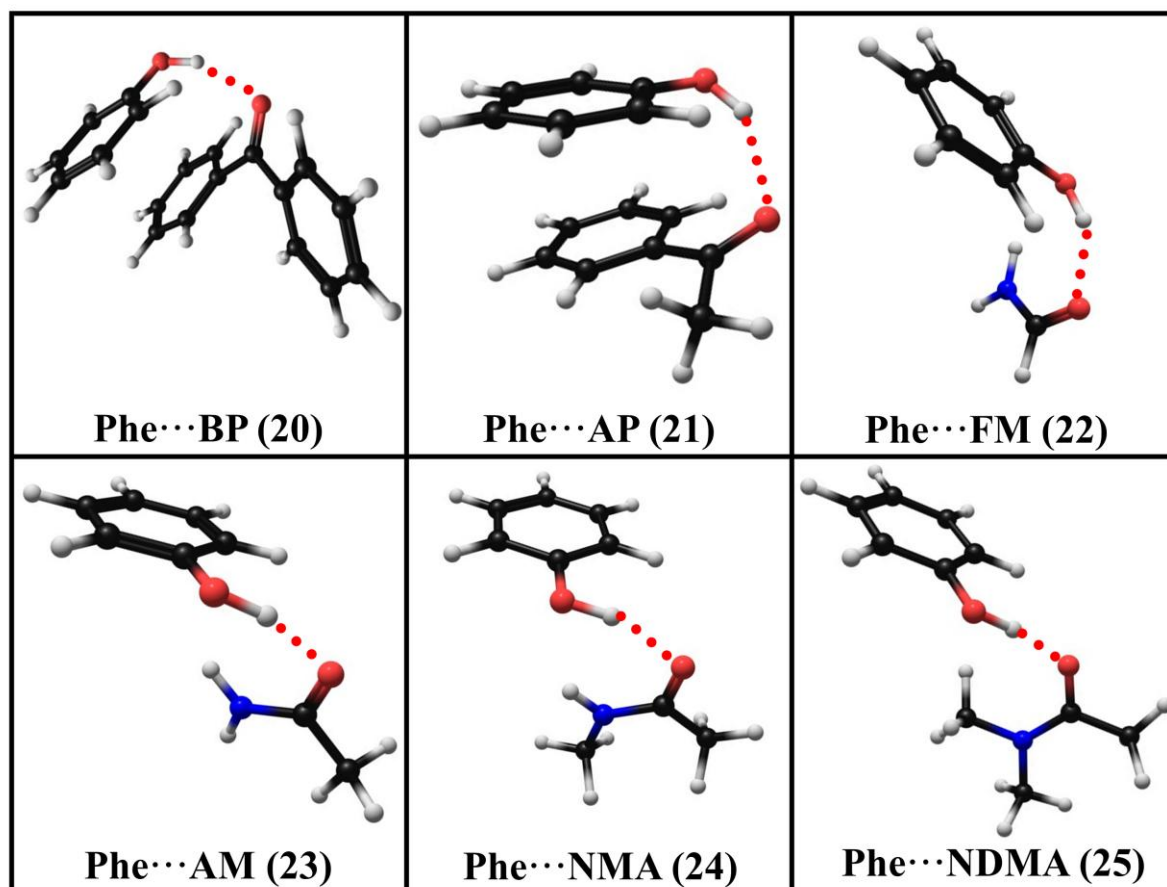


Figure S12. Structures of the O–H···O=C hydrogen bonded complexes optimized at the M06-2X/6-311++G(d,p) level. The number provided in the parenthesis next to the description of the complex indicates their identification number mentioned in Figure 1 of the manuscript.

3.5. Optimized structures of the O–H···O hydrogen bonded complexes:

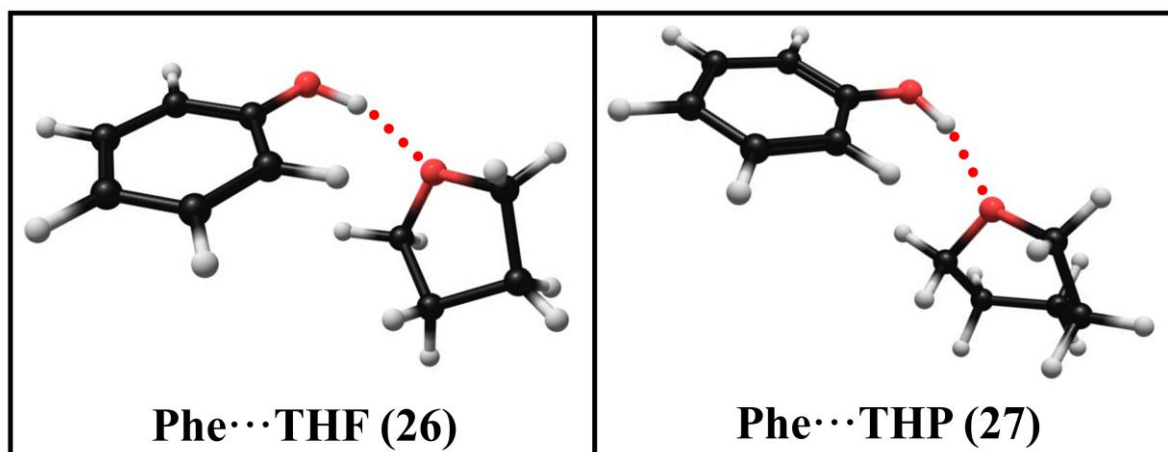


Figure S13. Structures of the O–H···O hydrogen bonded complexes optimized at the M06-2X/6-311++G(d,p) level. The number provided in the parenthesis next to the description of the complex indicates their identification number mentioned in Figure 1 of the manuscript.

3.6. Optimized structures of the O–H···N hydrogen bonded complexes:

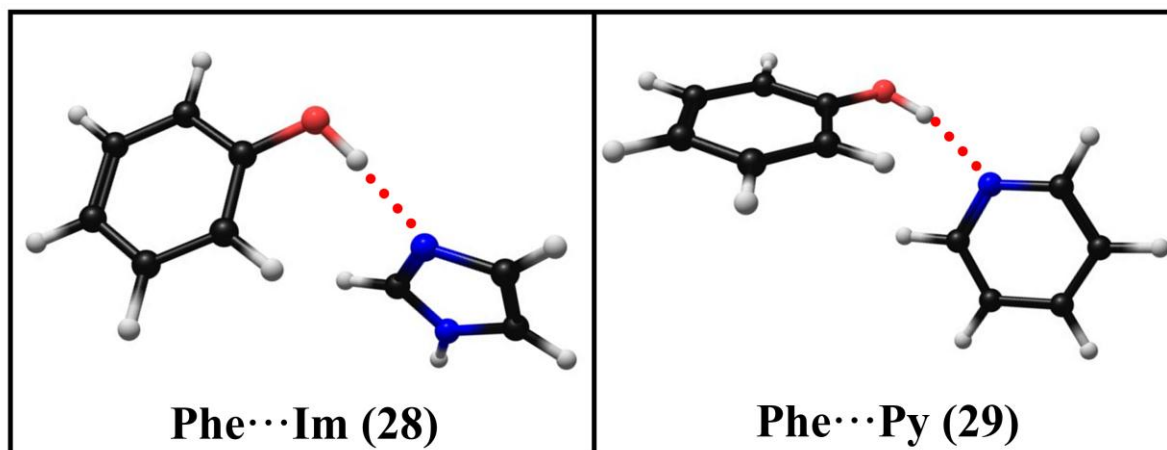


Figure S14. Structures of the O–H···N hydrogen bonded complexes optimized at the M06-2X/6-311++G(d,p) level. The number provided in the parenthesis next to the description of the complex indicates their identification number mentioned in Figure 1 of the manuscript.

4. ¹H NMR studies of indole, 7-azaindole, substituted indoles, and phenol in the presence of hydrogen bond acceptors:

4.1. Concentration dependent ¹H NMR spectra of indole:

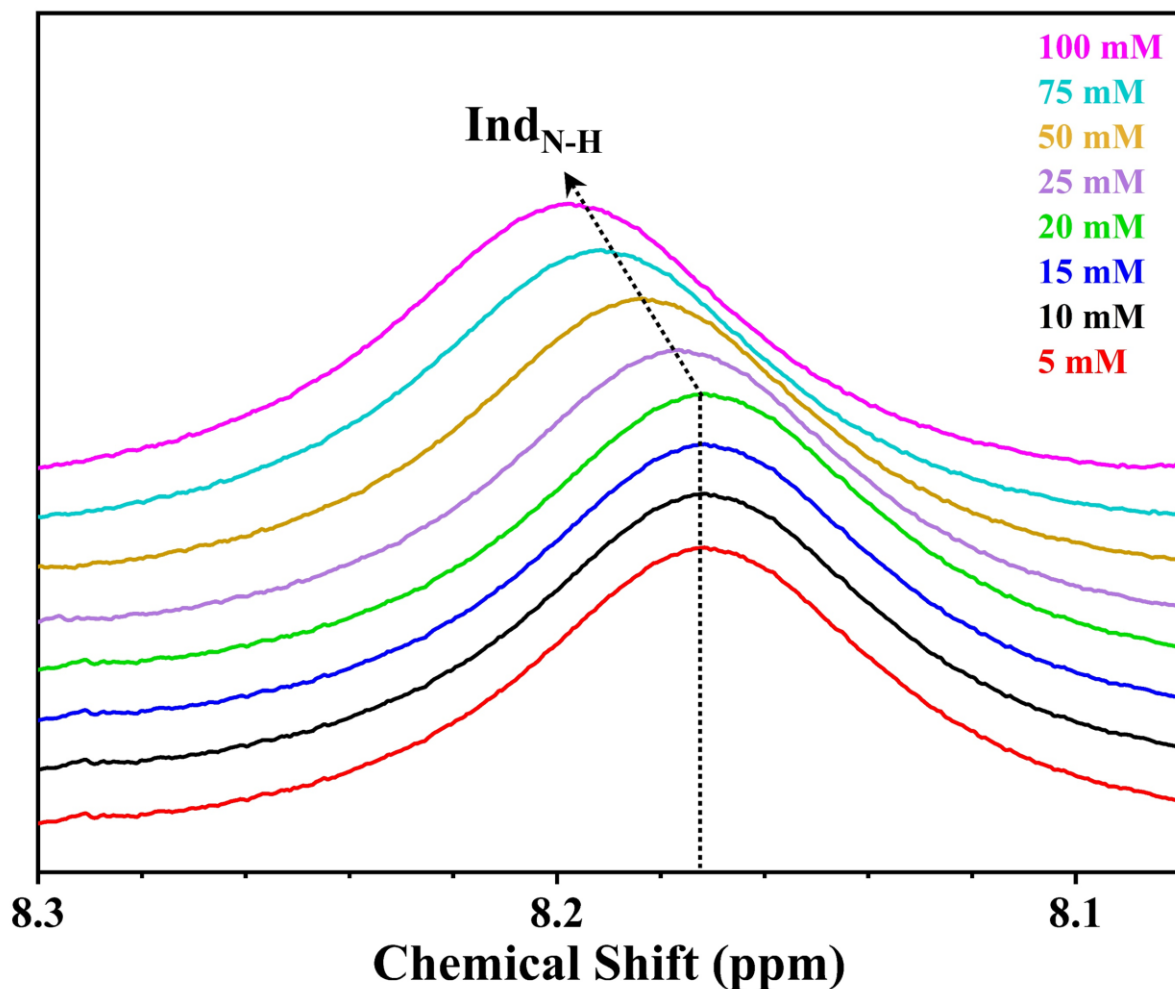


Figure S15. Concentration dependent ¹H NMR spectra of indole measured in CDCl₃ solution, displaying the changes in the chemical shift of the N–H proton. The reported ¹H NMR spectra of indole on a Bruker AV 400 NMR spectrometer in CDCl₃ obtained from BFEE electrolyte, shows N-H chemical shift at $\delta = 8.07$ ppm.¹⁴

4.2. Concentration dependent ^1H NMR spectra of 7-azaindole:

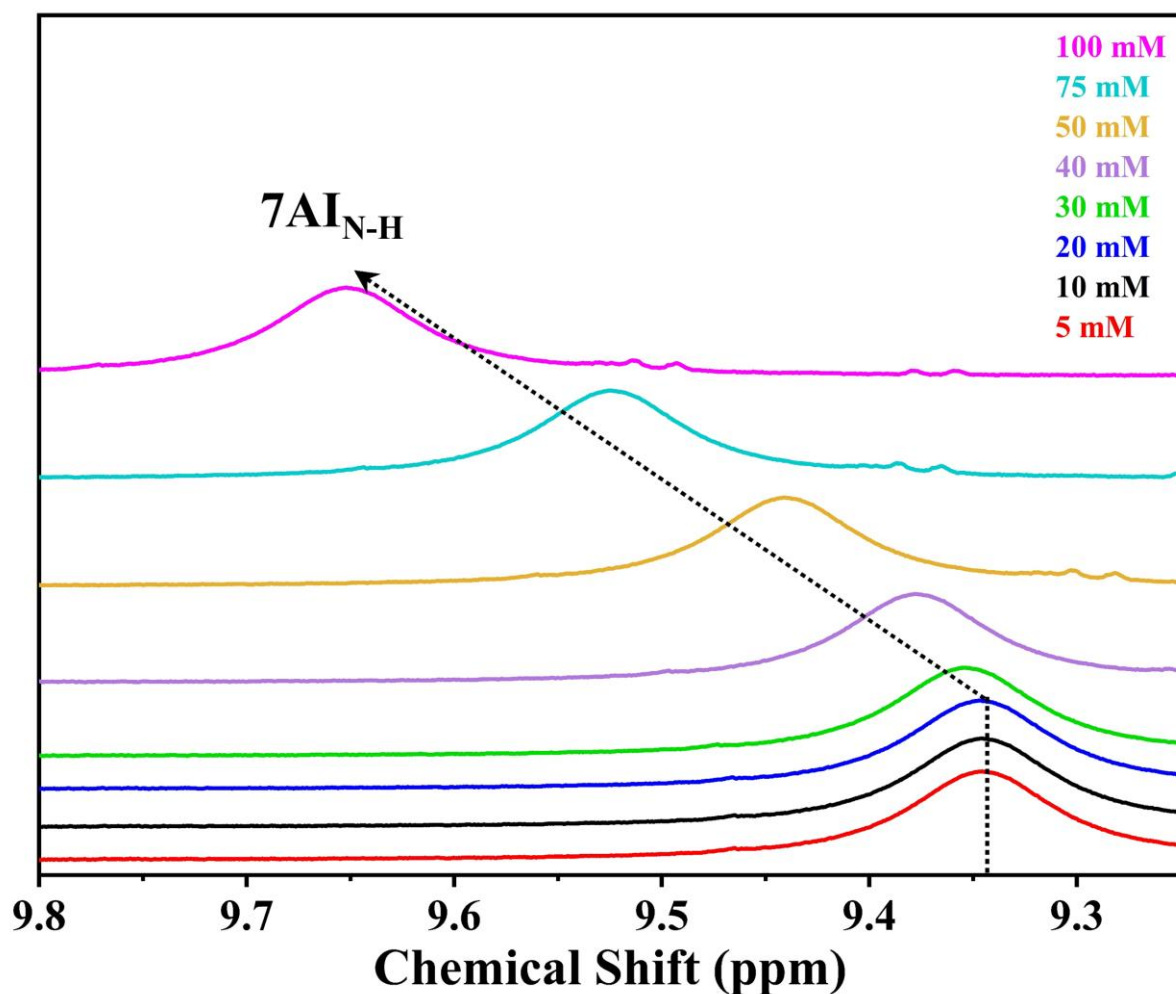


Figure S16. Concentration dependent ^1H NMR spectra of 7-azaindole measured in CDCl_3 solution, displaying the changes in the chemical shift of the N-H proton. The reported ^1H NMR spectra of 7-azaindole on a 400MHz JEOL NMR spectrometer in CCl_4 , shows N-H chemical shift at $\delta = 9.56$ ppm.¹⁵

4.3. Concentration dependent ^1H NMR spectra of phenol:

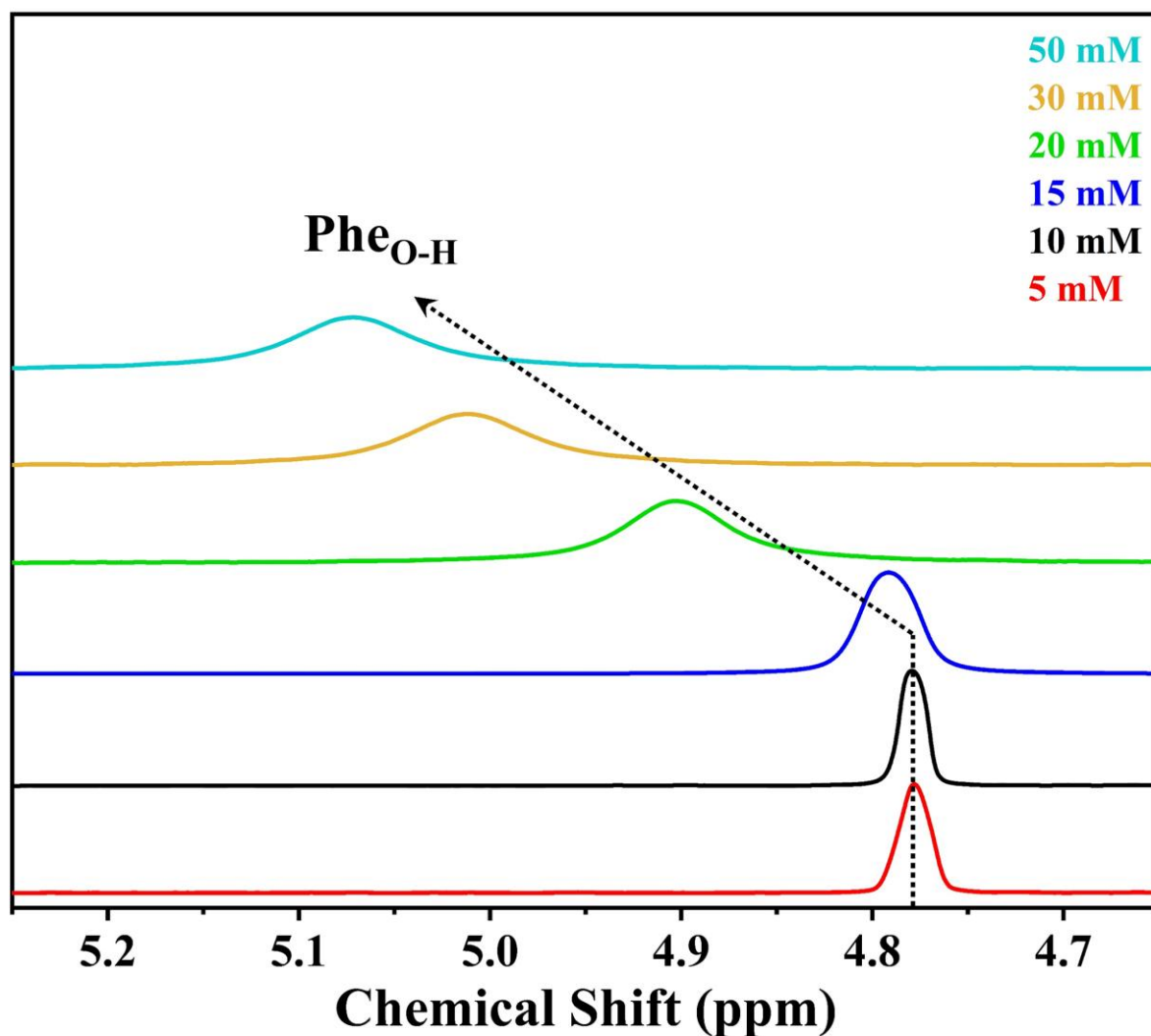


Figure S17. Concentration dependent ^1H NMR spectra of phenol measured in CDCl_3 solution, displaying the changes in the chemical shift of the O–H proton. The reported ^1H NMR spectra of phenol on a 400 MHz Bruker Avance spectrometer in CDCl_3 , shows O–H chemical shift at $\delta = 4.60$ ppm.¹⁶

4.4. ^1H NMR spectra of the complexes of indole:

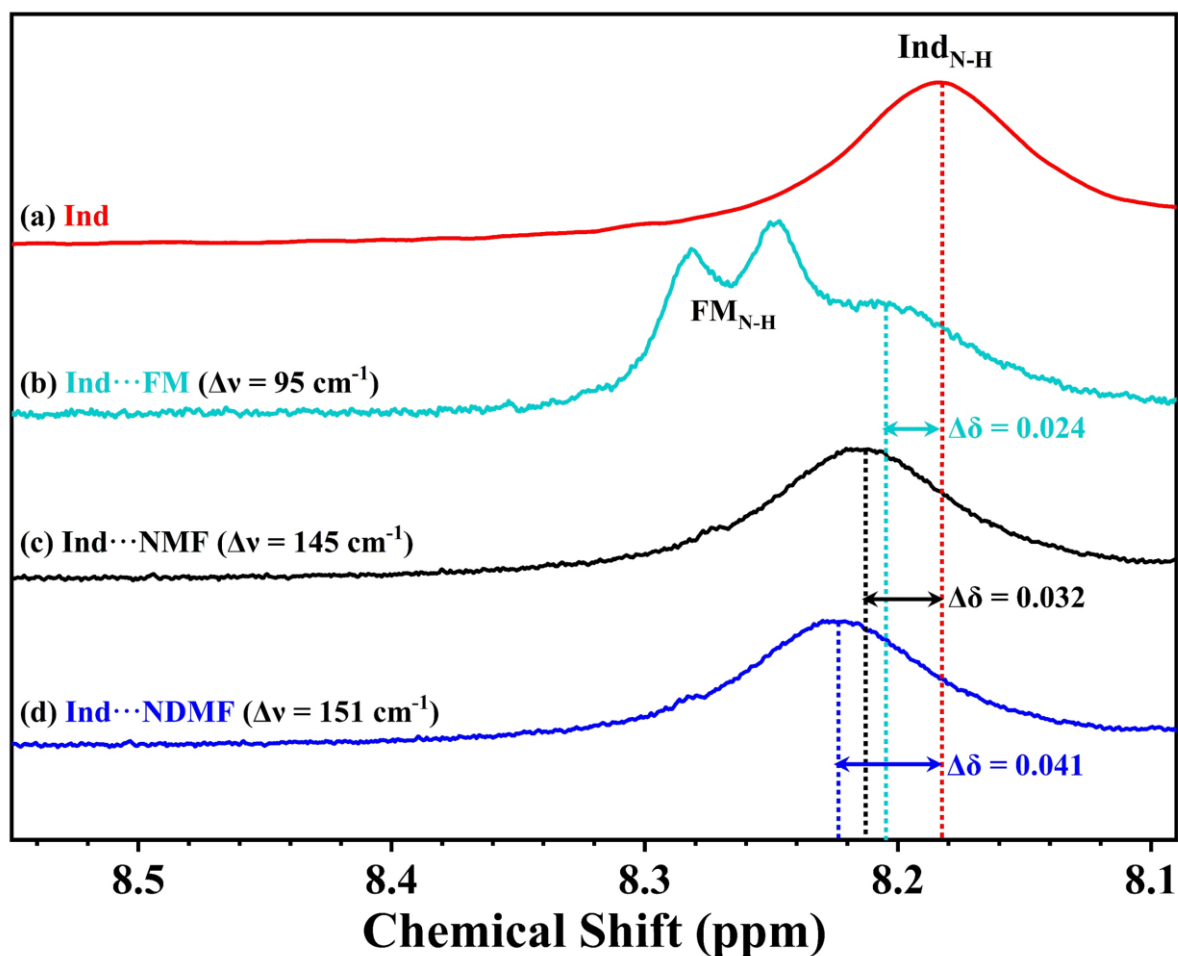


Figure S18. ^1H NMR spectra of (a) indole (Ind) monomer, (b) Ind \cdots FM (3), (c) Ind \cdots NMF (4), and (d) Ind \cdots NDMF (3) in CDCl_3 . The spectra are displayed only in the N-H chemical shift (δ) region. Changes in the N-H chemical shift ($\Delta\delta$) of the complexes with respect to that of the indole monomer are shown in the figure through a horizontal double-headed arrow. IR red-shift values ($\Delta\nu$) in the N-H stretching frequencies of the complexes are provided in parentheses alongside their names.

4.5. ^1H NMR spectra of the complexes of indole (continued):

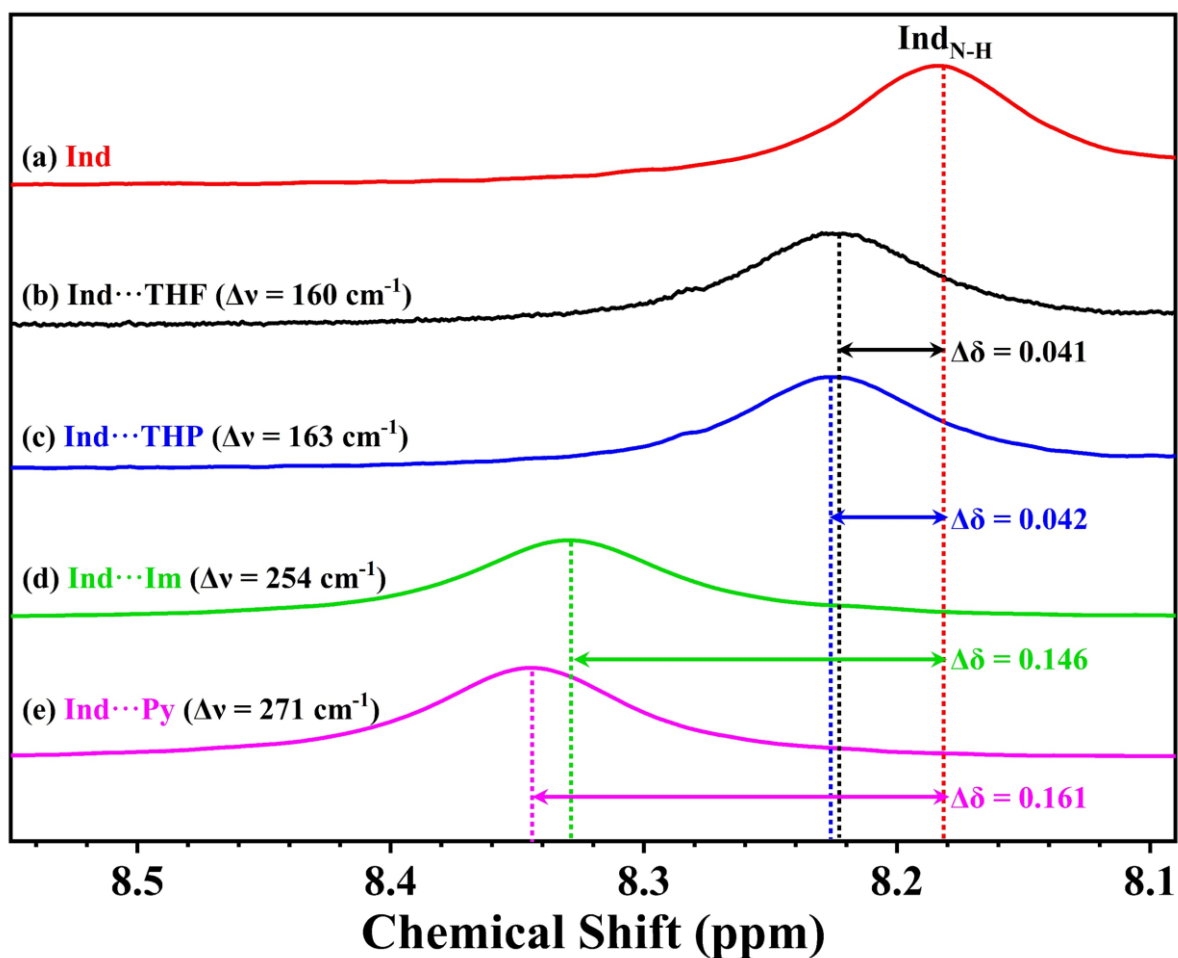


Figure S19. ^1H NMR spectra of (a) indole (Ind) monomer and (b) Ind...THF (12), (c) Ind...THP (13), (d) Ind...Im (16), and (e) Ind...Py (17) in CDCl_3 . The spectra are displayed only in the N-H chemical shift (δ) region. Changes in the N-H chemical shift ($\Delta\delta$) of the complexes with respect to that of the indole monomer are shown in the figure through a horizontal double-headed arrow. IR red-shift values ($\Delta\nu$) in the N-H stretching frequencies of the complexes are provided in parentheses alongside their names.

4.6. ^1H NMR spectra of the complexes of 7-azaindole (7AI):

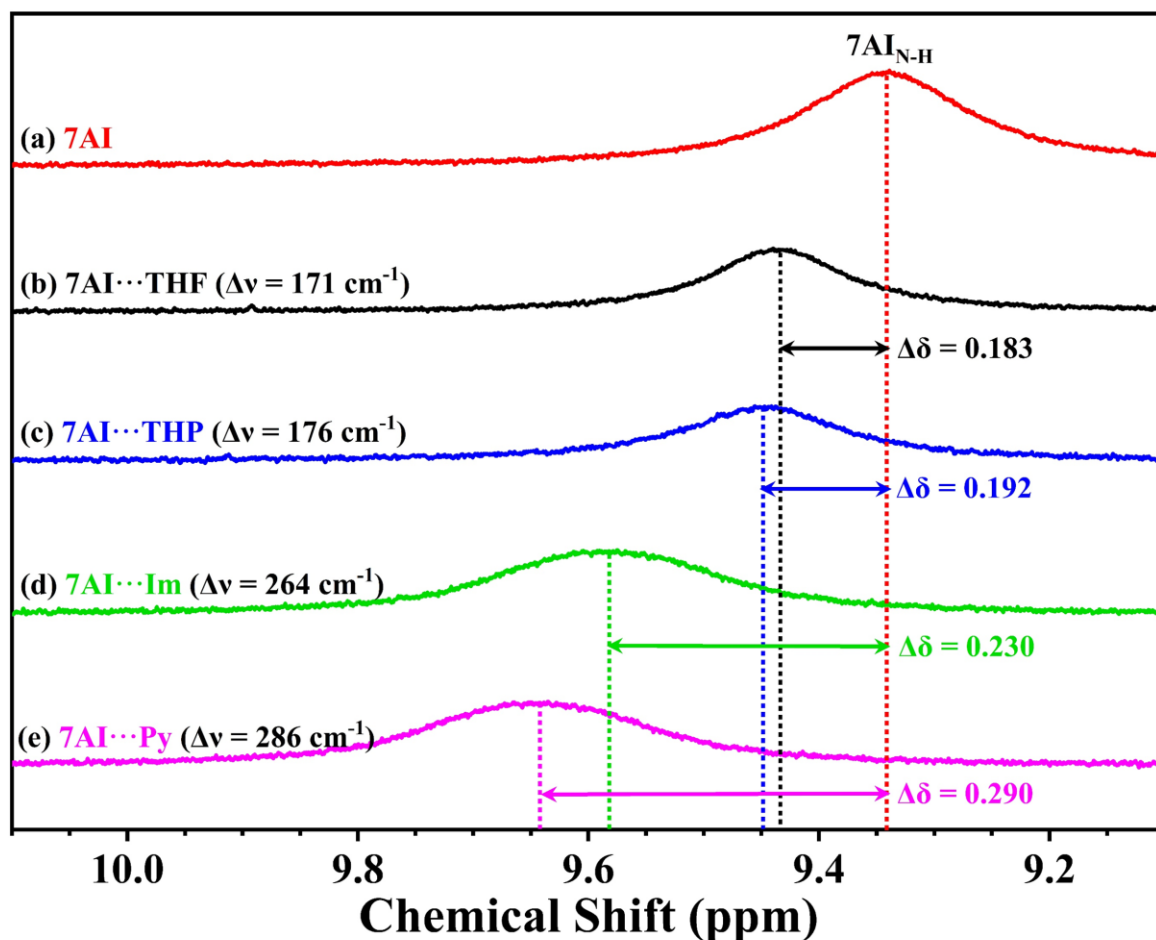


Figure S20. ^1H NMR spectra of (a) 7-azaindole (7AI) monomer, (b) 7AI \cdots THF (14), (c) 7AI \cdots THP (15), (d) 7AI \cdots Im (18), and (e) 7AI \cdots Py (19) in CDCl_3 . The spectra are displayed only in the N-H chemical shift (δ) region. Changes in the N-H chemical shift ($\Delta\delta$) of the complexes with respect to that of the indole monomer are shown in the figure through a horizontal double-headed arrow. IR red-shift values ($\Delta\nu$) in the N-H stretching frequencies of the complexes are provided in parentheses alongside their names.

4.7. ^1H NMR spectra of the complexes of substituted indole:

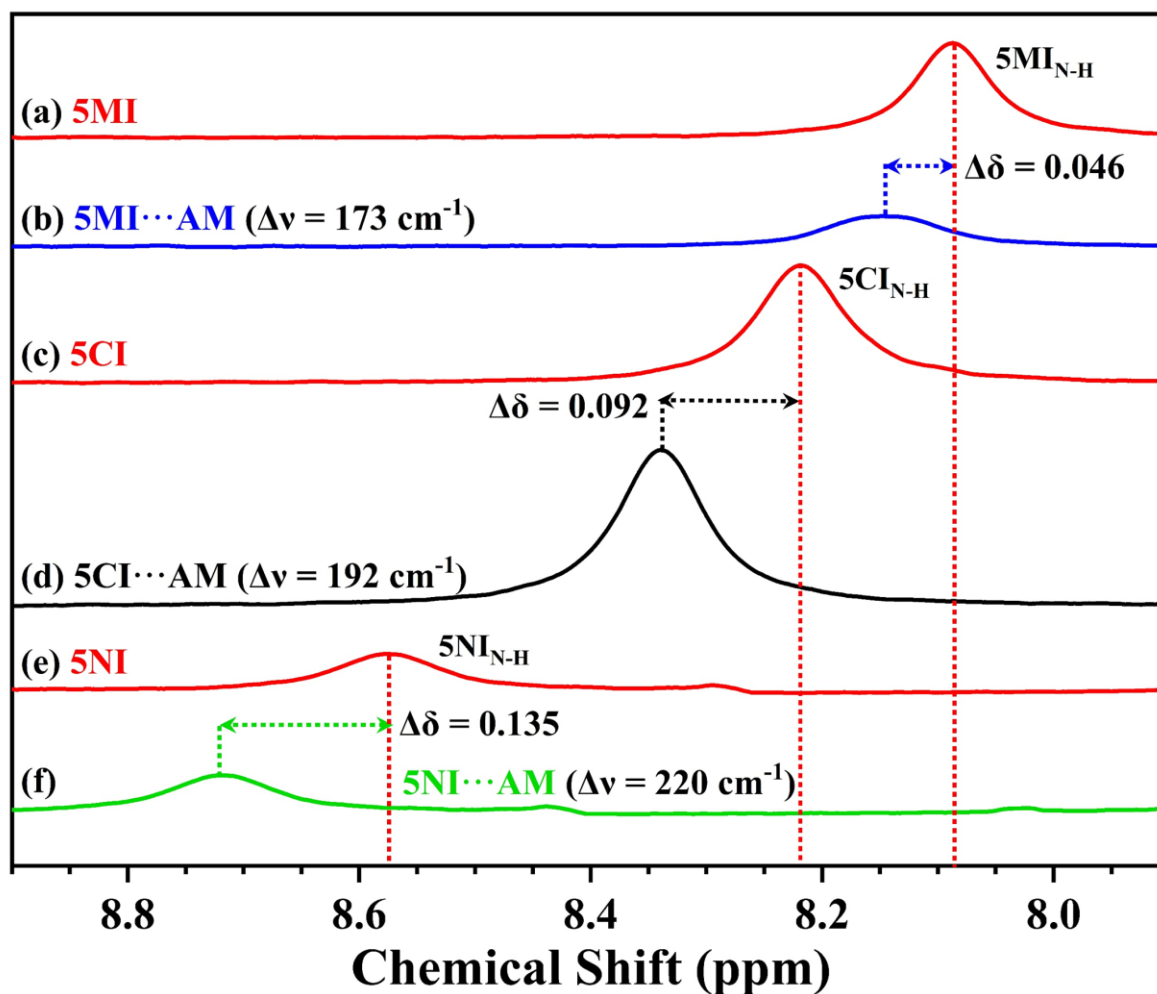


Figure S21. ^1H NMR spectra of (a) 5-methylindole (5MI), (b) 5MI...AM (9), (c) 5-chloroindole (5CI), (d) 5CI...AM (10), (e) 5-nitroindole (5NI), and (f) 5NI...AM (11) in CDCl_3 . The spectra are displayed only in the N-H chemical shift (δ) region. Changes in the N-H chemical shift ($\Delta\delta$) of the complexes with respect to that of the indole monomer are shown in the figure through a horizontal double-headed arrow. IR red-shift values ($\Delta\nu$) in the N-H stretching frequencies of the complexes are provided in parentheses alongside their names.

4.8. ^1H NMR spectra of the complexes of phenol (Phe):

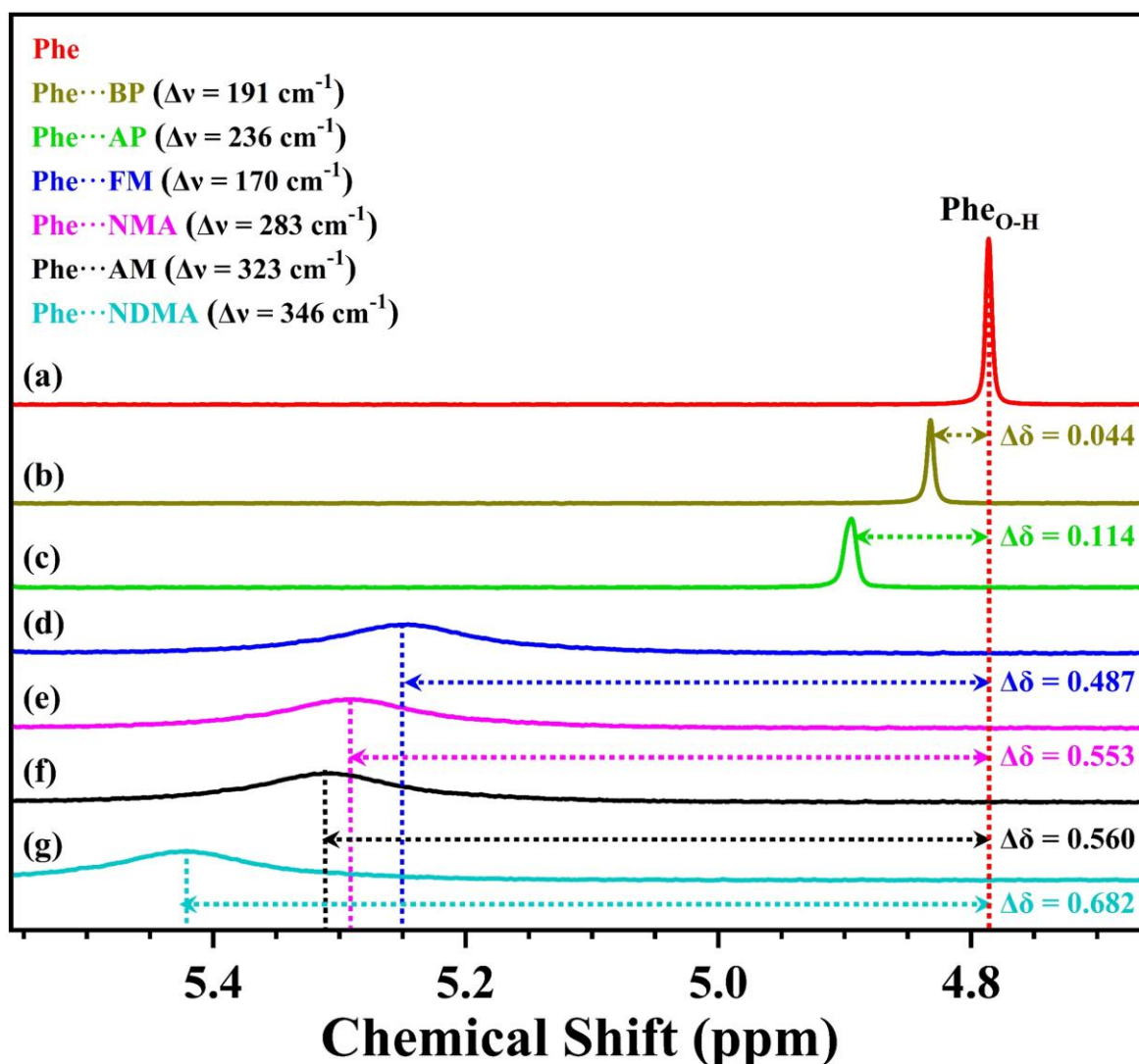


Figure S22. ^1H NMR spectra of (a) phenol (Phe) monomer (Phe) and (b) Phe...BP (20), (c) Phe...AP (21), (d) Phe...FM (22), (e) Phe...NMA (24), (f) Phe...AM (23), and (g) Phe...NDMA (25) in CDCl_3 . The spectra are displayed only in the N-H chemical shift (δ) region. Changes in the N-H chemical shift ($\Delta\delta$) of the complexes with respect to that of the indole monomer are shown in the figure through a horizontal double-headed arrow. IR red-shift values ($\Delta\nu$) in the N-H stretching frequencies of the complexes are provided in parentheses alongside their names.

4.9. ^1H NMR spectra of the complexes of phenol (continued):

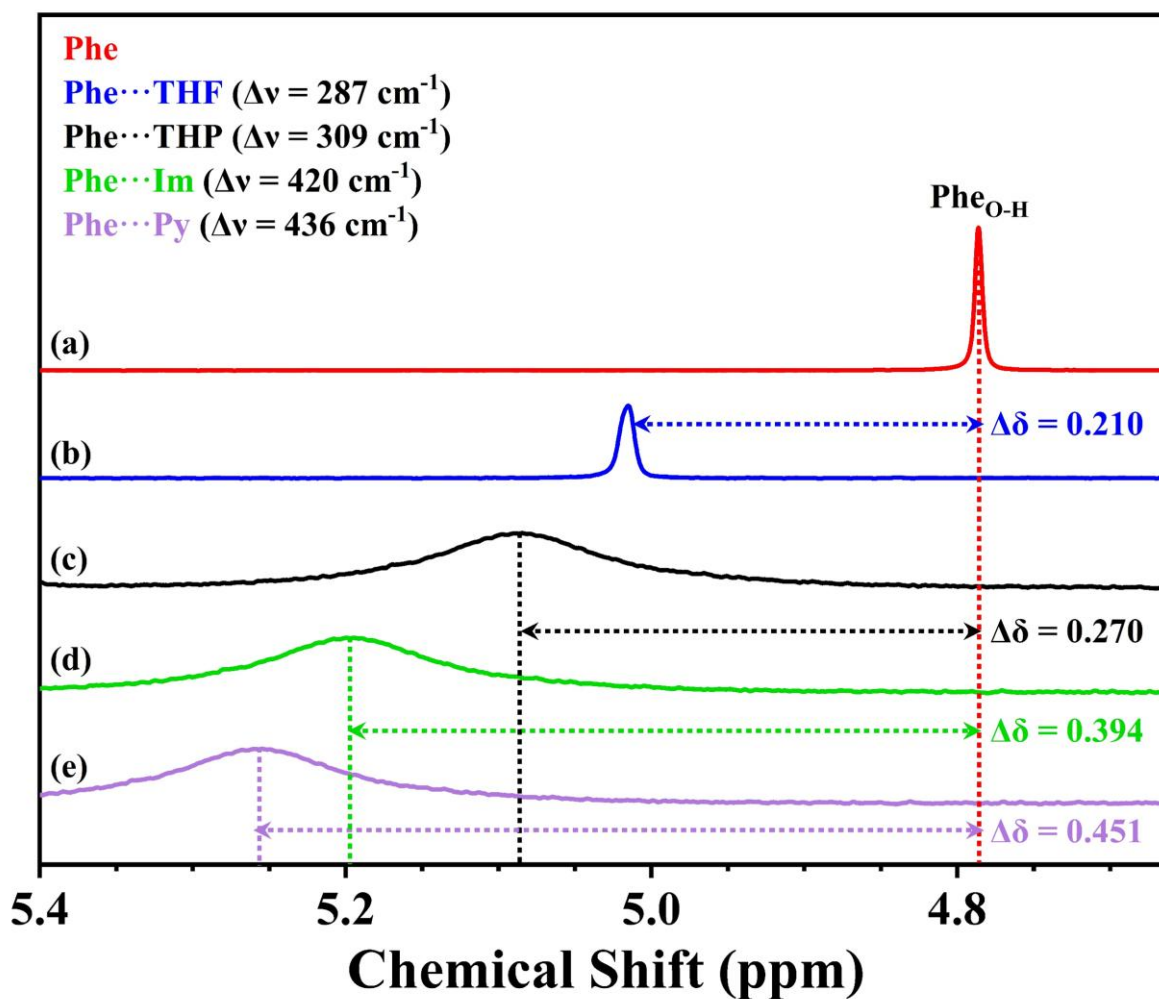


Figure S23. ^1H NMR spectra of (a) phenol monomer (Phe), (b) Phe···THF (26), (c) Phe···THP (27), (d) Phe···Im (28), and (e) Phe···Py (29) in CDCl_3 . The spectra are displayed only in the N-H chemical shift (δ) region. Changes in the N-H chemical shift ($\Delta\delta$) of the complexes with respect to that of the indole monomer are shown in the figure through a horizontal double-headed arrow. IR red-shift values ($\Delta\nu$) in the N-H stretching frequencies of the complexes are provided in parentheses alongside their names.

4.10. Variable-temperature (VT) ^1H NMR spectra of the $\text{Ind}_{\text{N-H}}$ and $\text{AM}_{\text{N-H}}$ protons of $\text{Ind}\cdots\text{AM}$ complex:

Variable-temperature (VT) ^1H NMR spectra were recorded in the temperature range of 278–318 K for the $\text{Ind}\cdots\text{AM}$ complex in CDCl_3 . The chemical shifts of both the $\text{Ind}_{\text{N-H}}$ and $\text{AM}_{\text{N-H}}$ protons were monitored throughout the experiment. At lower temperatures, both N-H resonances exhibit downfield shifts relative to their respective positions in the monomer. As the temperature increases, the peaks gradually shift toward their individual monomer positions. This behavior indicates the presence of an intermolecular hydrogen bond between the indole N-H and the acetamide C=O group, which dissociates at higher temperatures. Similarly, acetamide forms a self-associated dimer via $\text{N-H}\cdots\text{O=C}$ hydrogen bonding, which is also disrupted upon heating.

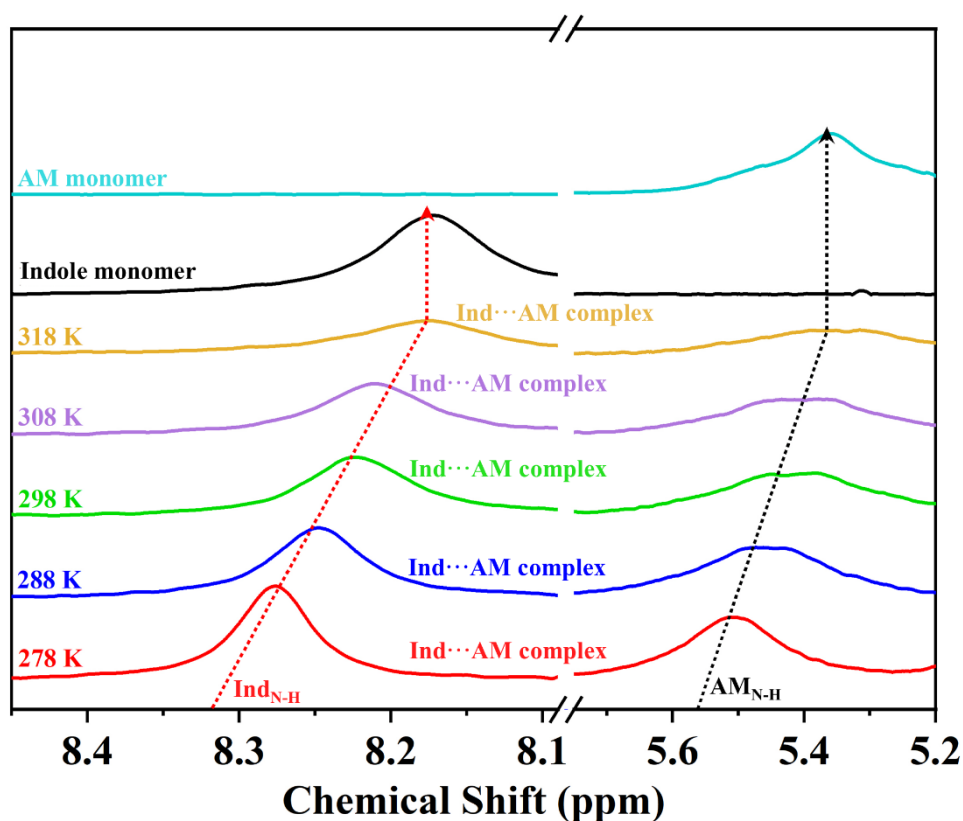


Figure S24. Variable-temperature (VT) ^1H NMR spectra of the $\text{Ind}\cdots\text{AM}$ complex, showing the chemical shifts of the $\text{Ind}_{\text{N-H}}$ and $\text{AM}_{\text{N-H}}$ protons, measured over 278–318 K in CDCl_3 . ^1H NMR spectra of the indole (Ind) and acetamide (AM) monomers are shown at the top for comparison.

4.10. ^1H NMR spectra of indole and Ind \cdots AM complex with increasing acetamide concentration

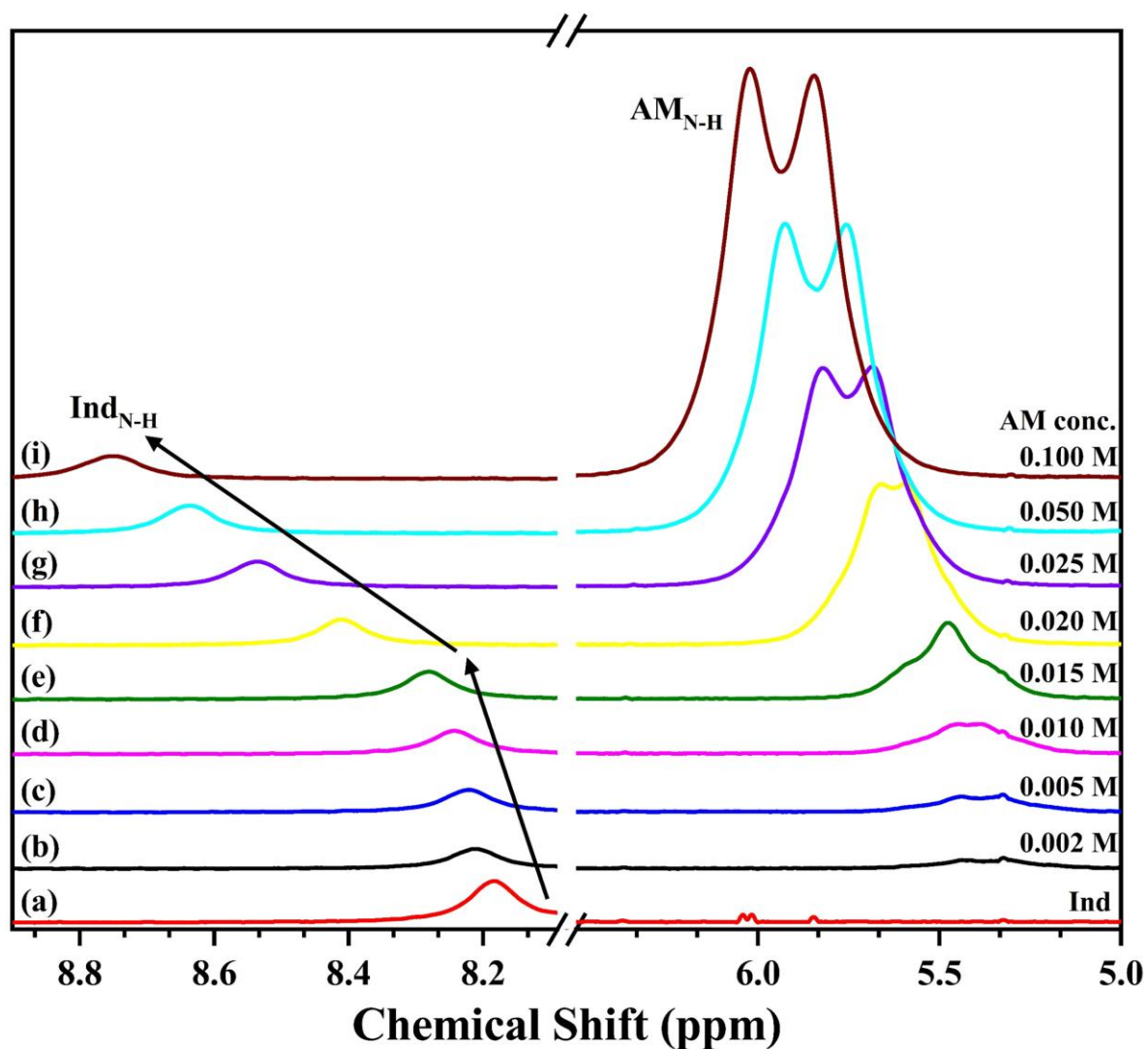


Figure S25. ^1H NMR spectra of (a) indole (Ind) and (b–i) Ind \cdots AM complex recorded at increasing acetamide (AM) concentrations ranging from 0.002 to 0.100 M. Variation in the chemical shift of both $\text{Ind}_{\text{N-H}}$ and $\text{AM}_{\text{N-H}}$ is observed.

5. Study of H/D exchange kinetics of the complexes following addition of D₂O using ¹H NMR spectroscopy:

5.1. Kinetics of H/D exchange in Ind···AM complex monitoring the Ind N–H and AM N–H NMR signals

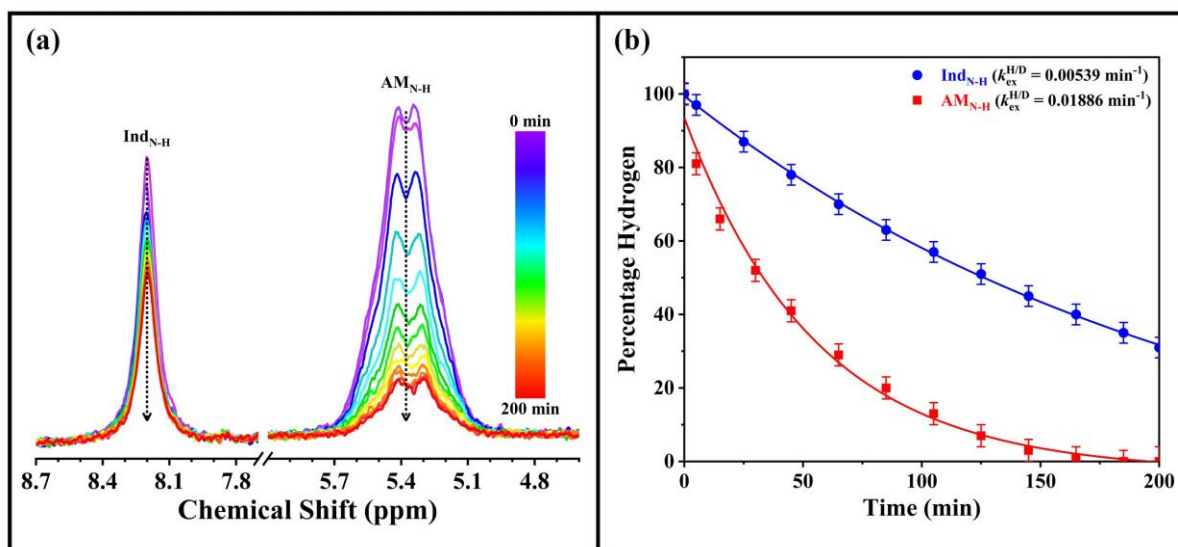


Figure S26. (a) ¹H NMR spectra of the Ind···AM complex in CDCl₃ measured as a function of time following the addition of D₂O, monitoring both the Ind N–H ($\delta \approx 8.2$ ppm) and AM N–H ($\delta \approx 5.4$ ppm) resonances. Both Ind and AM concentrations are kept fixed at 20 mM. (b) kinetic plots of the integrated intensities of the Ind N–H and AM N–H protons in Ind···AM complex in CDCl₃ after addition of D₂O. Standard error in the percentage hydrogen measurement at each time interval of the kinetics of every complex is provided with the plot, while the detailed procedure for the uncertainty calculation is given on page S9 in the supporting information.

5.2. H/D exchange kinetics of Ind \cdots AM complex at different AM concentrations:

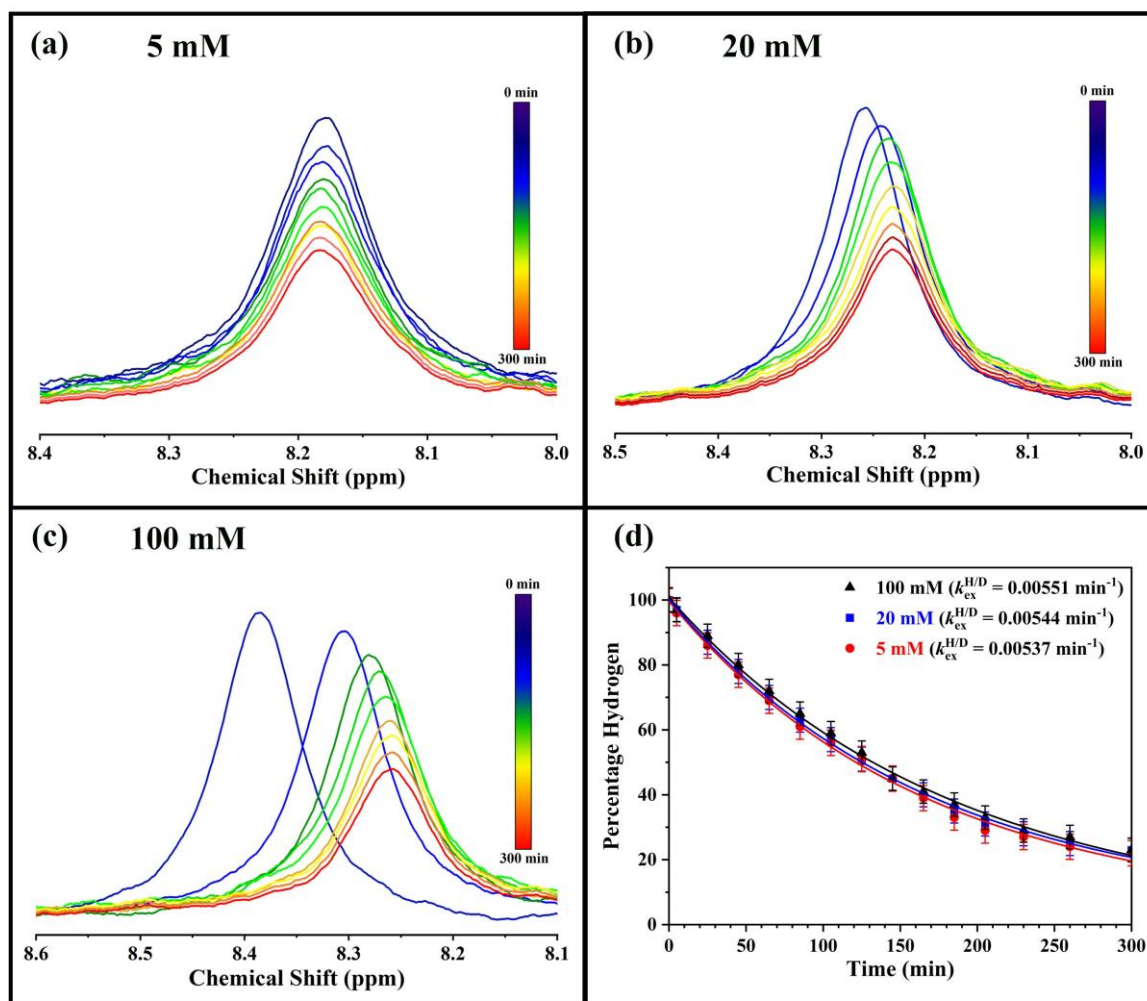


Figure S27. ^1H NMR spectra of the Ind \cdots AM complex measured as a function of time following the addition of D_2O , monitoring the Ind N–H signal at AM concentrations of (a) 5 mM, (b) 20 mM, and (c) 100 mM in CDCl_3 . (d) kinetic plots of the integrated intensities of the Ind N–H proton in Ind \cdots AM complex in CDCl_3 after addition of D_2O with AM concentrations of 5 mM, 20 mM, and 100 mM. Standard error in the percentage hydrogen measurement at each time interval of the kinetics of every complex is provided with the plot, while the detailed procedure for the uncertainty calculation is given on page S9 in the supporting information.

5.3. Determination of the average H/D exchange rate constant ($k_{\text{ex}}^{\text{avg}}$) from repeat kinetics measurements. For each complex, individual rate constants (k_1 , k_2 , k_3) are reported with their respective least-squares fitting errors, while $k_{\text{ex}}^{\text{avg}}$ is presented with its standard error. Details of these calculations are provided on pages S9-S10 in the supporting information.

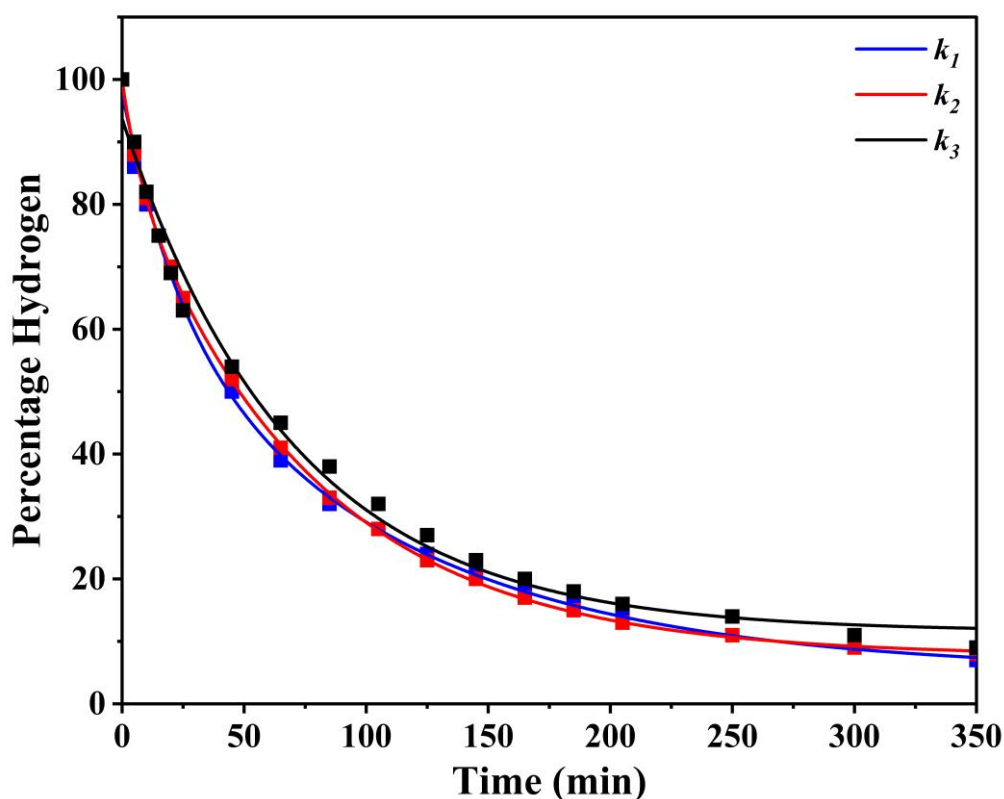


Figure S28. The H/D exchange rate constants (k_1 , k_2 , k_3) for the Ind \cdots BP complex (1) obtained from three independent experiments are compared, and the $k_{\text{ex}}^{\text{avg}}$ value was calculated as the average of the three measurements. The uncertainty reported for this complex was determined from the standard deviation of the repeated measurements.

$$k_1 = 0.01092 \pm 0.00065 \text{ min}^{-1}$$

$$k_2 = 0.01105 \pm 0.00059 \text{ min}^{-1}$$

$$k_3 = 0.00986 \pm 0.00059 \text{ min}^{-1}$$

$$k_{\text{ex}}^{\text{avg}} = 0.01061 \pm 0.00036 \text{ min}^{-1}$$

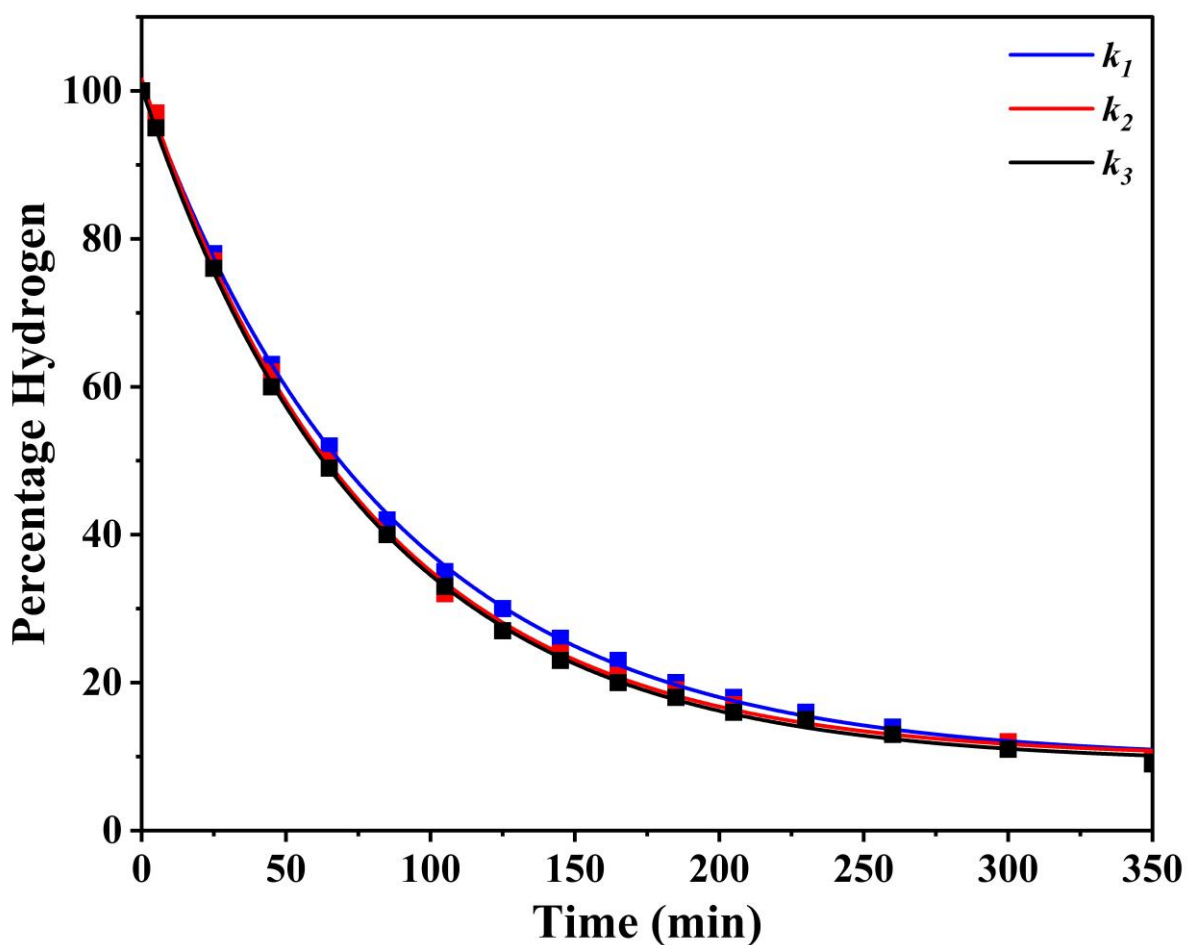


Figure S29. The H/D exchange rate constants (k_1 , k_2 , k_3) for the Ind \cdots AP complex (2) obtained from three independent experiments are compared, and the $k_{\text{ex}}^{\text{avg}}$ value was calculated as the average of the three measurements. The uncertainty reported for this complex was determined from the standard deviation of the repeated measurements.

$$k_1 = 0.00914 \pm 0.00039 \text{ min}^{-1}$$

$$k_2 = 0.00905 \pm 0.00042 \text{ min}^{-1}$$

$$k_3 = 0.00892 \pm 0.00034 \text{ min}^{-1}$$

$$k_{\text{ex}}^{\text{avg}} = 0.00903 \pm 0.00023 \text{ min}^{-1}$$

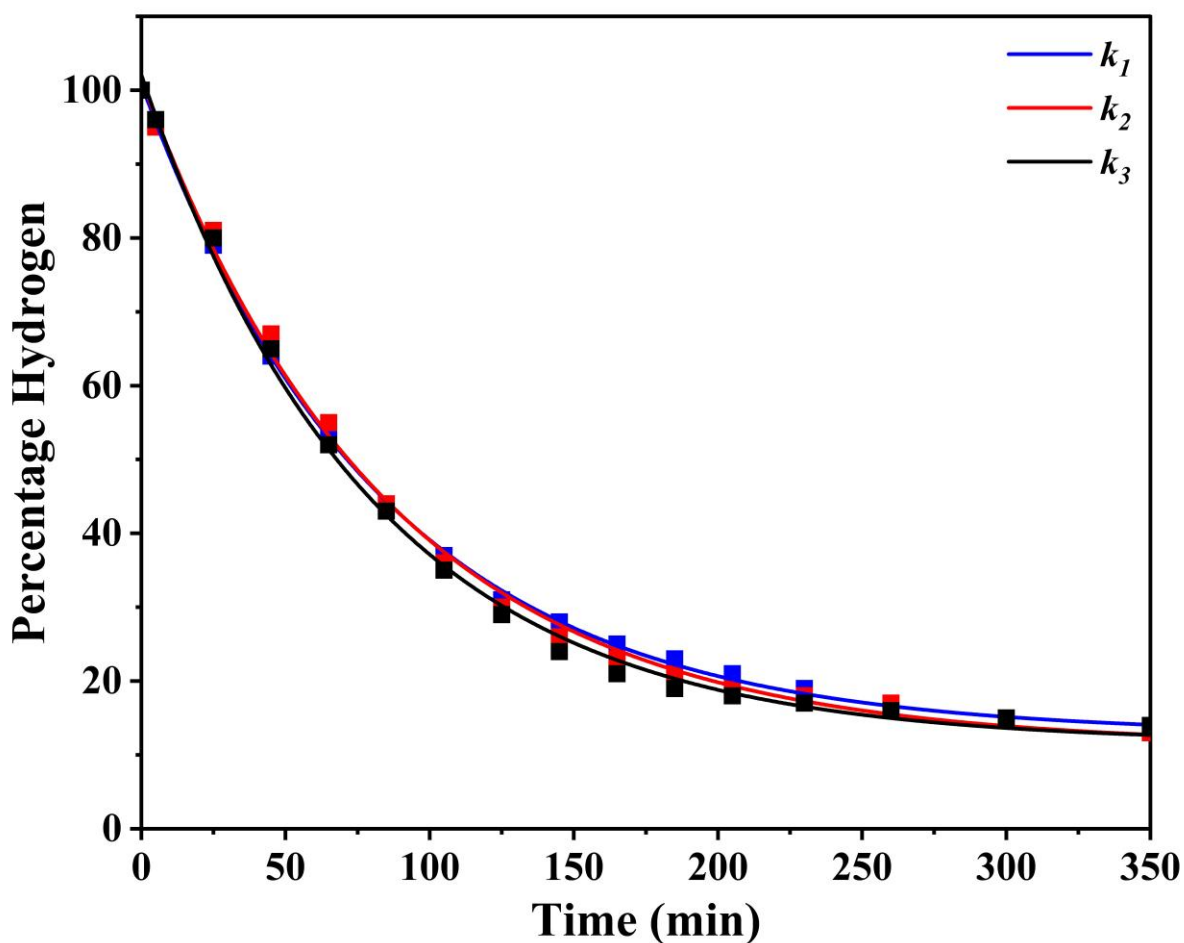


Figure S30. The H/D exchange rate constants (k_1 , k_2 , k_3) for Ind \cdots FM complex (3) obtained from three independent experiments are compared, and the $k_{\text{ex}}^{\text{avg}}$ value was calculated as the average of the three measurements. The uncertainty reported for this complex was determined from the standard deviation of the repeated measurements.

$$k_1 = 0.00846 \pm 0.00040 \text{ min}^{-1}$$

$$k_2 = 0.00839 \pm 0.00040 \text{ min}^{-1}$$

$$k_3 = 0.00817 \pm 0.00047 \text{ min}^{-1}$$

$$k_{\text{ex}}^{\text{avg}} = 0.00834 \pm 0.00025 \text{ min}^{-1}$$

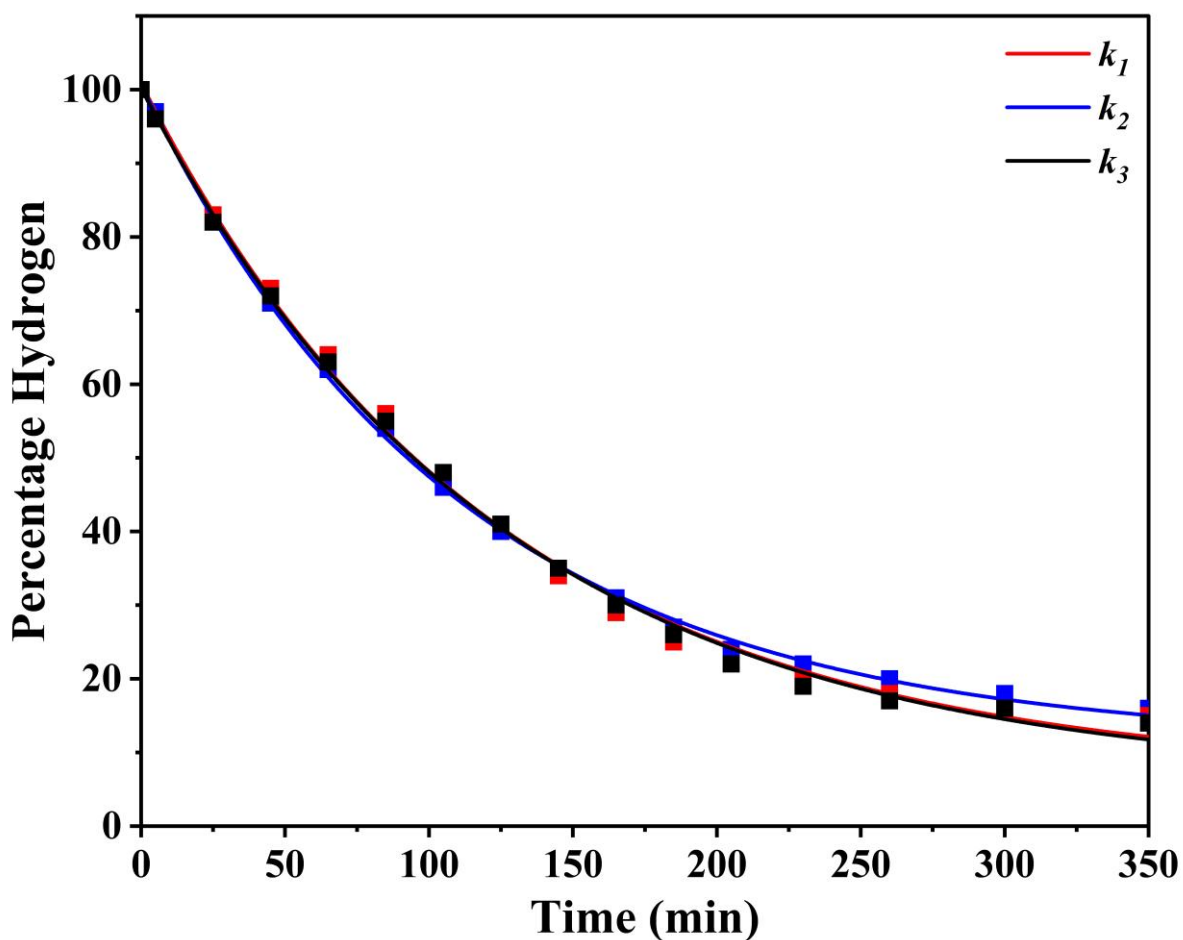


Figure S31. The H/D exchange rate constants (k_1 , k_2 , k_3) for Ind···NMF complex (4) obtained from three independent experiments are compared, and the $k_{\text{ex}}^{\text{avg}}$ value was calculated as the average of the three measurements. The uncertainty reported for this complex was determined from the standard deviation of the repeated measurements.

$$k_1 = 0.00675 \pm 0.00022 \text{ min}^{-1}$$

$$k_2 = 0.00696 \pm 0.00018 \text{ min}^{-1}$$

$$k_3 = 0.00696 \pm 0.00015 \text{ min}^{-1}$$

$$k_{\text{ex}}^{\text{avg}} = 0.00689 \pm 0.00017 \text{ min}^{-1}$$

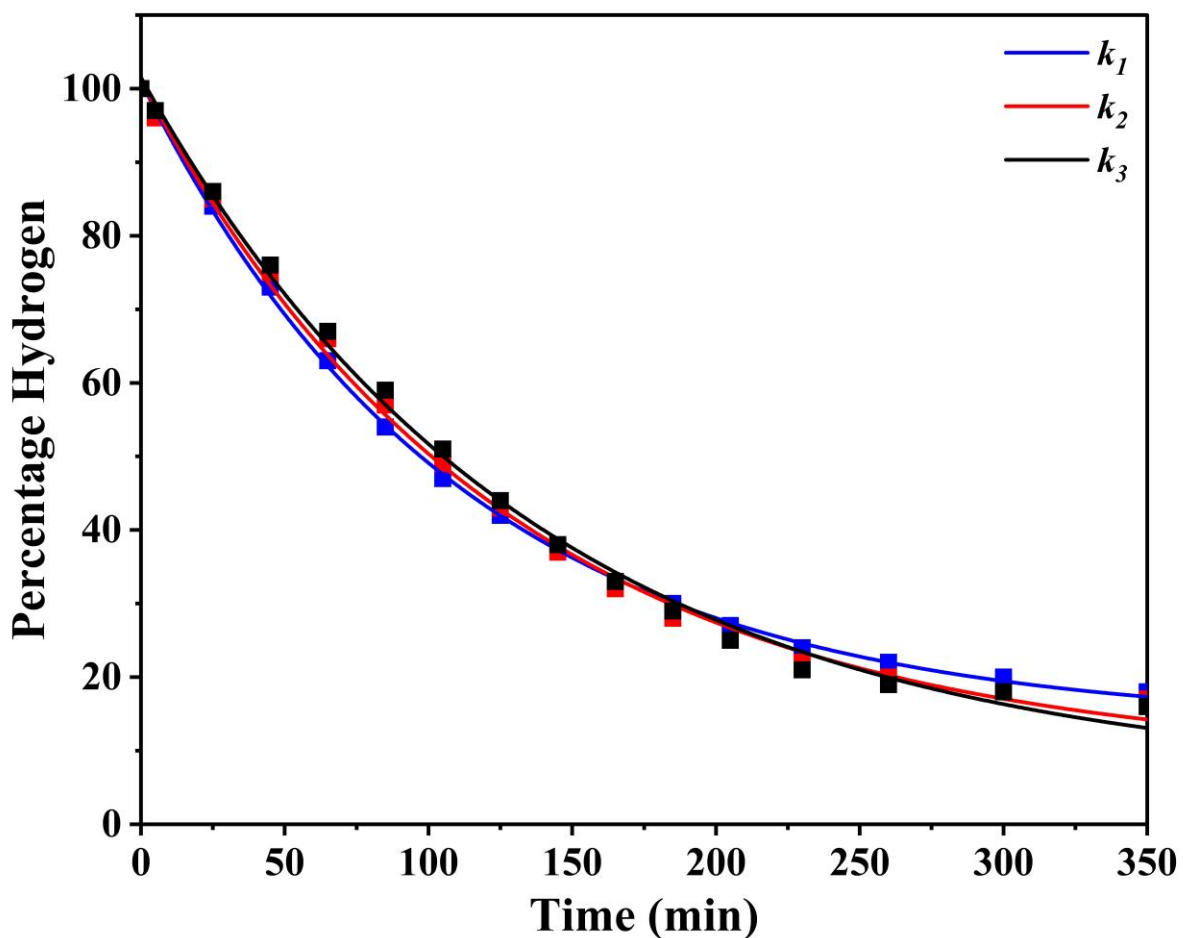


Figure S32. The H/D exchange rate constants (k_1 , k_2 , k_3) for Ind...NDMF complex (5) obtained from three independent experiments are compared, and the $k_{\text{ex}}^{\text{avg}}$ value was calculated as the average of the three measurements. The uncertainty reported for this complex was determined from the standard deviation of the repeated measurements.

$$k_1 = 0.00648 \pm 0.00017 \text{ min}^{-1}$$

$$k_2 = 0.00633 \pm 0.00023 \text{ min}^{-1}$$

$$k_3 = 0.00645 \pm 0.00014 \text{ min}^{-1}$$

$$k_{\text{ex}}^{\text{avg}} = 0.00642 \pm 0.00011 \text{ min}^{-1}$$

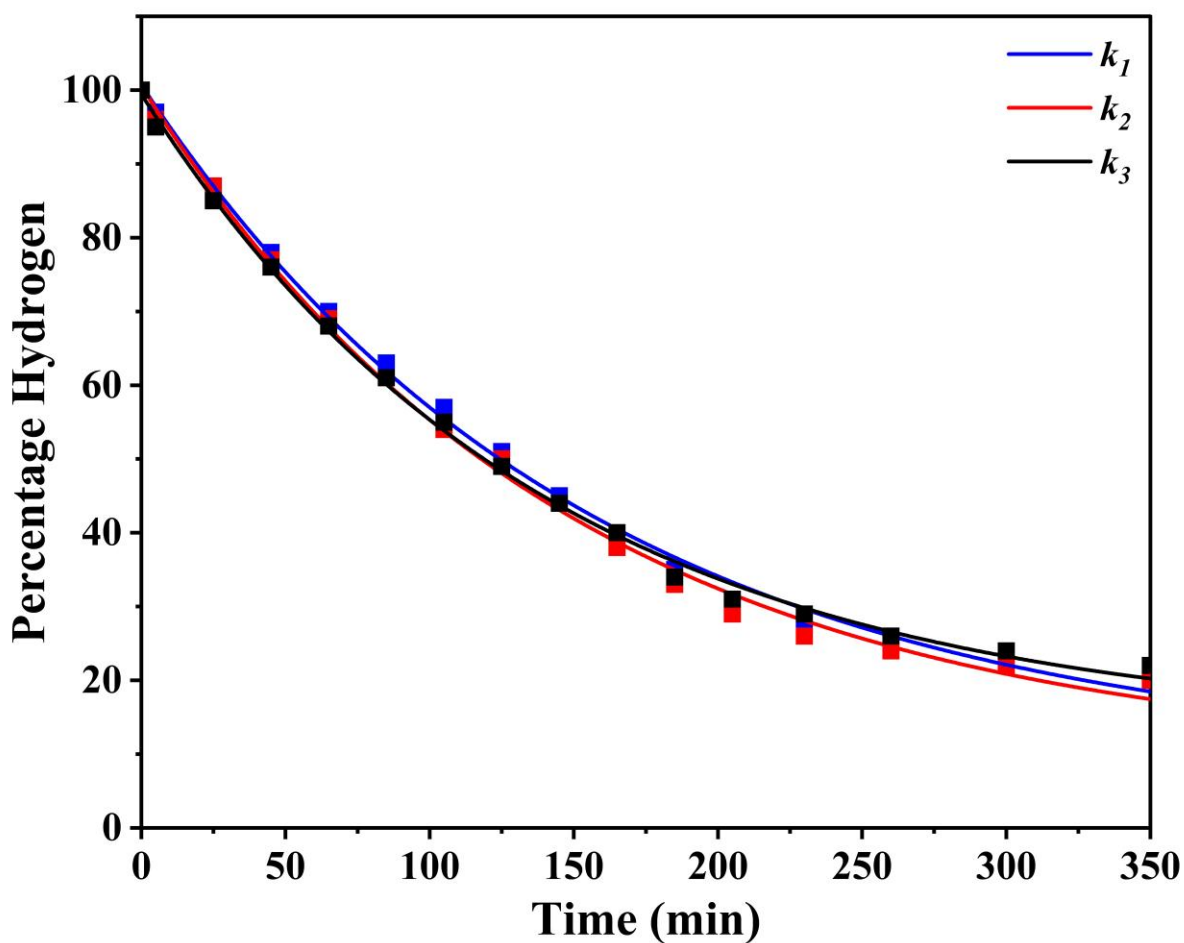


Figure S33. The H/D exchange rate constants (k_1 , k_2 , k_3) for Ind \cdots AM complex (6) obtained from three independent experiments are compared, and the $k_{\text{ex}}^{\text{avg}}$ value was calculated as the average of the three measurements. The uncertainty reported for this complex was determined from the standard deviation of the repeated measurements.

$$k_1 = 0.00558 \pm 0.00014 \text{ min}^{-1}$$

$$k_2 = 0.00527 \pm 0.00015 \text{ min}^{-1}$$

$$k_3 = 0.00533 \pm 0.00012 \text{ min}^{-1}$$

$$k_{\text{ex}}^{\text{avg}} = 0.00539 \pm 0.00016 \text{ min}^{-1}$$

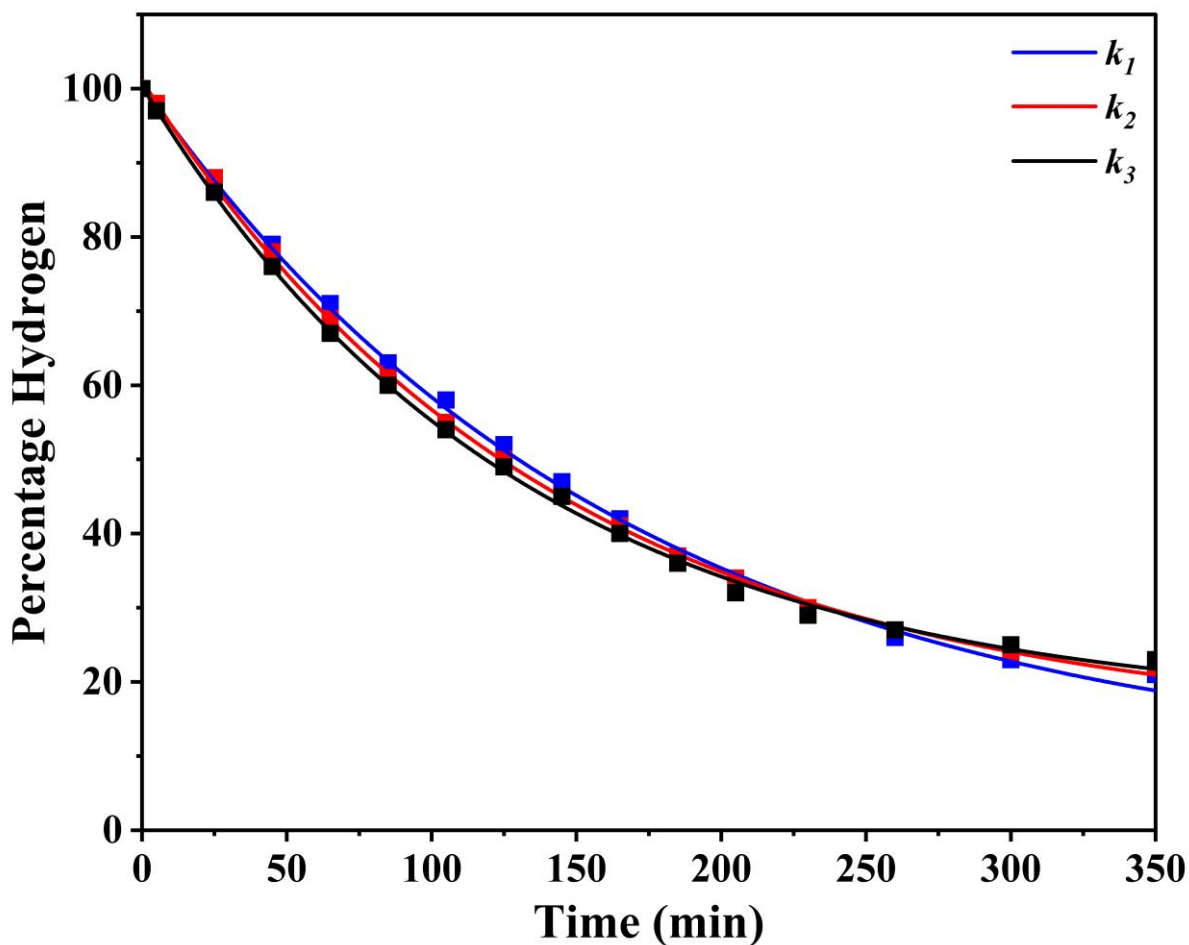


Figure S34. The H/D exchange rate constants (k_1 , k_2 , k_3) for Ind···NMA complex (7) obtained from three independent experiments are compared, and the $k_{\text{ex}}^{\text{avg}}$ value was calculated as the average of the three measurements. The uncertainty reported for this complex was determined from the standard deviation of the repeated measurements.

$$k_1 = 0.00516 \pm 0.00009 \text{ min}^{-1}$$

$$k_2 = 0.00519 \pm 0.00013 \text{ min}^{-1}$$

$$k_3 = 0.00521 \pm 0.00017 \text{ min}^{-1}$$

$$k_{\text{ex}}^{\text{avg}} = 0.00519 \pm 0.00008 \text{ min}^{-1}$$

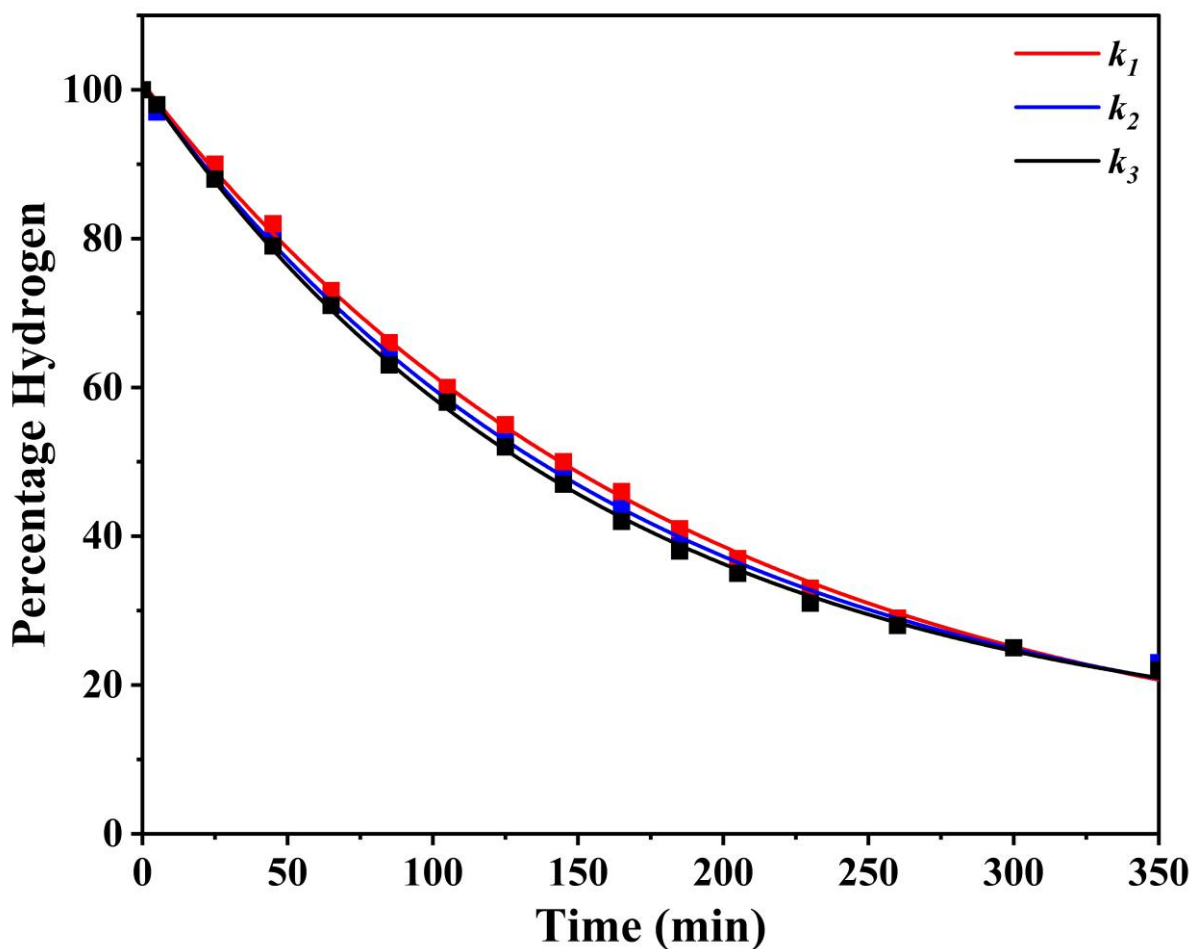


Figure S35. The H/D exchange rate constants (k_1 , k_2 , k_3) for Ind···NDMA complex (8) obtained from three independent experiments are compared, and the $k_{\text{ex}}^{\text{avg}}$ value was calculated as the average of the three measurements. The uncertainty reported for this complex was determined from the standard deviation of the repeated measurements.

$$k_1 = 0.00488 \pm 0.00009 \text{ min}^{-1}$$

$$k_2 = 0.00495 \pm 0.00005 \text{ min}^{-1}$$

$$k_3 = 0.00500 \pm 0.00011 \text{ min}^{-1}$$

$$k_{\text{ex}}^{\text{avg}} = 0.00494 \pm 0.00006 \text{ min}^{-1}$$

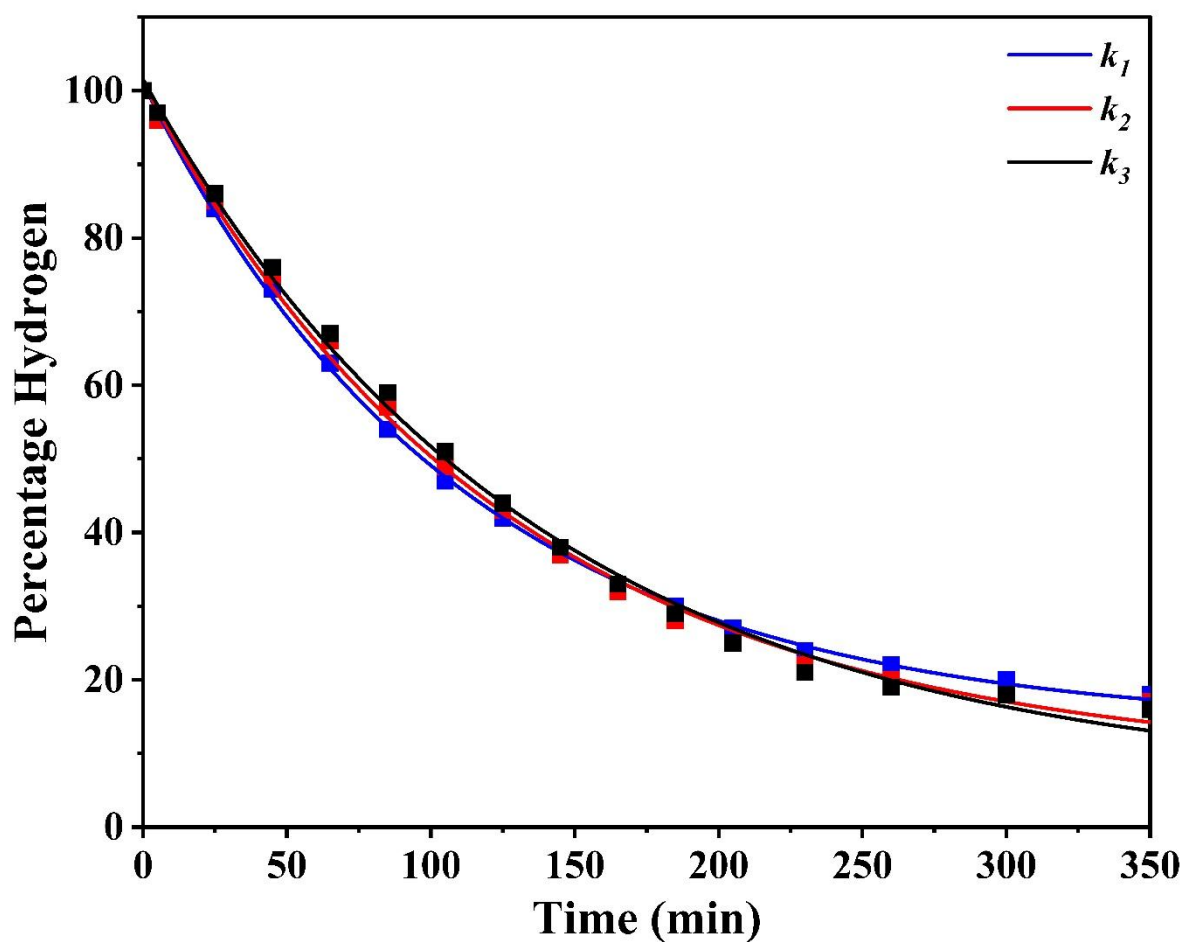


Figure 36. The H/D exchange rate constants (k_1 , k_2 , k_3) for Ind \cdots THF complex (12) obtained from three independent experiments are compared, and the $k_{\text{ex}}^{\text{avg}}$ value was calculated as the average of the three measurements. The uncertainty reported for this complex was determined from the standard deviation of the repeated measurements.

$$k_1 = 0.00607 \pm 0.00009 \text{ min}^{-1}$$

$$k_2 = 0.00624 \pm 0.00008 \text{ min}^{-1}$$

$$k_3 = 0.00627 \pm 0.00031 \text{ min}^{-1}$$

$$k_{\text{ex}}^{\text{avg}} = 0.00619 \pm 0.00011 \text{ min}^{-1}$$

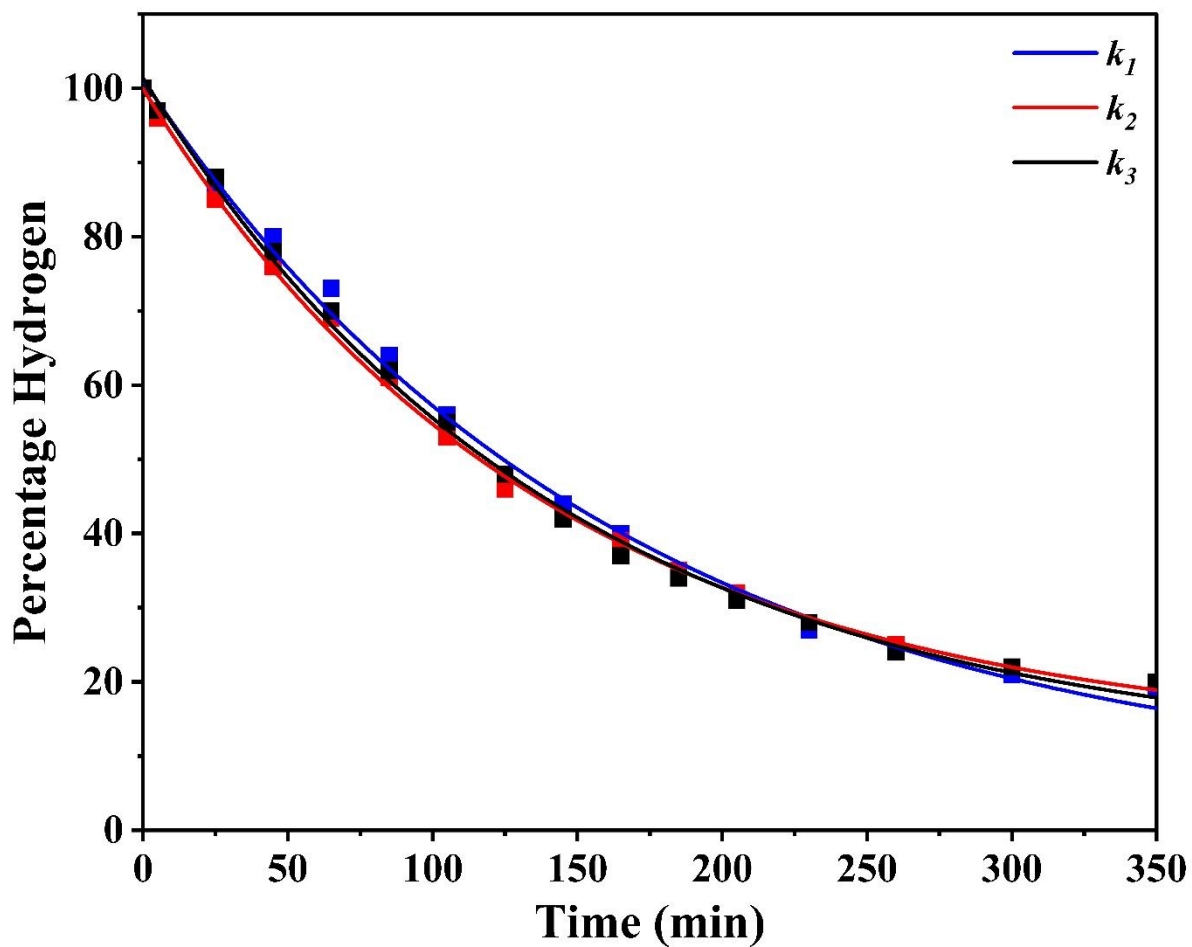


Figure S37. The H/D exchange rate constants (k_1 , k_2 , k_3) for Ind...THP complex (13) obtained from three independent experiments are compared, and the $k_{\text{ex}}^{\text{avg}}$ value was calculated as the average of the three measurements. The uncertainty reported for this complex was determined from the standard deviation of the repeated measurements.

$$k_1 = 0.00591 \pm 0.00021 \text{ min}^{-1}$$

$$k_2 = 0.00618 \pm 0.00032 \text{ min}^{-1}$$

$$k_3 = 0.00609 \pm 0.00026 \text{ min}^{-1}$$

$$k_{\text{ex}}^{\text{avg}} = 0.00606 \pm 0.00015 \text{ min}^{-1}$$

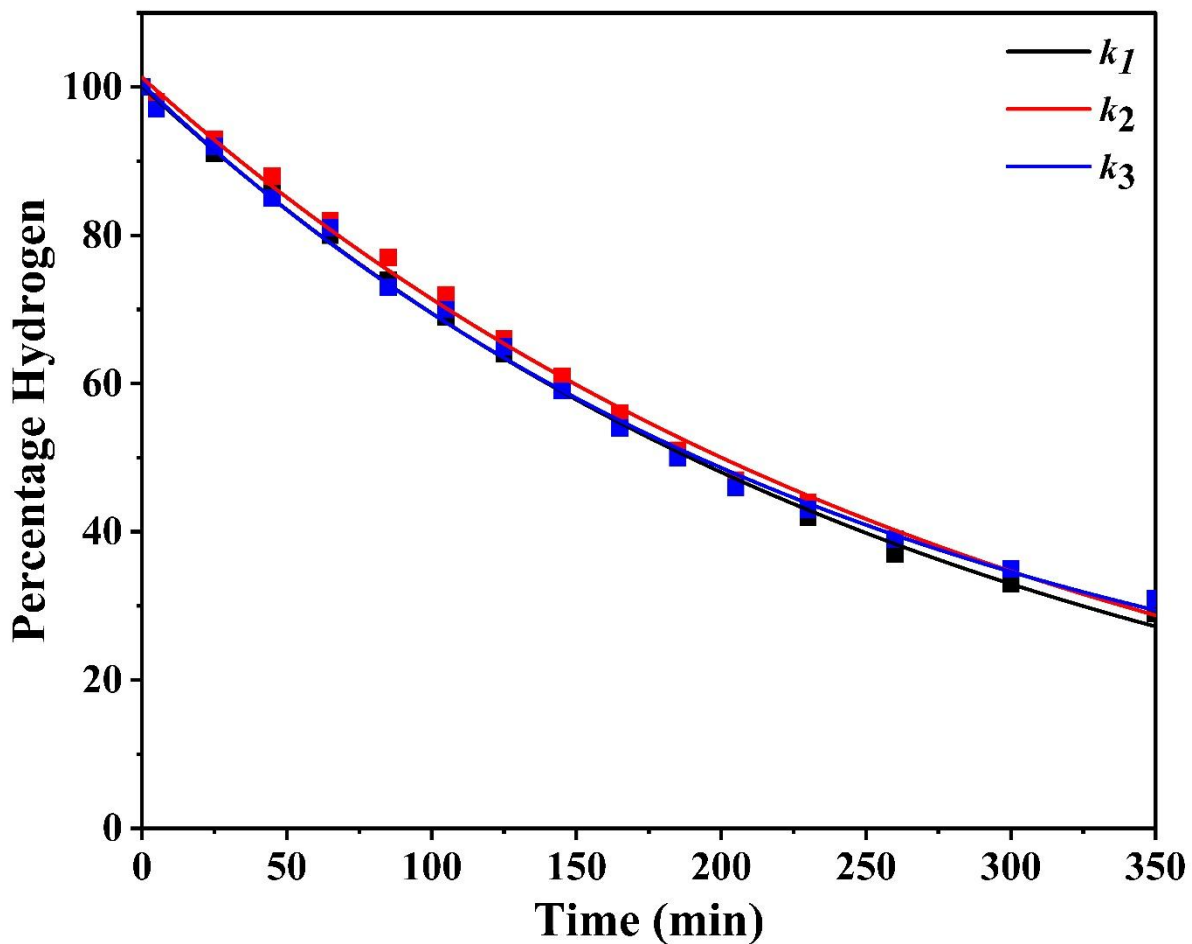


Figure S38. The H/D exchange rate constants (k_1 , k_2 , k_3) for Ind···Im complex (16) obtained from three independent experiments are compared, and the $k_{\text{ex}}^{\text{avg}}$ value was calculated as the average of the three measurements. The uncertainty reported for this complex was determined from the standard deviation of the repeated measurements.

$$k_1 = 0.00390 \pm 0.00022 \text{ min}^{-1}$$

$$k_2 = 0.00395 \pm 0.00027 \text{ min}^{-1}$$

$$k_3 = 0.00378 \pm 0.00018 \text{ min}^{-1}$$

$$k_{\text{ex}}^{\text{avg}} = 0.00388 \pm 0.00013 \text{ min}^{-1}$$

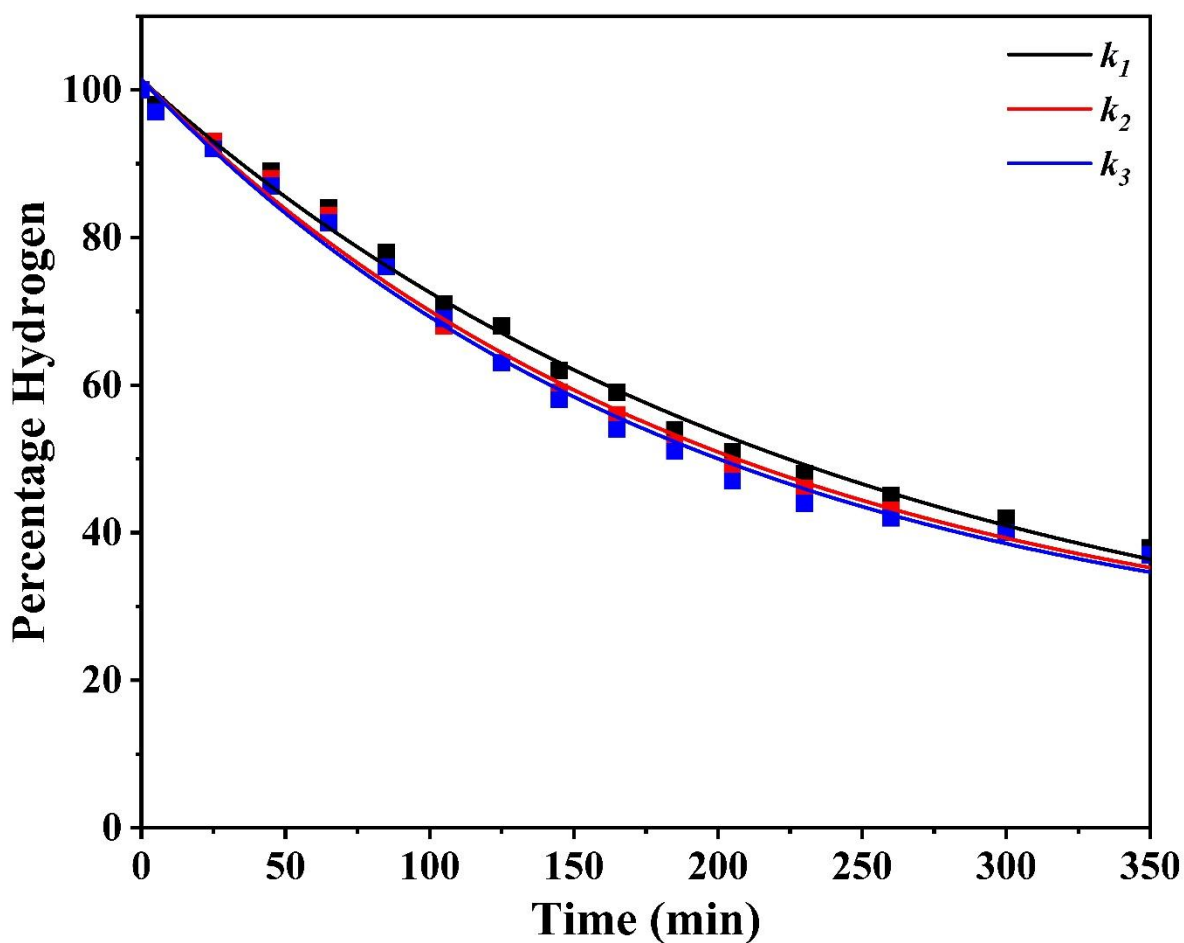


Figure S39. The H/D exchange rate constants (k_1 , k_2 , k_3) for Ind \cdots Py complex (17) obtained from three independent experiments are compared, and the $k_{\text{ex}}^{\text{avg}}$ value was calculated as the average of the three measurements. The uncertainty reported for this complex was determined from the standard deviation of the repeated measurements.

$$k_1 = 0.00361 \pm 0.00009 \text{ min}^{-1}$$

$$k_2 = 0.00343 \pm 0.00005 \text{ min}^{-1}$$

$$k_3 = 0.00339 \pm 0.00011 \text{ min}^{-1}$$

$$k_{\text{ex}}^{\text{avg}} = 0.00348 \pm 0.00012 \text{ min}^{-1}$$

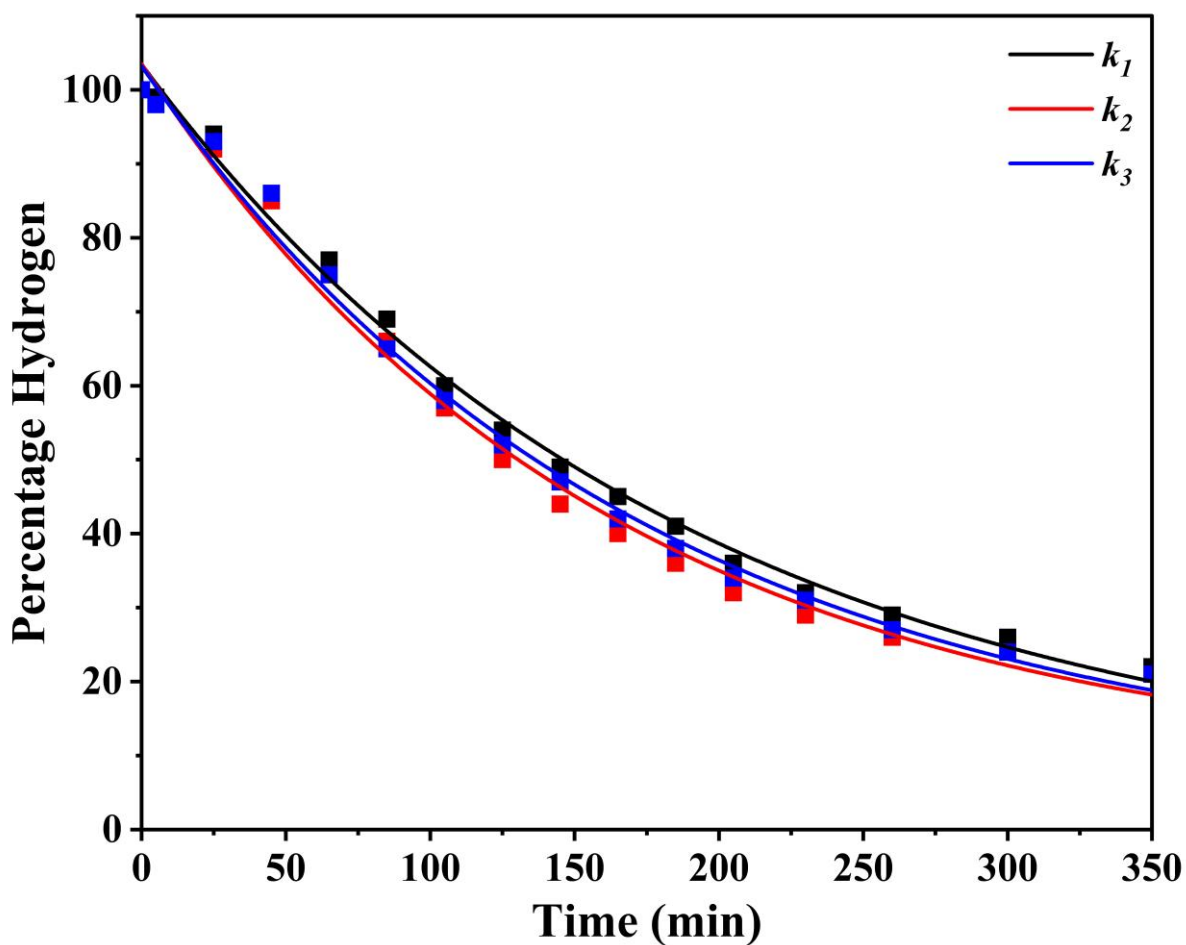


Figure S40. The H/D exchange rate constants (k_1 , k_2 , k_3) for Phe...BP complex (20) obtained from three independent experiments are compared, and the $k_{\text{ex}}^{\text{avg}}$ value was calculated as the average of the three measurements. The uncertainty reported for this complex was determined from the standard deviation of the repeated measurements.

$$k_1 = 0.00516 \pm 0.00014 \text{ min}^{-1}$$

$$k_2 = 0.00496 \pm 0.00017 \text{ min}^{-1}$$

$$k_3 = 0.00488 \pm 0.00012 \text{ min}^{-1}$$

$$k_{\text{ex}}^{\text{avg}} = 0.00500 \pm 0.00014 \text{ min}^{-1}$$

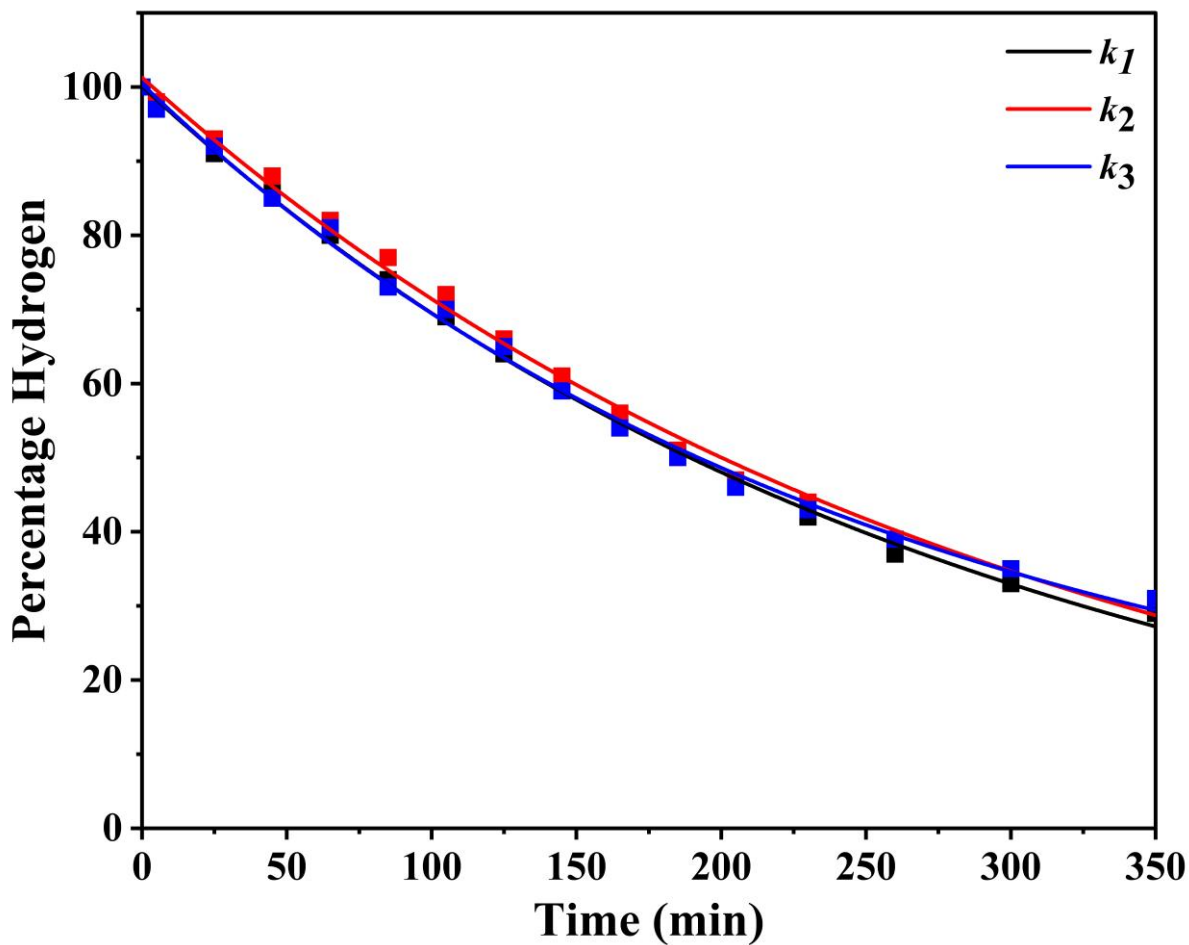


Figure S41. The H/D exchange rate constants (k_1 , k_2 , k_3) for Phe...AP complex (21) obtained from three independent experiments are compared, and the $k_{\text{ex}}^{\text{avg}}$ value was calculated as the average of the three measurements. The uncertainty reported for this complex was determined from the standard deviation of the repeated measurements.

$$k_1 = 0.00359 \pm 0.00021 \text{ min}^{-1}$$

$$k_2 = 0.00367 \pm 0.00056 \text{ min}^{-1}$$

$$k_3 = 0.00355 \pm 0.00061 \text{ min}^{-1}$$

$$k_{\text{ex}}^{\text{avg}} = 0.00360 \pm 0.00042 \text{ min}^{-1}$$

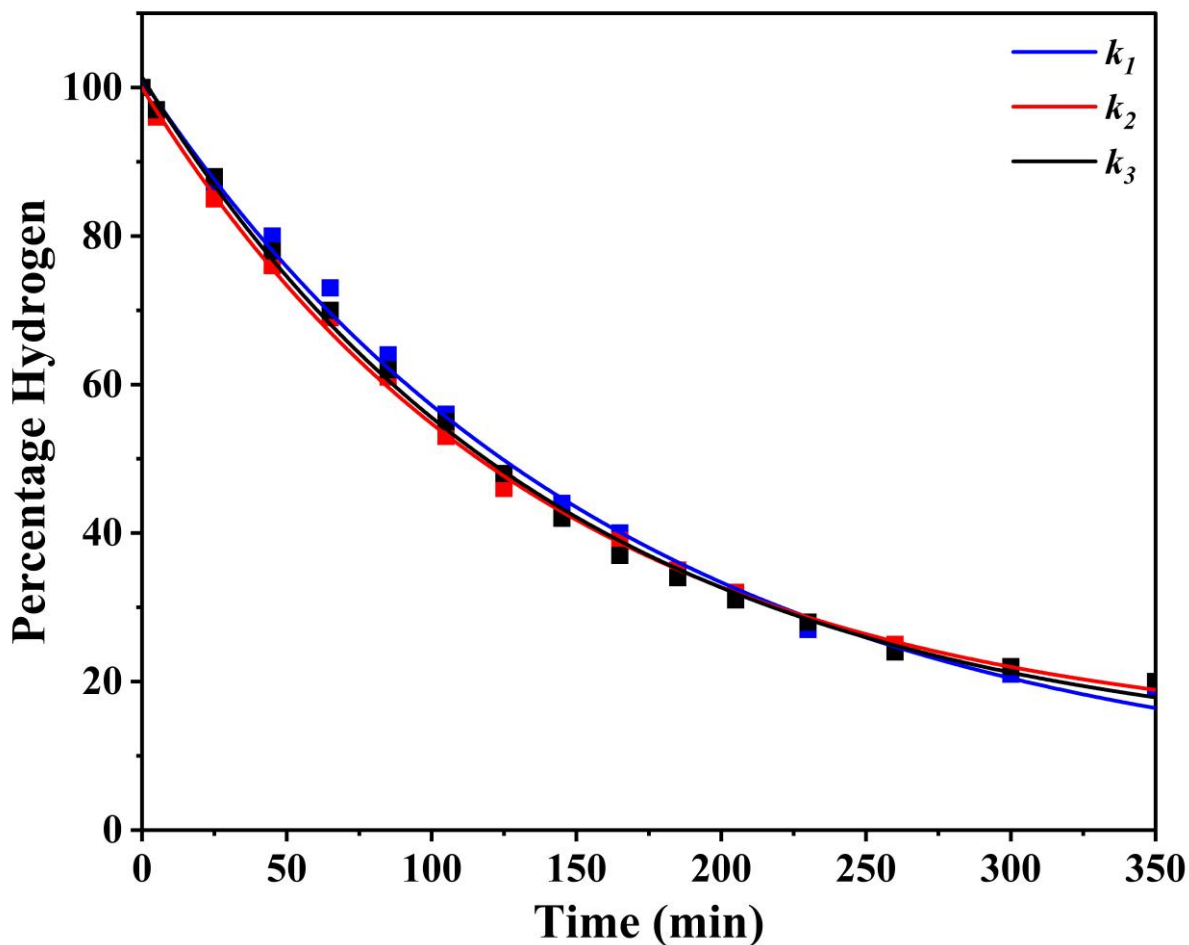


Figure S42. The H/D exchange rate constants (k_1 , k_2 , k_3) for Phe...FM complex (22) obtained from three independent experiments are compared, and the $k_{\text{ex}}^{\text{avg}}$ value was calculated as the average of the three measurements. The uncertainty reported for this complex was determined from the standard deviation of the repeated measurements.

$$k_1 = 0.00558 \pm 0.00011 \text{ min}^{-1}$$

$$k_2 = 0.00547 \pm 0.00014 \text{ min}^{-1}$$

$$k_3 = 0.00550 \pm 0.00013 \text{ min}^{-1}$$

$$k_{\text{ex}}^{\text{avg}} = 0.00552 \pm 0.00009 \text{ min}^{-1}$$

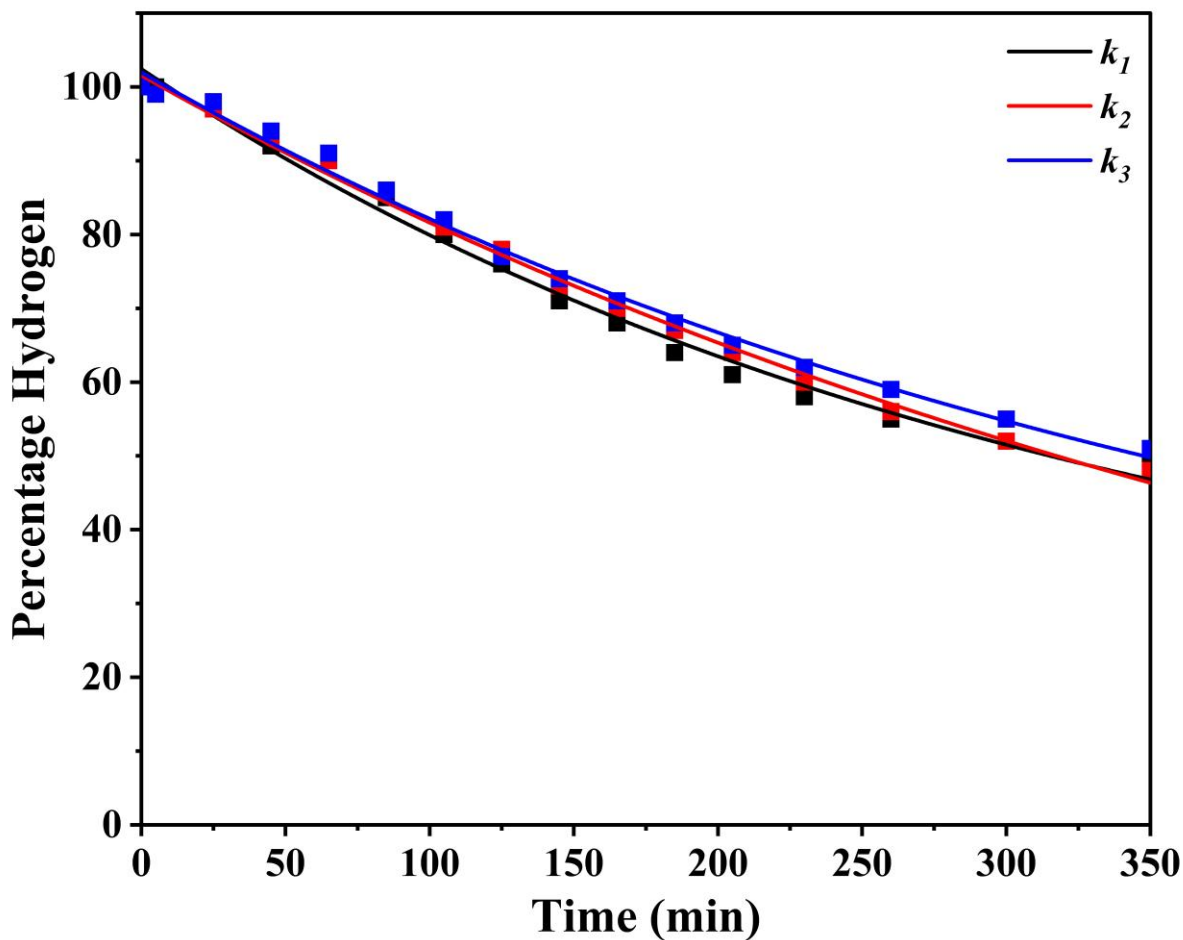


Figure S43. The H/D exchange rate constants (k_1 , k_2 , k_3) for Phe···AM complex (23) obtained from three independent experiments are compared, and the $k_{\text{ex}}^{\text{avg}}$ value was calculated as the average of the three measurements. The uncertainty reported for this complex was determined from the standard deviation of the repeated measurements.

$$k_1 = 0.00208 \pm 0.00006 \text{ min}^{-1}$$

$$k_2 = 0.00222 \pm 0.00049 \text{ min}^{-1}$$

$$k_3 = 0.00232 \pm 0.00042 \text{ min}^{-1}$$

$$k_{\text{ex}}^{\text{avg}} = 0.00221 \pm 0.00022 \text{ min}^{-1}$$

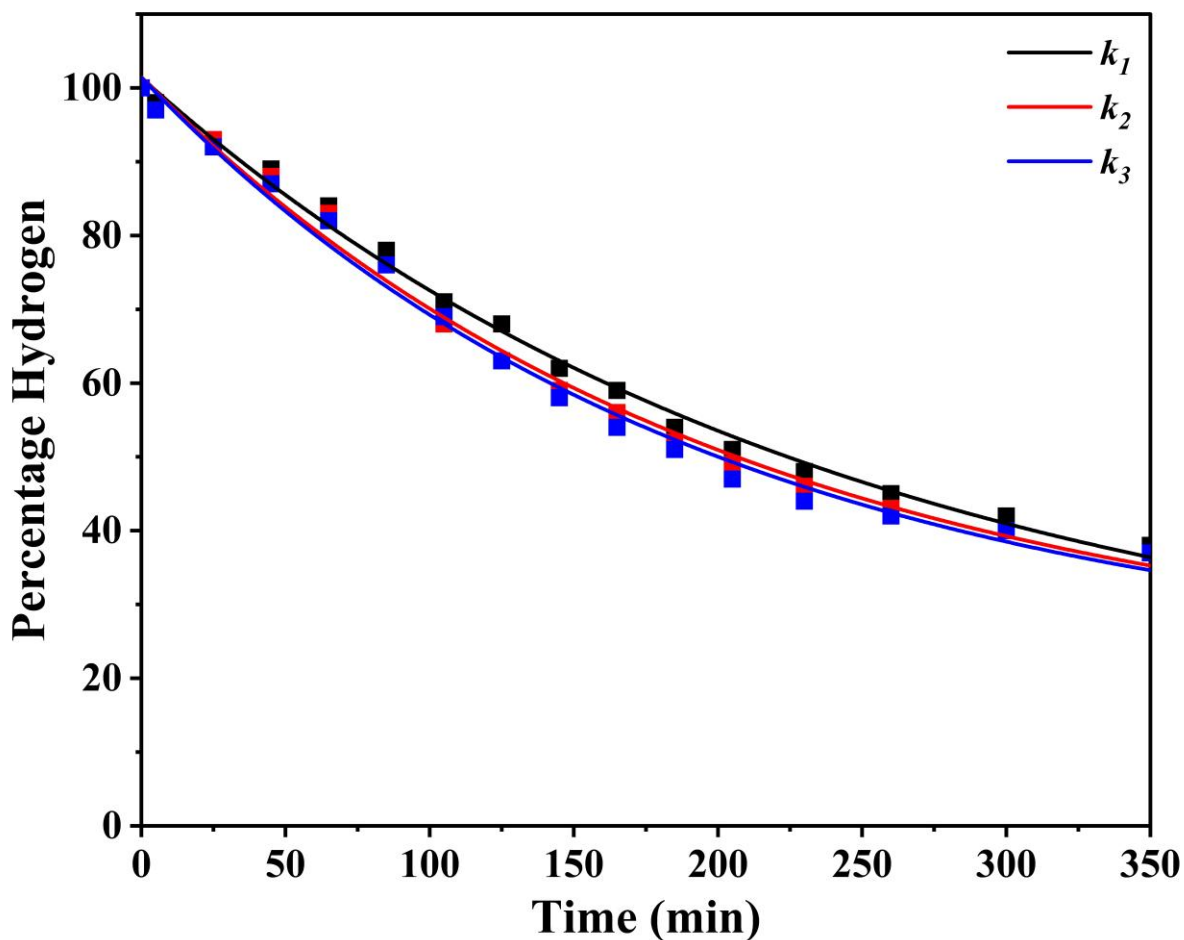


Figure S44. The H/D exchange rate constants (k_1 , k_2 , k_3) for Phe...NMA complex (24) obtained from three independent experiments are compared, and the $k_{\text{ex}}^{\text{avg}}$ value was calculated as the average of the three measurements. The uncertainty reported for this complex was determined from the standard deviation of the repeated measurements.

$$k_1 = 0.00329 \pm 0.00011 \text{ min}^{-1}$$

$$k_2 = 0.00317 \pm 0.00008 \text{ min}^{-1}$$

$$k_3 = 0.00309 \pm 0.00012 \text{ min}^{-1}$$

$$k_{\text{ex}}^{\text{avg}} = 0.00318 \pm 0.0001 \text{ min}^{-1}$$

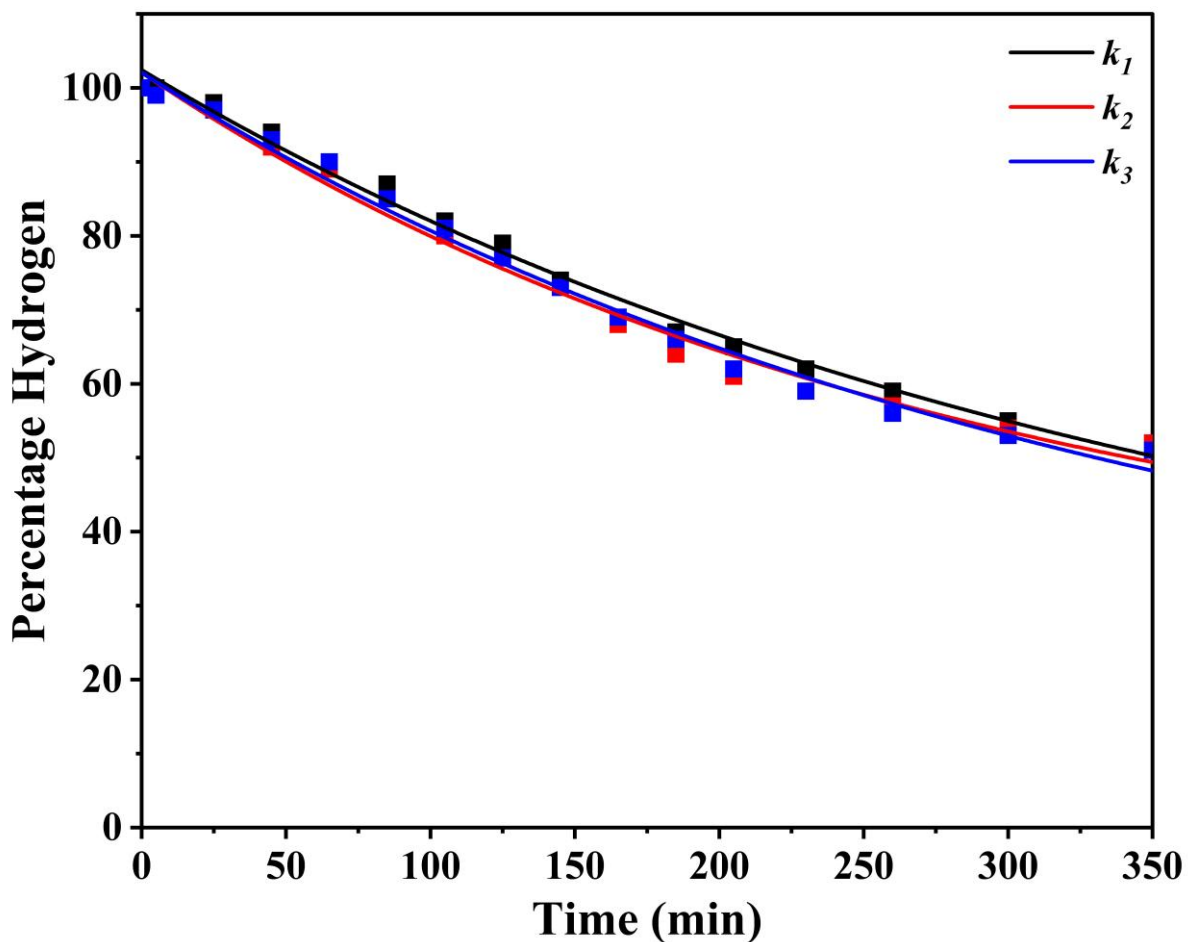


Figure S45. The H/D exchange rate constants (k_1 , k_2 , k_3) for Phe...NDMA complex (25) obtained from three independent experiments are compared, and the $k_{\text{ex}}^{\text{avg}}$ value was calculated as the average of the three measurements. The uncertainty reported for this complex was determined from the standard deviation of the repeated measurements.

$$k_1 = 0.00221 \pm 0.00006 \text{ min}^{-1}$$

$$k_2 = 0.00218 \pm 0.00007 \text{ min}^{-1}$$

$$k_3 = 0.00209 \pm 0.00005 \text{ min}^{-1}$$

$$k_{\text{ex}}^{\text{avg}} = 0.00216 \pm 0.00006 \text{ min}^{-1}$$

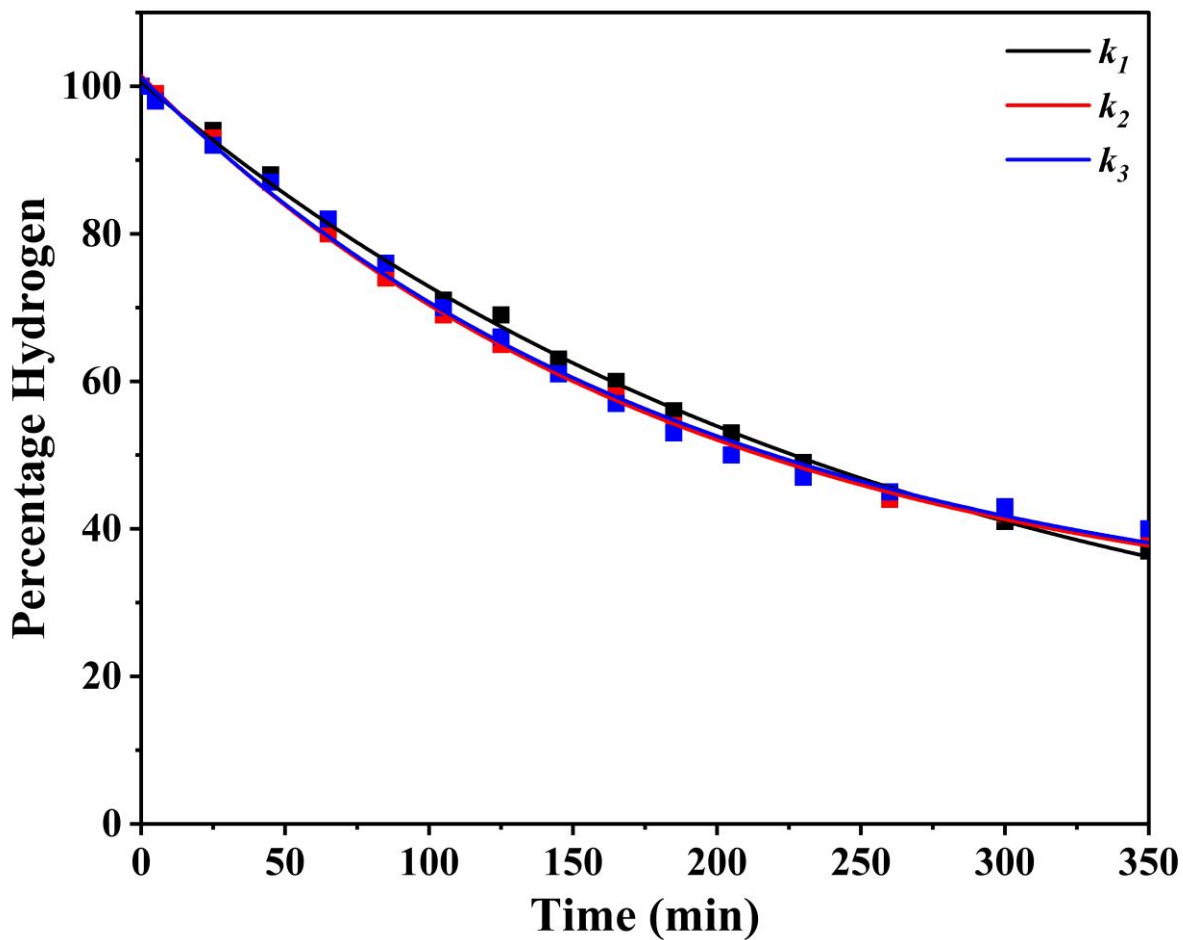


Figure S46. The H/D exchange rate constants (k_1 , k_2 , k_3) for Phe...THF complex (26) obtained from three independent experiments are compared, and the $k_{\text{ex}}^{\text{avg}}$ value was calculated as the average of the three measurements. The uncertainty reported for this complex was determined from the standard deviation of the repeated measurements.

$$k_1 = 0.00304 \pm 0.00048 \text{ min}^{-1}$$

$$k_2 = 0.00313 \pm 0.00010 \text{ min}^{-1}$$

$$k_3 = 0.00308 \pm 0.00011 \text{ min}^{-1}$$

$$k_{\text{ex}}^{\text{avg}} = 0.00308 \pm 0.00025 \text{ min}^{-1}$$

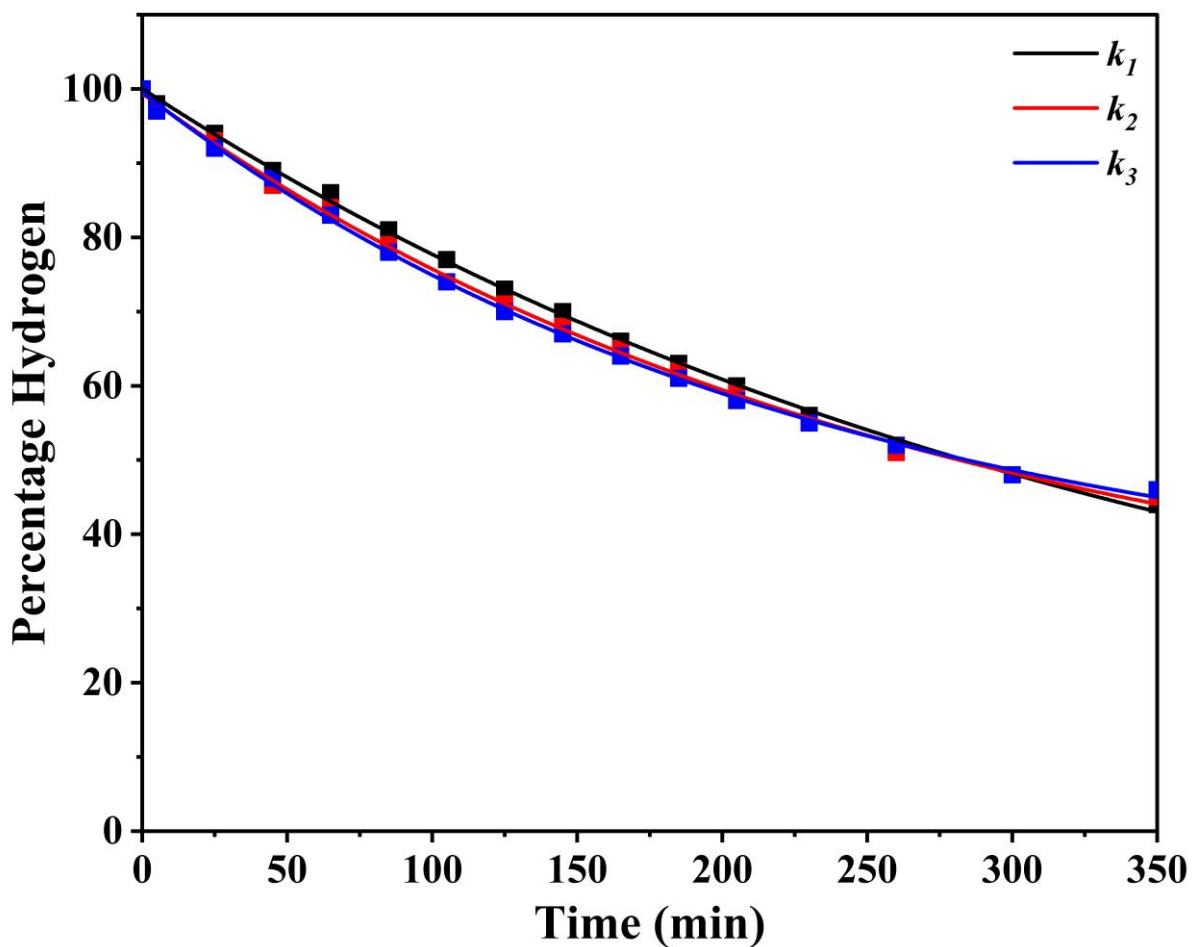


Figure S47. The H/D exchange rate constants (k_1 , k_2 , k_3) for Phe...THP complex (27) obtained from three independent experiments are compared, and the $k_{\text{ex}}^{\text{avg}}$ value was calculated as the average of the three measurements. The uncertainty reported for this complex was determined from the standard deviation of the repeated measurements.

$$k_1 = 0.00245 \pm 0.00002 \text{ min}^{-1}$$

$$k_2 = 0.00245 \pm 0.00005 \text{ min}^{-1}$$

$$k_3 = 0.00245 \pm 0.00006 \text{ min}^{-1}$$

$$k_{\text{ex}}^{\text{avg}} = 0.00245 \pm 0.00004 \text{ min}^{-1}$$

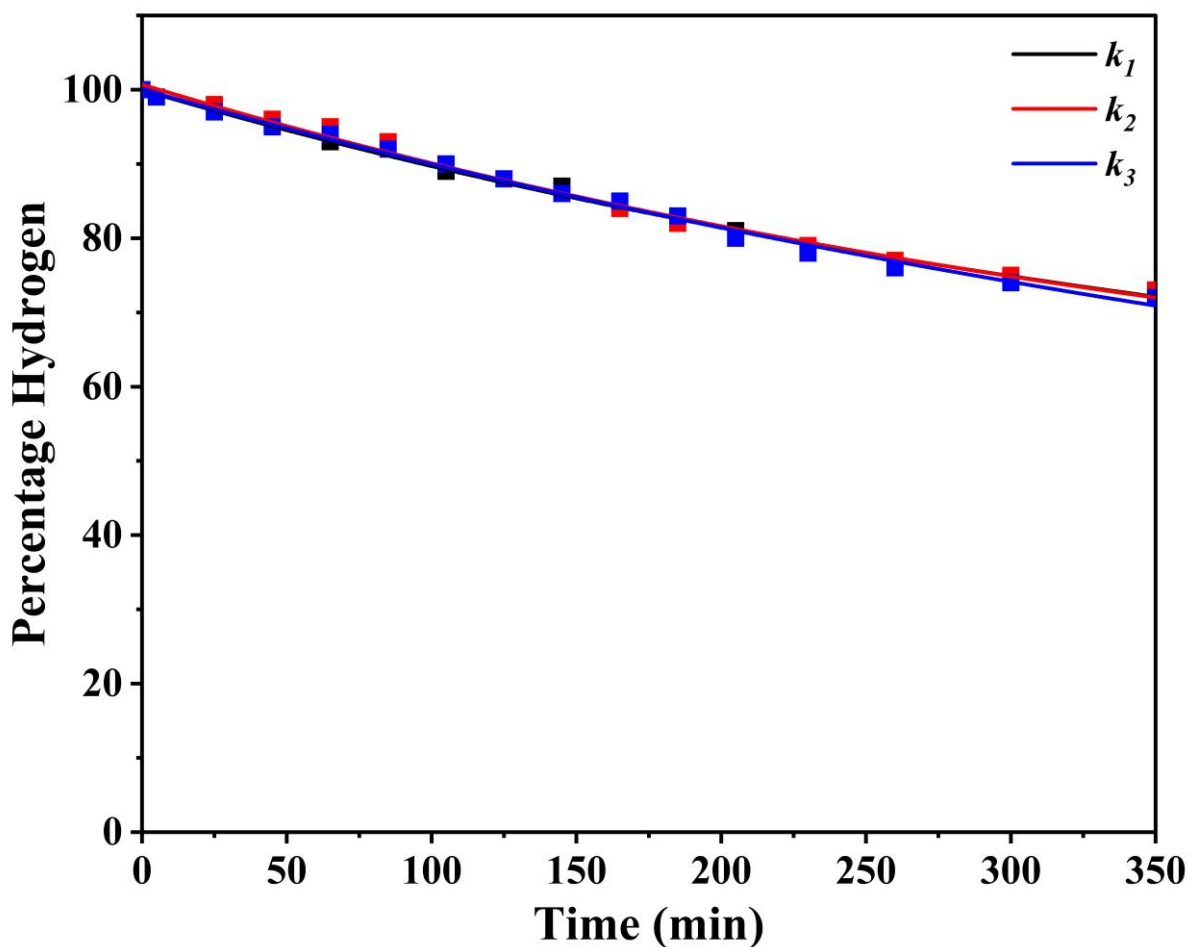


Figure S48. The H/D exchange rate constants (k_1 , k_2 , k_3) for Phe...Im complex (28) obtained from three independent experiments are compared, and the $k_{\text{ex}}^{\text{avg}}$ value was calculated as the average of the three measurements. The uncertainty reported for this complex was determined from the standard deviation of the repeated measurements.

$$k_1 = 0.00096 \pm 0.00002 \text{ min}^{-1}$$

$$k_2 = 0.00099 \pm 0.00002 \text{ min}^{-1}$$

$$k_3 = 0.00098 \pm 0.00003 \text{ min}^{-1}$$

$$k_{\text{ex}}^{\text{avg}} = 0.00098 \pm 0.00002 \text{ min}^{-1}$$

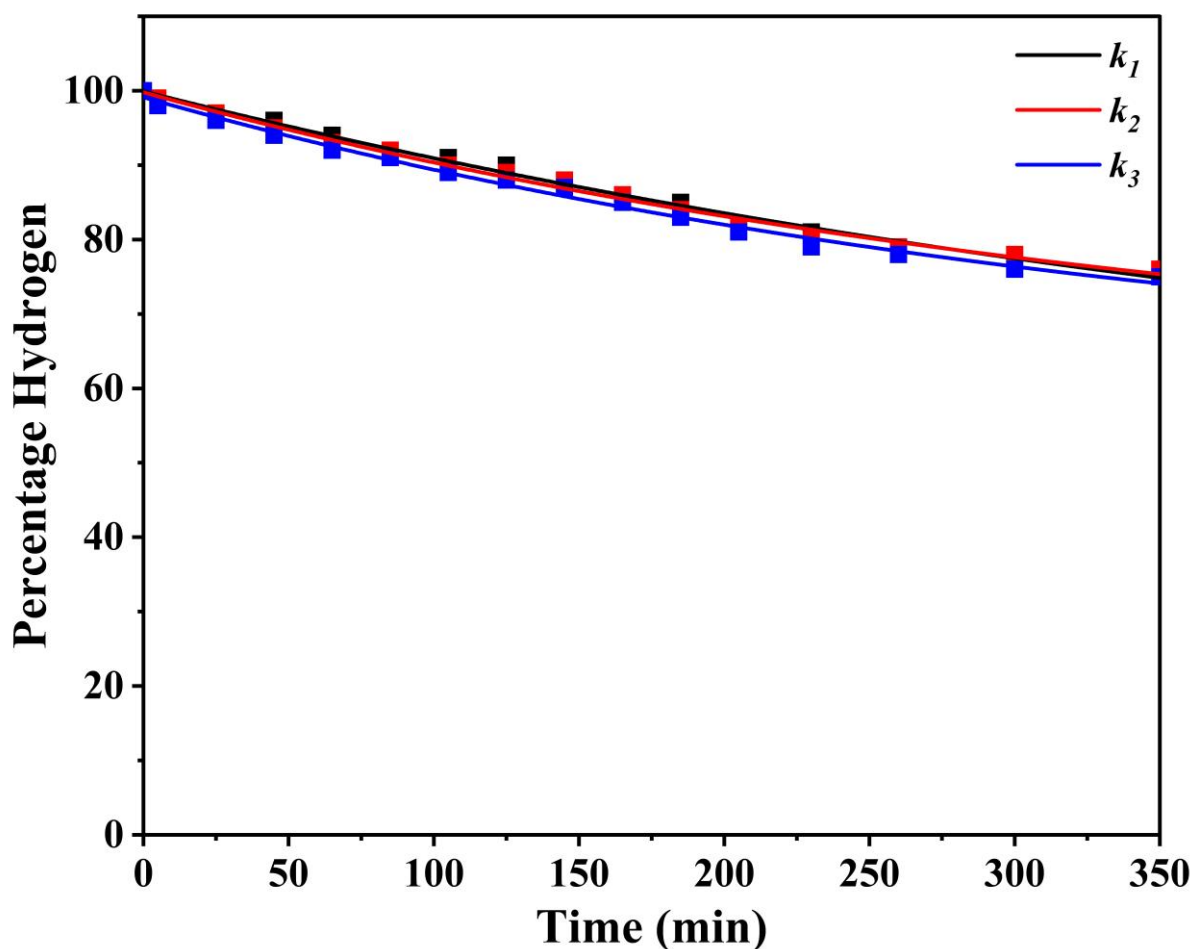


Figure S49. The H/D exchange rate constants (k_1 , k_2 , k_3) for Phe...Py complex (29) obtained from three independent experiments are compared, and the $k_{\text{ex}}^{\text{avg}}$ value was calculated as the average of the three measurements. The uncertainty reported for this complex was determined from the standard deviation of the repeated measurements.

$$k_1 = 0.00086 \pm 0.00023 \text{ min}^{-1}$$

$$k_2 = 0.00085 \pm 0.00009 \text{ min}^{-1}$$

$$k_3 = 0.00083 \pm 0.00028 \text{ min}^{-1}$$

$$k_{\text{ex}}^{\text{avg}} = 0.00085 \pm 0.00018 \text{ min}^{-1}$$

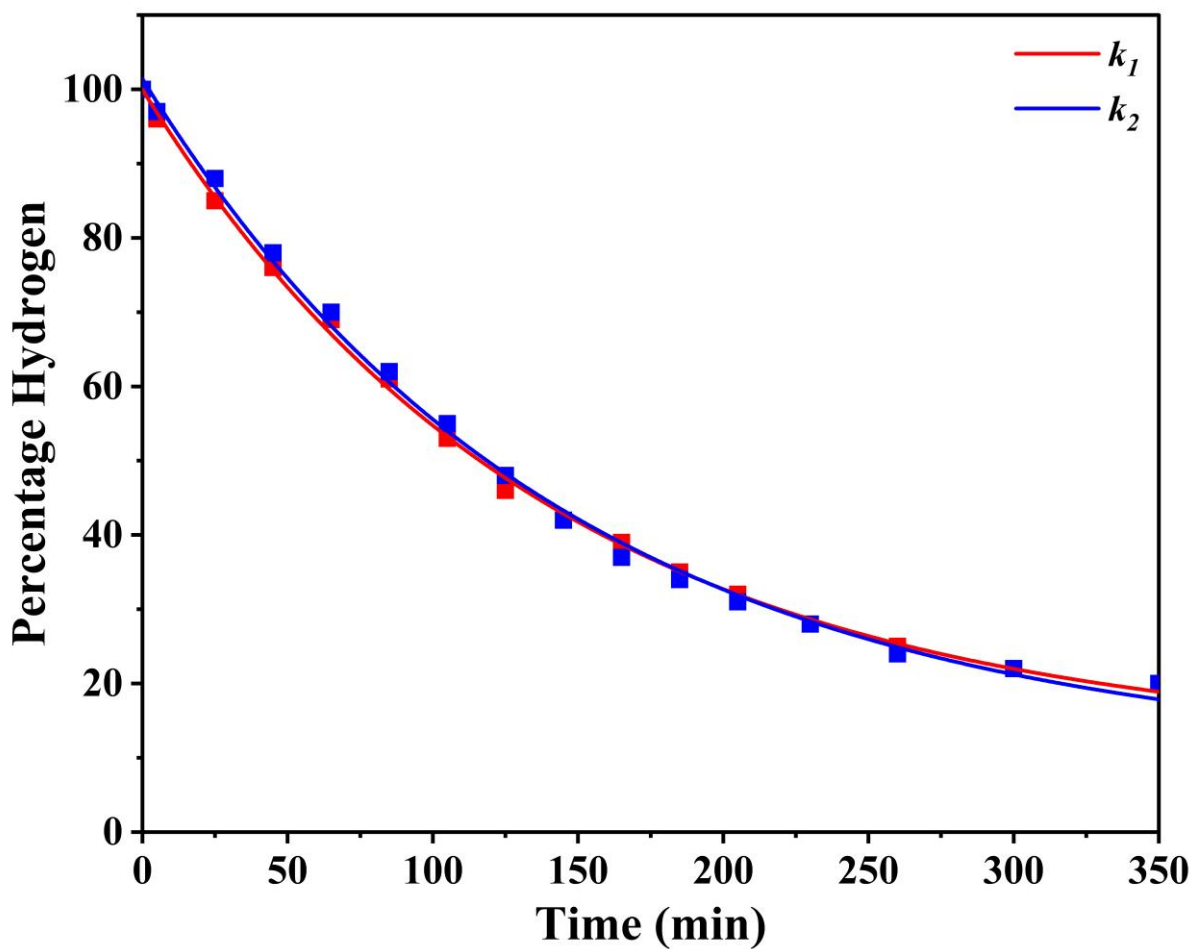


Figure S50. The H/D exchange rate constants (k_1 , k_2) for 7Al...THF complex (14) obtained from two independent experiments are compared, and the $k_{\text{ex}}^{\text{avg}}$ value was calculated as the average of the two measurements. The uncertainty reported for this complex was determined from the standard deviation of the repeated measurements.

$$k_1 = 0.00575 \pm 0.0001 \text{ min}^{-1}$$

$$k_2 = 0.00559 \pm 0.0001 \text{ min}^{-1}$$

$$k_{\text{ex}}^{\text{avg}} = 0.00567 \pm 0.00008 \text{ min}^{-1}$$

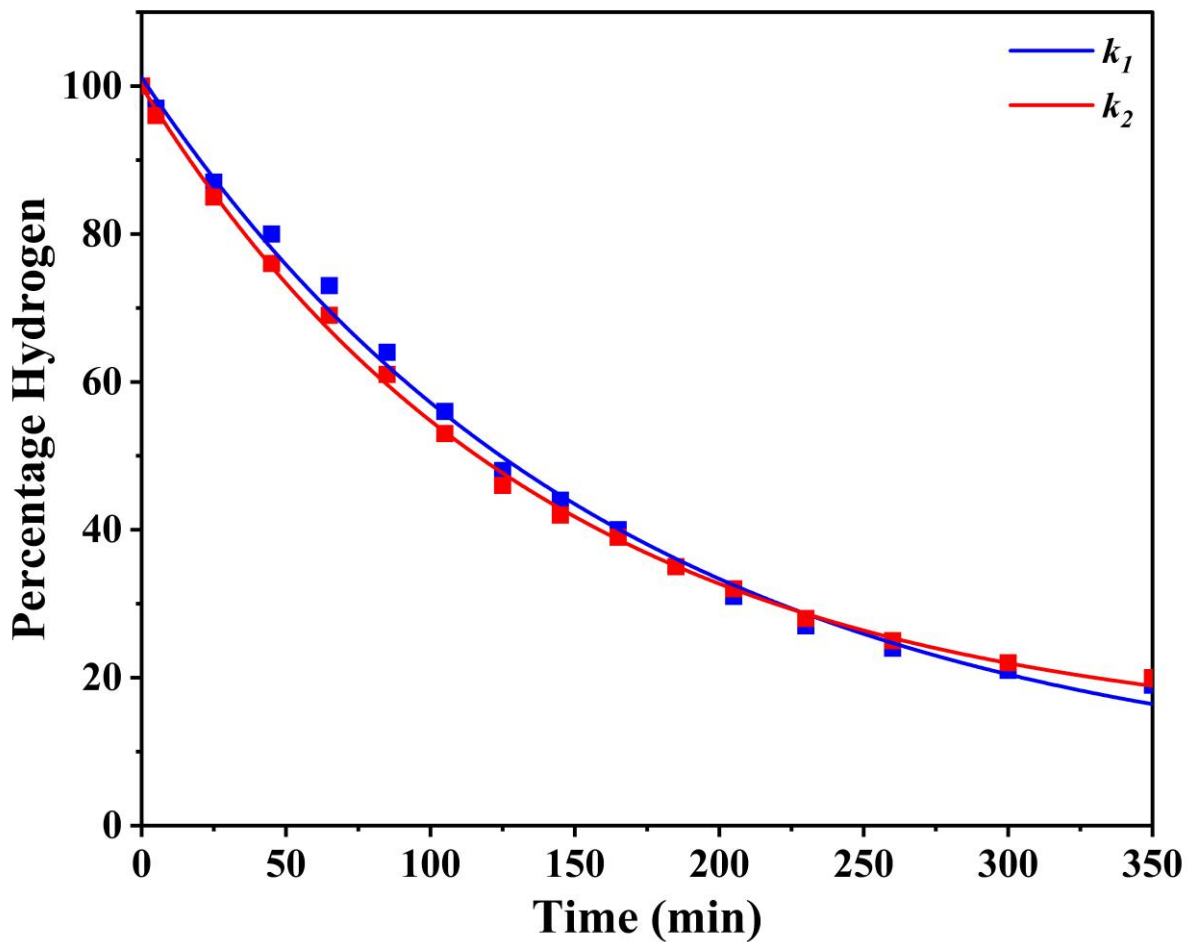


Figure S51. The H/D exchange rate constants (k_1, k_2) for 7AI...THP complex (15) obtained from two independent experiments are compared, and the $k_{\text{ex}}^{\text{avg}}$ value was calculated as the average of the two measurements. The uncertainty reported for this complex was determined from the standard deviation of the repeated measurements.

$$k_1 = 0.00588 \pm 0.00025 \text{ min}^{-1}$$

$$k_2 = 0.00576 \pm 0.00019 \text{ min}^{-1}$$

$$k_{\text{ex}}^{\text{avg}} = 0.00582 \pm 0.00016 \text{ min}^{-1}$$

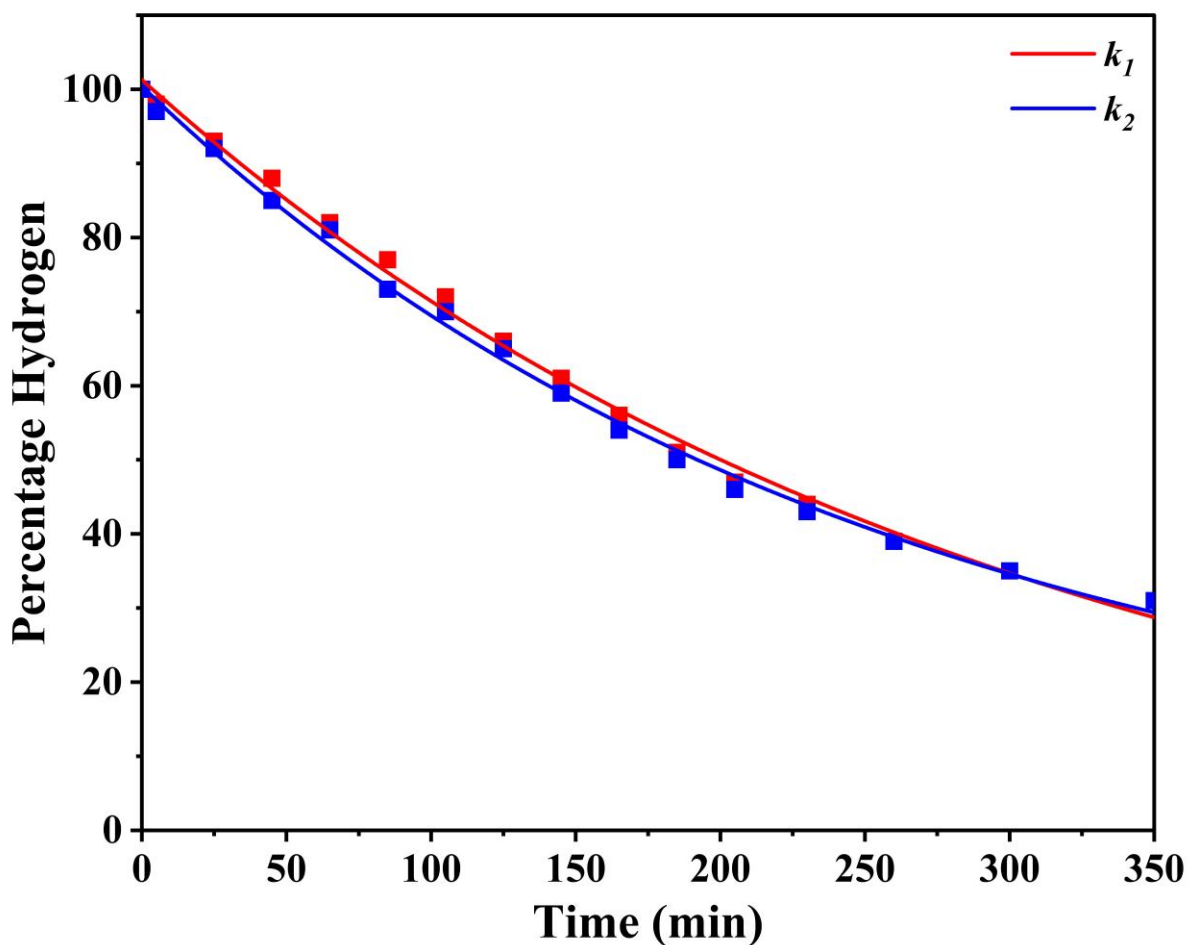


Figure S52. The H/D exchange rate constants (k_1 , k_2) for 7AI...Im complex (18) obtained from two independent experiments are compared, and the $k_{\text{ex}}^{\text{avg}}$ value was calculated as the average of the two measurements. The uncertainty reported for this complex was determined from the standard deviation of the repeated measurements.

$$k_1 = 0.00362 \pm 0.00034 \text{ min}^{-1}$$

$$k_2 = 0.00357 \pm 0.00061 \text{ min}^{-1}$$

$$k_{\text{ex}}^{\text{avg}} = 0.00360 \pm 0.00031 \text{ min}^{-1}$$

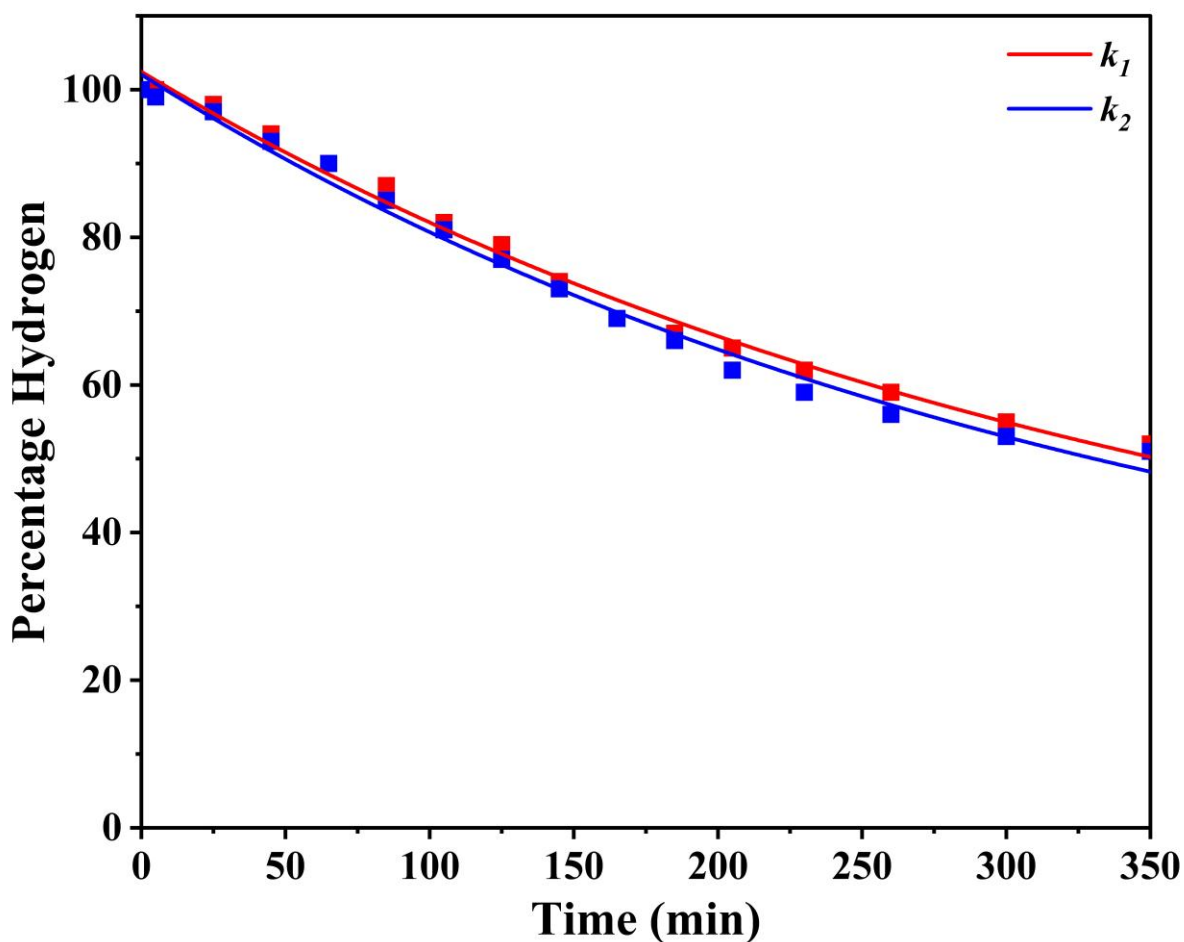


Figure S53. The H/D exchange rate constants (k_1 , k_2) for 7AI...Py complex (19) obtained from two independent experiments are compared, and the $k_{\text{ex}}^{\text{avg}}$ value was calculated as the average of the two measurements. The uncertainty reported for this complex was determined from the standard deviation of the repeated measurements.

$$k_1 = 0.00314 \pm 0.00004 \text{ min}^{-1}$$

$$k_2 = 0.00299 \pm 0.00008 \text{ min}^{-1}$$

$$k_{\text{ex}}^{\text{avg}} = 0.00307 \pm 0.00011 \text{ min}^{-1}$$

5.4. A comparison of H/D exchange kinetics of N-H \cdots O=C hydrogen bond complexes upon addition of D₂O. Standard errors for the percentage hydrogen measurements at each time interval for all complexes and monomers are shown in the figure.

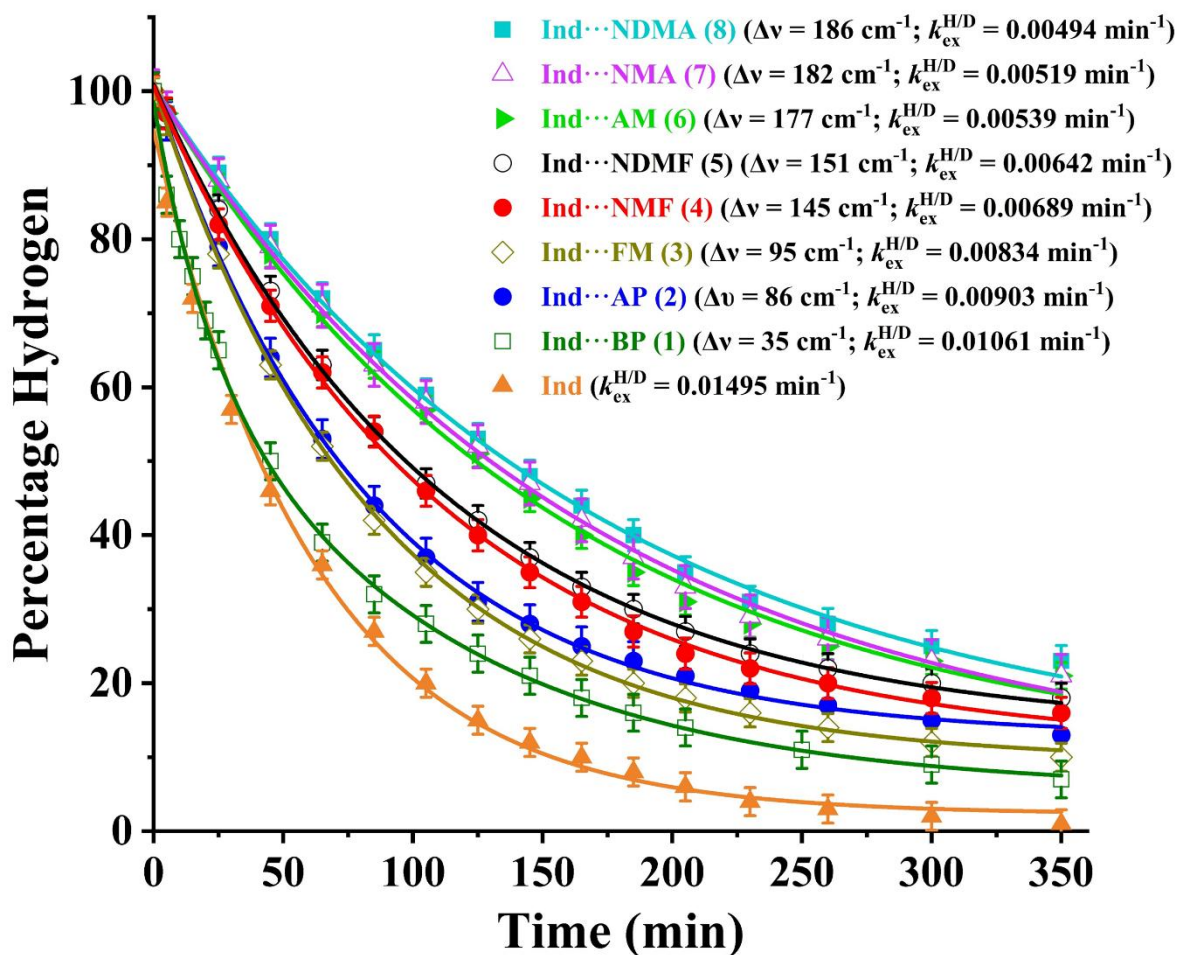


Figure S54. Kinetics of H/D exchange for N-H ¹H NMR signals in the complexes (CDCl₃) featuring N-H \cdots O=C hydrogen bonding upon addition of D₂O. H/D exchange kinetic profile of the Ind monomer is also provided in the figure. The identification numbers (IDs), $k_{ex}^{H/D}$, and $\Delta\nu$ of the complexes are provided in parentheses alongside their names in the inset. In the cases of the monomers, only $k_{ex}^{H/D}$ values are provided. The $k_{ex}^{H/D}$ value provided in parentheses is the average rate constant from the repeated kinetic measurement. Standard error in the percentage hydrogen measurement at each time interval of the kinetics of every complex is provided with the plot, while the detailed procedure for the uncertainty calculation is given on page S9 in the supporting information.

5.5. A comparison of H/D exchange kinetics of N-H \cdots O and N-H \cdots N hydrogen bond complexes upon addition of D₂O. Standard errors for the percentage hydrogen measurements at each time interval for all complexes and monomers are shown in the figure.

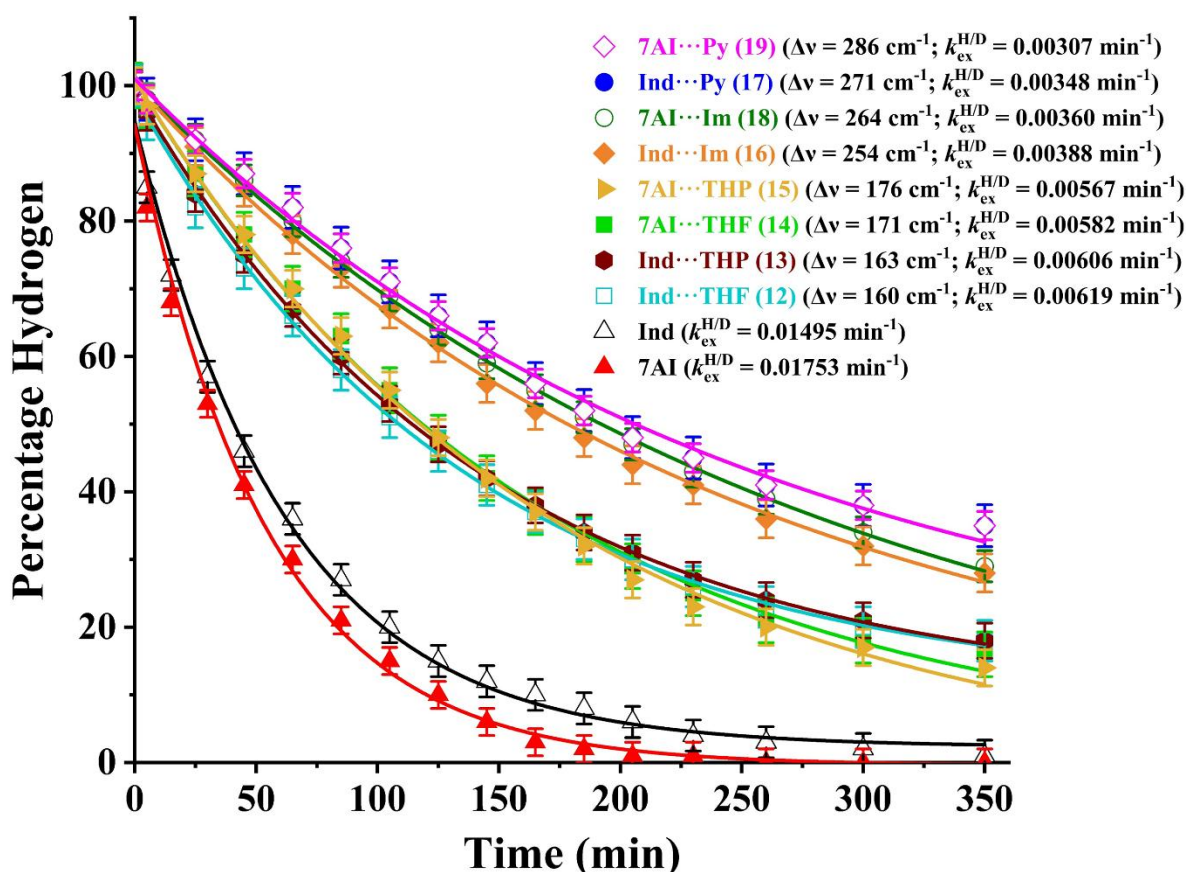


Figure S55. Kinetics of H/D exchange for N-H ¹H NMR signals in the complexes (CDCl₃) featuring N-H \cdots O and N-H \cdots N hydrogen bonding upon addition of D₂O. H/D exchange kinetic profiles of the Ind and 7AI monomers are also provided in the figure. The identification numbers (IDs), $k_{\text{ex}}^{\text{H/D}}$, and $\Delta\nu$ of the complexes are provided in parentheses alongside their names in the inset. In the cases of the monomers, only $k_{\text{ex}}^{\text{H/D}}$ values are provided. The $k_{\text{ex}}^{\text{H/D}}$ value provided in parentheses is the average rate constant from the repeated kinetic measurement. Standard error in the percentage hydrogen measurement at each time interval of the kinetics of every complex is provided with the plot, while the detailed procedure for the uncertainty calculation is given on page S9 in the supporting information.

5.6. A comparison of H/D exchange kinetics of O-H···O=C, O-H···O, and O-H···N hydrogen bond complexes. Standard errors for the percentage hydrogen measurements at each time interval for all complexes and monomers are shown in the figure.

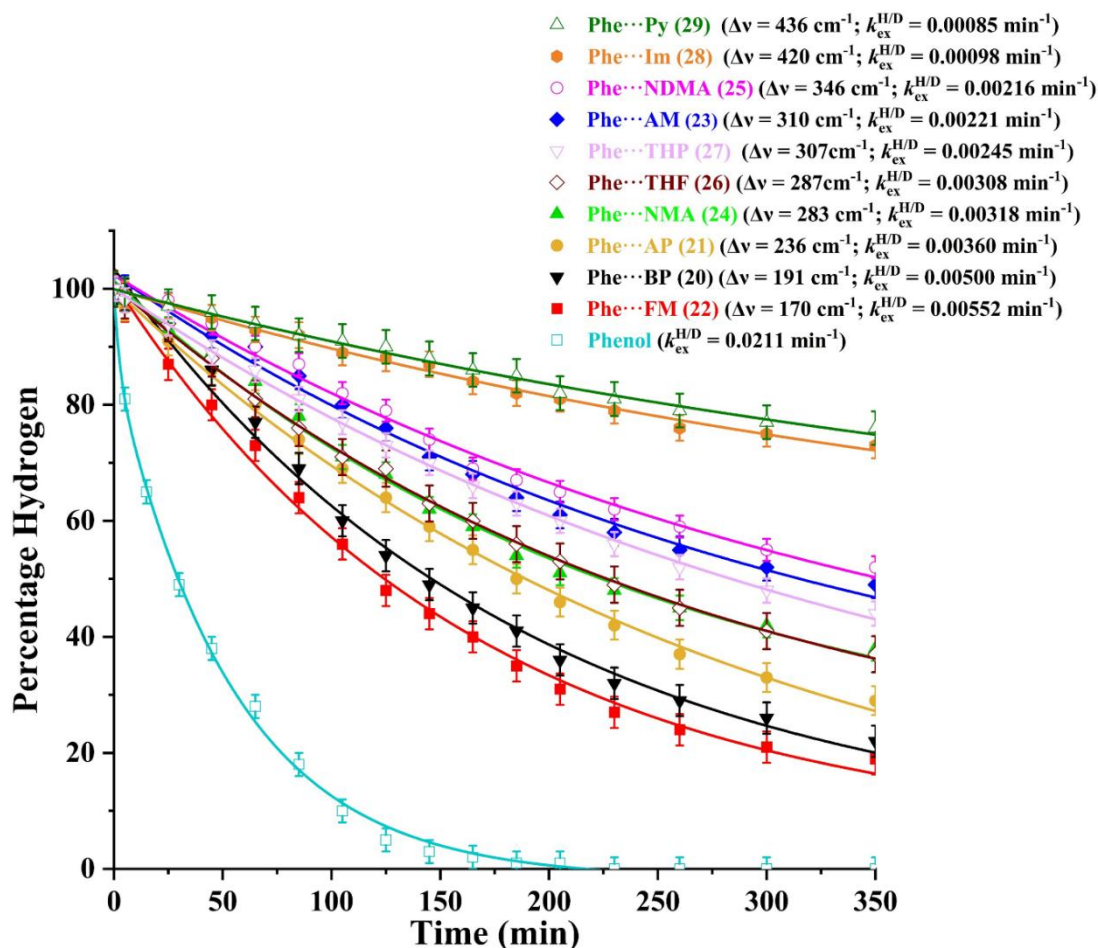


Figure S56. Kinetics of H/D exchange for O-H ^1H NMR signals in the complexes (CDCl_3) featuring O-H···O=C, O-H···O and O-H···N hydrogen bonding upon addition of D_2O . The H/D exchange kinetic profile of the Phe monomer is also provided in the figure. The identification numbers (IDs), $k_{ex}^{H/D}$, and $\Delta\nu$ of the complexes are provided in parentheses alongside their names in the inset. In the cases of the monomers, only $k_{ex}^{H/D}$ values are provided. The $k_{ex}^{H/D}$ value provided in parentheses is the average from the repeated kinetic measurement. Standard error in the percentage hydrogen measurement at each time interval of the kinetics of every complex is provided with the plot, while the detailed procedure for the uncertainty calculation is given on page S9 in the supporting information.

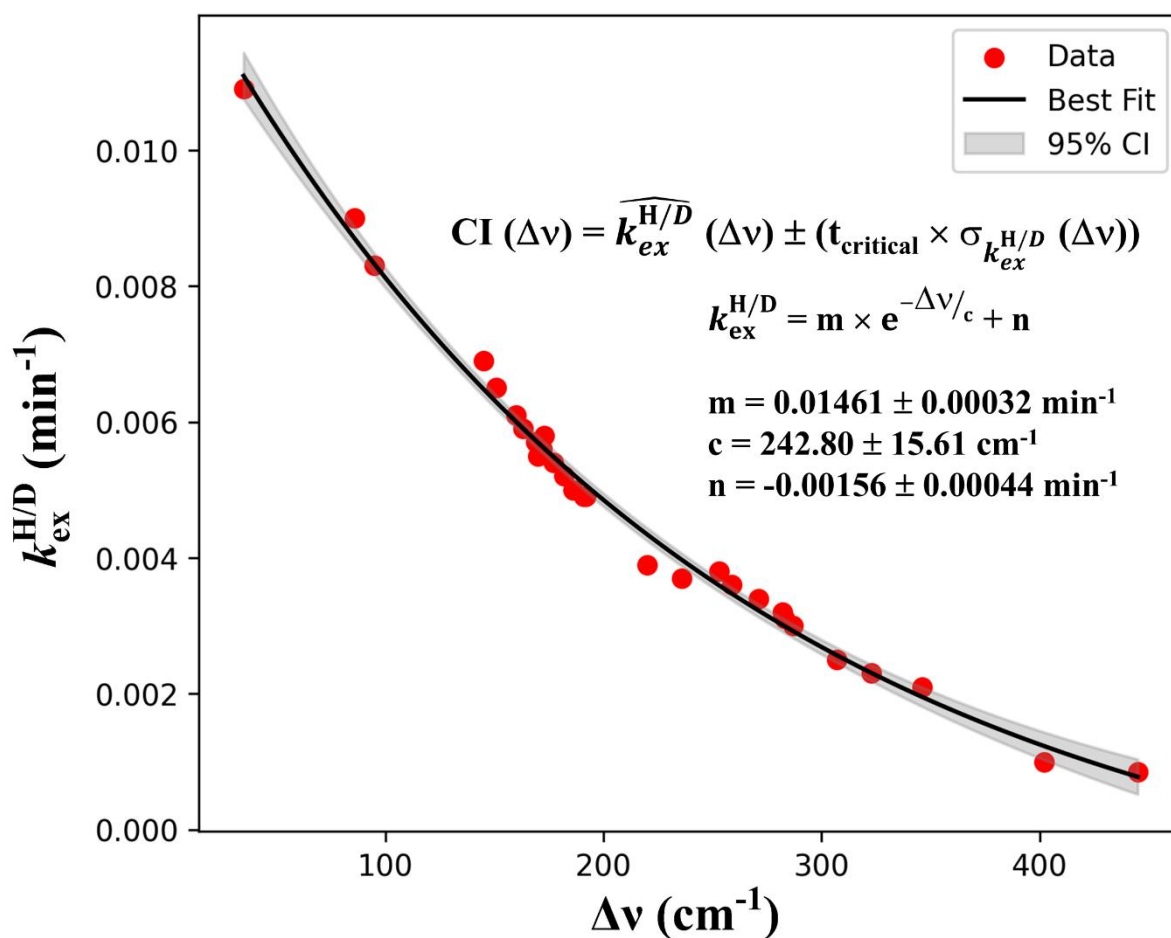


Figure S57. Correlation between the H/D exchange rate constants ($k_{ex}^{H/D}$) and the IR red shift ($\Delta\nu$) for all 29 complexes with the exponential fit ($R^2 = 0.993$). The shaded grey area shows the 95% confidence band, determined from the confidence interval (CI) calculations: $CI(\Delta\nu) = \widehat{k_{ex}^{H/D}}(\Delta\nu) \pm (t_{\text{critical}} \times \sigma_{k_{ex}^{H/D}}(\Delta\nu))$; where $\widehat{k_{ex}^{H/D}}(\Delta\nu)$ is the fitted value of $k_{ex}^{H/D}$ at a specific $\Delta\nu$ value, t_{critical} is calculated based on the Student's t-distribution, and $\sigma_{k_{ex}^{H/D}}(\Delta\nu)$ is the standard deviation of the fit ($\sigma_{k_{ex}^{H/D}}$) at a specific $\Delta\nu$ point. The detailed method for CI calculation is discussed on pages S10-S11 in the supporting information. This confidence band represents the region within which we are 95% confident that new data will fit the proposed empirical model.

Table S1. Comparison of the experimental IR red shift ($\Delta\nu$) values in the N–H and O–H stretching regions of all 29 complexes measured in CHCl_3 solution with respect to those obtained from the calculations performed in the gas and solution phases. Experimental IR red-shift values of some of the complexes measured in CCl_4 solution or gas phase and reported in the literature are also listed in the table

Complexes Description	Interaction	IR red shift ($\Delta\nu$) (cm^{-1})				Complexes Description	Interaction	IR red shift ($\Delta\nu$) (cm^{-1})			
		Experiment		Calculation				Experiment		Calculation	
		This work	Reported	Gas-phase	Solution-phase			This work	Reported	Gas-phase	Solution-phase
Ind \cdots BP (1)	N-H \cdots O=C	35	23 ^a	50	48	5CI \cdots AM (10)	N-H \cdots O=C	192	-	173	171
Ind \cdots AP (2)	N-H \cdots O=C	86	86 ^b	65	57	5NI \cdots AM (11)	N-H \cdots O=C	220	-	194	190
Ind \cdots FM (3)	N-H \cdots O=C	95	-	111	109	Phe \cdots AP (21)	O-H \cdots O=C	236	243 ^g	245	239
Ind \cdots NMF (4)	N-H \cdots O=C	145	-	127	121	Ind \cdots Im (16)	N-H \cdots N	254	256 ^h	213	208
Ind \cdots NDMF (5)	N-H \cdots O=C	151	-	131	129	7AI \cdots Im (18)	N-H \cdots N	264	-	215	212
Ind \cdots THF (12)	N-H \cdots O	160	162 ^c	134	131	Ind \cdots Py (17)	N-H \cdots N	271	257 ⁱ	217	216
Ind \cdots THP (13)	N-H \cdots O	163	168 ^d	146	145	Phe \cdots NMA (24)	O-H \cdots O=C	283	-	285	282
Phe \cdots FM (22)	O-H \cdots O=C	170	-	165	163	7AI \cdots Py (19)	N-H \cdots N	286	-	271	264
7AI \cdots THF (14)	N-H \cdots O	171	-	151	147	Phe \cdots THF (26)	O-H \cdots O	287	285 ^j	256	255
5MI \cdots AM (9)	N-H \cdots O=C	173	-	149	147	Phe \cdots THP (27)	O-H \cdots O	309	-	273	268
7AI \cdots THP (15)	N-H \cdots O	176	-	160	158	Phe \cdots AM (23)	O-H \cdots O=C	323	310 ^k	332	330
Ind \cdots AM (6)	N-H \cdots O=C	177	-	156	150	Phe \cdots NDMA (25)	O-H \cdots O=C	346	345 ^l	272	269

Ind⋯NMA (7)	N-H⋯O=C	182	218 ^e	160	159	Phe⋯Im (28)	O-H⋯N	420	-	394	391
Ind⋯NDMA (8)	N-H⋯O=C	186	-	161	160	Phe⋯Py (29)	O-H⋯N	436	465 ^m	403	399
Phe⋯BP (20)	O-H⋯O=C	191	198 ^f	176	170						

^aIR red shift of Ind⋯BP complex in CCl₄ solvent (Ref 17), ^bIR red shift of Ind⋯AP complex in CCl₄ solvent (Ref 17), ^cIR red shift of Ind⋯THF complex in CCl₄ solvent (Ref 18), ^dIR red shift of Ind⋯THP complex in CCl₄ solvent (Ref 18), ^eIR red shift of Ind⋯NMA complex in gas phase (Ref 19), ^fIR red shift of Phe⋯BP complex in CCl₄ solvent (Ref 20), ^gIR red shift of Phe⋯AP complex in CCl₄ solvent (Ref 20), ^hIR red shift of Ind⋯Im complex in gas phase (Ref 21), ⁱIR red shift of Ind⋯Py complex in gas phase (Ref 22), ^jIR red shift of Phe⋯THF complex in CCl₄ solvent (Ref 23), ^kIR red shift of Phe⋯AM complex in CCl₄ solvent (Ref 20), ^lIR red shift of Phe⋯NDMA complex in CCl₄ solvent (Ref 24), ^mIR red shift of Phe⋯Py complex in CCl₄ solvent (Ref 24).

Table S2: Observed change in chemical shift ($\Delta\delta$) values in ^1H NMR for the N-H and O-H protons in all 29 complexes with respect to those in the monomers. $\Delta\delta$ values are provided with their standard errors, i.e., $\Delta\delta \pm \text{Standard Error}$

Complex	Interaction	IR Shift ($\Delta\nu$) (cm^{-1})	Change in Chemical Shift (ppm) ($\Delta\delta$) \pm Standard Error	Complex	Interaction	IR Shift ($\Delta\nu$) (cm^{-1})	Change in Chemical Shift (ppm) ($\Delta\delta$) \pm Standard Error
Ind \cdots BP (1)	N-H \cdots O=C	35	0.0125 ± 0.0001	5CI \cdots AM (10)	N-H \cdots O=C	192	0.0915 ± 0.0007
Ind \cdots AP (2)	N-H \cdots O=C	86	0.0167 ± 0.0001	5NI \cdots AM (11)	N-H \cdots O=C	220	0.1354 ± 0.0007
Ind \cdots FM (3)	N-H \cdots O=C	95	0.0242 ± 0.0004	Phe \cdots AP (21)	O-H \cdots O=C	236	0.1140 ± 0.0003
Ind \cdots NMF (4)	N-H \cdots O=C	145	0.0319 ± 0.0003	Ind \cdots Im (16)	N-H \cdots N	254	0.1463 ± 0.0008
Ind \cdots NDMF (5)	N-H \cdots O=C	151	0.0412 ± 0.0002	7AI \cdots Im (18)	N-H \cdots N	264	0.2303 ± 0.0012
Ind \cdots THF (12)	N-H \cdots O	160	0.0415 ± 0.0006	Ind \cdots Py (17)	N-H \cdots N	271	0.1608 ± 0.0012
Ind \cdots THP (13)	N-H \cdots O	163	0.0424 ± 0.0005	Phe \cdots NMA (24)	O-H \cdots O=C	283	0.5527 ± 0.0030
Phe \cdots FM (22)	O-H \cdots O=C	170	0.4872 ± 0.0009	7AI \cdots Py (19)	N-H \cdots N	286	0.2902 ± 0.0023
7AI \cdots THF (14)	N-H \cdots O	171	0.1825 ± 0.0013	Phe \cdots THF (26)	O-H \cdots O	287	0.2100 ± 0.0011
5MI \cdots AM (9)	N-H \cdots O=C	173	0.0458 ± 0.0005	Phe \cdots THP (27)	O-H \cdots O	309	0.2695 ± 0.0011
7AI \cdots THP (15)	N-H \cdots O	176	0.1916 ± 0.0009	Phe \cdots AM (23)	O-H \cdots O=C	323	0.5603 ± 0.0039
Ind \cdots AM (6)	N-H \cdots O=C	177	0.0495 ± 0.0007	Phe \cdots NDMA (25)	O-H \cdots O=C	346	0.6819 ± 0.0039
Ind \cdots NMA (7)	N-H \cdots O=C	182	0.0602 ± 0.0005	Phe \cdots Im (28)	O-H \cdots N	420	0.3940 ± 0.0043
Ind \cdots NDMA (8)	N-H \cdots O=C	186	0.1044 ± 0.0006	Phe \cdots Py (29)	O-H \cdots N	436	0.4513 ± 0.0060
Phe \cdots BP (20)	O-H \cdots O=C	191	0.0442 ± 0.0003				

Table S3: List of experimentally observed IR red shifts ($\Delta\nu$) (cm^{-1}) and average H/D exchange rate constants ($k_{\text{ex}}^{\text{H/D}}$) (min^{-1}) of the N–H and O–H groups in all 29 complexes. Average $k_{\text{ex}}^{\text{H/D}}$ values are provided with their uncertainties, obtained from the standard deviation errors from the repeat measurement of the kinetic data.

Complexes Description	Interaction	IR Shift ($\Delta\nu$) (cm^{-1})	H/D exchange rates ($k_{\text{ex}}^{\text{H/D}}$) (min^{-1}) \pm Standard Error	Complexes Description	Interaction	IR Shift ($\Delta\nu$) (cm^{-1})	H/D exchange rates ($k_{\text{ex}}^{\text{H/D}}$) (min^{-1}) \pm Standard Error
Ind \cdots BP (1)	N-H \cdots O=C	35	0.01061 ± 0.00036	Phe \cdots FM (22)	O-H \cdots O=C	170	0.00552 ± 0.00009
Ind \cdots AP (2)	N-H \cdots O=C	86	0.00903 ± 0.00023	7AI \cdots THF (14)	N-H \cdots O	171	0.00567 ± 0.00016
Ind \cdots FM (3)	N-H \cdots O=C	95	0.00834 ± 0.00025	5MI \cdots AM (9)	N-H \cdots O=C	173	0.00580 ± 0.00021
Ind \cdots NMF (4)	N-H \cdots O=C	145	0.00689 ± 0.00017	7AI \cdots THP (15)	N-H \cdots O	176	0.00582 ± 0.00008
Ind \cdots NDMF (5)	N-H \cdots O=C	151	0.00642 ± 0.00011	Ind \cdots AM (6)	N-H \cdots O=C	177	0.00539 ± 0.00016
Ind \cdots THF (12)	N-H \cdots O	160	0.00619 ± 0.00011	Ind \cdots NMA (7)	N-H \cdots O=C	182	0.00519 ± 0.00008
Ind \cdots THP (13)	N-H \cdots O	163	0.00606 ± 0.00015	Ind \cdots NDMA (8)	N-H \cdots O=C	186	0.00494 ± 0.00006

Phe...BP (20)	O-H...O=C	191	0.00500 ± 0.00014	7AI...Py (19)	N-H...N	286	0.00207 ± 0.00011
5CI...AM (10)	N-H...O=C	192	0.00491 ± 0.00021	Phe...THF (26)	O-H...O	287	0.00308 ± 0.00025
5NI...AM (11)	N-H...O=C	220	0.00386 ± 0.00005	Phe...THP (27)	O-H...O	309	0.00245 ± 0.00004
Phe...AP (21)	O-H...O=C	236	0.00360 ± 0.00042	Phe...AM (23)	O-H...O=C	323	0.00221 ± 0.00022
Ind...Im (16)	N-H...N	254	0.00388 ± 0.00013	Phe...NDMA (25)	O-H...O=C	346	0.00216 ± 0.00006
7AI...Im (18)	N-H...N	264	0.00360 ± 0.00031	Phe...Im (28)	O-H...N	420	0.00098 ± 0.00002
Ind...Py (17)	N-H...N	271	0.00348 ± 0.00012	Phe...Py (29)	O-H...N	436	0.00085 ± 0.00018
Phe...NMA (24)	O-H...O=C	283	0.00318 ± 0.00010				

10. References:

1. Pracht, P.; Bohle, F.; Grimme, S., Automated exploration of the low-energy chemical space with fast quantum chemical methods. *Phys. Chem. Chem. Phys.* **2020**, *22* (14), 7169-7192.
2. Grimme, S.; Bannwarth, C.; Shushkov, P., A robust and accurate tight-binding quantum chemical method for structures, vibrational frequencies, and noncovalent interactions of large molecular systems parametrized for all spd-block elements ($Z= 1-86$). *J. Chem. Theory Comput.* **2017**, *13* (5), 1989-2009.
3. Halgren, T. A., Merck molecular force field. I. Basis, form, scope, parameterization, and performance of MMFF94. *J. Comput. Chem.* **1996**, *17* (5-6), 490-519.
4. O'Boyle, N. M.; Banck, M.; James, C. A.; Morley, C.; Vandermeersch, T.; Hutchison, G. R., Open Babel: An open chemical toolbox. *J. Cheminform.* **2011**, *3* (1), 33.
5. Frisch, M. J.; Trucks, G. W.; Schlegel, H. B.; Scuseria, G. E.; Robb, M. A.; Cheeseman, J. R.; Scalmani, G.; Barone, V.; Petersson, G. A.; Nakatsuji, H.; Li, X.; Caricato, M.; Marenich, A. V.; Bloino, J.; Janesko, B. G.; Gomperts, R.; Mennucci, B.; Hratchian, H. P.; Ortiz, J. V.; Izmaylov, A. F.; Sonnenberg, J. L.; Williams; Ding, F.; Lipparini, F.; Egidi, F.; Goings, J.; Peng, B.; Petrone, A.; Henderson, T.; Ranasinghe, D.; Zakrzewski, V. G.; Gao, J.; Rega, N.; Zheng, G.; Liang, W.; Hada, M.; Ehara, M.; Toyota, K.; Fukuda, R.; Hasegawa, J.; Ishida, M.; Nakajima, T.; Honda, Y.; Kitao, O.; Nakai, H.; Vreven, T.; Throssell, K.; Montgomery Jr., J. A.; Peralta, J. E.; Ogliaro, F.; Bearpark, M. J.; Heyd, J. J.; Brothers, E. N.; Kudin, K. N.; Staroverov, V. N.; Keith, T. A.; Kobayashi, R.; Normand, J.; Raghavachari, K.; Rendell, A. P.; Burant, J. C.; Iyengar, S. S.; Tomasi, J.; Cossi, M.; Millam, J. M.; Klene, M.; Adamo, C.; Cammi, R.; Ochterski, J. W.; Martin, R. L.; Morokuma, K.; Farkas, O.; Foresman, J. B.; Fox, D. J. *Gaussian 09*, Revision D.01; Gaussian, Inc.: Wallingford CT, 2009.
6. Dunning Jr, T. H., Gaussian basis sets for use in correlated molecular calculations. I. The atoms boron through neon and hydrogen. *J. Chem. Phys.* **1989**, *90* (2), 1007-1023.
7. Zhao, Y.; Truhlar, D. G., The M06 suite of density functionals for main group thermochemistry, thermochemical kinetics, noncovalent interactions, excited states, and transition elements: two new functionals and systematic testing of four M06-class functionals and 12 other functionals. *Theor. Chem. Acc.* **2008**, *120* (1), 215-241.
8. Miertuš, S.; Scrocco, E.; Tomasi, J., Electrostatic interaction of a solute with a continuum. A direct utilization of AB initio molecular potentials for the prevision of solvent effects. *Chem. Phys.* **1981**, *55* (1), 117-129.
9. Dennington, R.; Keith, T. A.; Millam, J. M. *GaussView 6.0.*, 2016.
10. Saggiu, M.; Levinson, N. M.; Boxer, S. G., Experimental Quantification of Electrostatics in X-H \cdots π Hydrogen Bonds. *J. Am. Chem. Soc.* **2012**, *134* (46), 18986-18997.
11. Whetsel, K. B.; Lady, J. H. Self-Association of Phenol in Nonpolar Solvents. In *Spectrometry of Fuels*; Eriedel, R.A., Eds.; Springer, Boston, MA, 1970, pp 259-279.
12. Stingel, A. M.; Petersen, P. B. Couplings Across the Vibrational Spectrum Caused by Strong Hydrogen Bonds: A Continuum 2D IR Study of the 7-Azaindole-Acetic Acid Heterodimer. *J. Phys. Chem. B* **2016**, *120* (41), 10768-10779.
13. Walmsley, J. A., Self-association of 7-azaindole in nonpolar solvents. *J. phys. Chem.* **1981**, *85* (21), 3181-3187.
14. Xu, J.; Hou, J.; Zhou, W.; Nie, G.; Pu, S.; Zhang, S., ¹H NMR spectral studies on the polymerization mechanism of indole and its derivatives. *Spectrochim. Acta, Part A* **2006**, *63* (3), 723-728.
15. Shirota, H.; Fukuda, T.; Kato, T., Solvent dependence of 7-azaindole dimerization. *J. Phys. Chem. B* **2013**, *117* (50), 16196-16205.

16. Abraham, R. J.; Mobli, M., An NMR, IR and theoretical investigation of ^1H Chemical Shifts and hydrogen bonding in phenols. *Magn. Reson. Chem.* **2007**, *45* (10), 865-877.
17. Jović, B.; Negru, N.; Dimić, D.; Kordić, B., Vibrational Spectroscopic and Quantum-Chemical Study of Indole–Ketone Hydrogen-Bonded Complexes. *Molecules* **2025**, *30* (13), 2685.
18. Kordić, B.; Kovačević, M.; Sloboda, T.; Vidović, A.; Jović, B., FT-IR and NIR spectroscopic investigation of hydrogen bonding in indole-ether systems. *J. Mol. Struct.* **2017**, *1144*, 159-165.
19. Sakota, K.; Shimazaki, Y.; Sekiya, H., Formation of a dual hydrogen bond in the $\text{N}-\text{H}\cdots\text{C}=\text{O}$ moiety in the indole-(N-methylacetamide) 1 cluster revealed by IR-dip spectroscopy with natural bond orbital analysis. *J. Chem. Phys.* **2009**, *130* (23), 231105.
20. Thijs, R.; Zeegers-Huyskens, T., Infrared and Raman studies of hydrogen bonded complexes involving acetone, acetophenone and benzophenone—I. Thermodynamic constants and frequency shifts of the νOH and νCO stretching vibrations. *Spectrochim. Acta A* **1984**, *40* (3), 307-313.
21. Kumar, S.; Mukherjee, A.; Das, A., Structure of indole \cdots imidazole heterodimer in a supersonic jet: a gas phase study on the interaction between the aromatic side chains of tryptophan and histidine residues in proteins. *J. Phys. Chem. A* **2012**, *116* (47), 11573-11580.
22. Kumar, S.; Biswas, P.; Kaul, I.; Das, A., Competition between hydrogen bonding and dispersion interactions in the indole \cdots pyridine dimer and (Indole) $_2\cdots$ pyridine trimer studied in a supersonic jet. *J. Phys. Chem. A* **2011**, *115* (26), 7461-7472.
23. Epley, T. D.; Drago, R. S., Calorimetric studies on some hydrogen-bonded adducts. *J. Am. Chem. Soc.* **1967**, *89* (23), 5770-5773.
24. Drago, R. S.; Epley, T. D., Enthalpies of hydrogen bonding and changes in hydroxy frequency shifts for a series of adducts with substituted phenols. *J. Am. Chem. Soc.* **1969**, *91* (11), 2883-2890.

11. Cartesian co-ordinate of optimized structures of the series of hydrogen-bonded complexes:

11.1. Cartesian co-ordinate of optimized structures of the series of N-H \cdots O=C hydrogen-bonded complexes (1-11):

Ind \cdots BP

C	2.81817800	-0.98413700	0.24994300
C	1.68563600	-1.34857000	-0.51649400
C	0.58102900	-1.99693800	0.04388100
C	0.61497600	-2.25592200	1.40195900
C	1.72768400	-1.89311300	2.18669500
C	2.82655000	-1.27079700	1.62350700
C	3.73639300	-0.34297000	-0.64900400
C	3.13932000	-0.32750000	-1.87648600
H	-0.27064500	-2.27999000	-0.56433600
H	-0.22762000	-2.75162200	1.87002400
H	1.72127100	-2.11605600	3.24714100
H	3.68123400	-1.00161200	2.23409700
H	4.70987300	0.05544200	-0.41177700
H	3.49288700	0.08011000	-2.81073000
N	1.91382700	-0.95142700	-1.81154600
O	-0.84182000	0.07085000	-2.16545100
H	1.17867800	-0.86143500	-2.49895500
C	-1.12029100	0.48422100	-1.05441600
C	-2.46701800	0.19288700	-0.46906600
C	-3.13253400	-0.96138200	-0.88817900
C	-3.09203000	1.06444500	0.42481300
C	-4.39589900	-1.25690400	-0.39663000
H	-2.64490900	-1.61252300	-1.60424900
C	-4.36752200	0.77803700	0.89914400
H	-2.59005700	1.97415900	0.73220300
C	-5.01469200	-0.38585200	0.49763900
H	-4.90320100	-2.16021000	-0.71345300
H	-4.85558600	1.46341100	1.58151100
H	-6.00448400	-0.61241200	0.87633600
C	-0.12058600	1.25966400	-0.26023200
C	-0.05404200	1.15885100	1.13227300
C	0.84179300	2.00009500	-0.94872400
C	0.97035000	1.79175500	1.82439500
H	-0.76738100	0.54260500	1.66597300
C	1.85109500	2.64944200	-0.25208600
H	0.78967700	2.04738000	-2.03037400
C	1.91756600	2.54215400	1.13432600
H	1.03926200	1.68331000	2.89997900
H	2.59644200	3.22358200	-0.78916500
H	2.71660300	3.03424800	1.67664000

Ind...AP

C	-1.99782700	-0.08164800	0.15778600
C	-1.07738500	-0.98982700	0.73346300
C	-0.55995800	-2.07901200	0.02664600
C	-0.95789200	-2.23133000	-1.28945300
C	-1.86190300	-1.33122800	-1.88811400
C	-2.38934100	-0.26983900	-1.17628700
C	-2.30614400	0.89032600	1.16863500
C	-1.57179800	0.55956500	2.27044900
H	0.12646000	-2.77432500	0.49746900
H	-0.57810400	-3.06558900	-1.86857400
H	-2.15418300	-1.48449900	-2.92018200
H	-3.09033700	0.41316500	-1.64276500
H	-2.97939300	1.72817000	1.08314300
H	-1.50619500	1.04955100	3.22934800
N	-0.84336800	-0.58308100	2.02389800
O	2.14818600	-0.87296900	1.68898000
H	-0.06450400	-0.90605800	2.57941400
C	2.20115100	-0.67872300	0.49137400
C	1.55765300	0.52643600	-0.11716300
C	1.25674400	0.58571400	-1.47960100
C	1.19874600	1.58601900	0.71743000
C	0.58400200	1.68610100	-1.99555600
H	1.51031200	-0.23955400	-2.13398300
C	0.54225300	2.69171000	0.19724200
H	1.43417100	1.51925500	1.77304300
C	0.22790900	2.73881000	-1.15838400
H	0.32763600	1.71672600	-3.04765500
H	0.26093000	3.51036800	0.84879200
H	-0.29847300	3.59583100	-1.56235400
C	2.90659800	-1.65519200	-0.42049200
H	2.17733200	-2.13630500	-1.07760000
H	3.63310700	-1.13870900	-1.05120000
H	3.40249200	-2.41000700	0.18612700

Ind...FM

C	-0.45880300	0.19233900	-0.45623600
C	-1.62628400	0.64073200	0.20878500
C	-2.63216700	-0.29103900	0.51026100
C	-2.44858500	-1.61510900	0.15809000
C	-1.27782000	-2.03910800	-0.50151400
C	-0.27062000	-1.14620900	-0.82185800
C	-1.46178100	2.05061700	0.42238900
H	-3.53911200	0.02507500	1.01297500
H	-3.21802900	-2.34273700	0.38667800
H	-1.16887800	-3.08289700	-0.77091200
H	0.62868400	-1.45819900	-1.34120100

H	1.31577600	1.20553100	-0.97124300
H	-2.15829600	2.72417200	0.89499200
C	-0.24223500	2.38771600	-0.09467500
H	0.25242100	3.34583000	-0.12463600
N	0.36319800	1.27816800	-0.63333600
C	3.24069300	-0.45663200	0.33412500
N	2.32718600	-0.79671500	1.26446500
O	2.98735400	0.05967900	-0.73659000
H	1.33934900	-0.67066200	1.07786400
H	2.60728500	-1.24437500	2.12045400
H	4.27487900	-0.68919700	0.63364500

Ind...NMF

C	-0.83576400	0.31730600	-0.48641000
C	-1.93522400	0.40935200	0.40170500
C	-2.73103700	-0.72818300	0.61174300
C	-2.41197100	-1.90163500	-0.04546000
C	-1.31149000	-1.97059800	-0.92318100
C	-0.51194600	-0.86679200	-1.16025100
C	-1.94818000	1.75505400	0.90097100
H	-3.58296400	-0.68511700	1.28077500
H	-3.01913700	-2.78545300	0.10954600
H	-1.09421600	-2.90361800	-1.42944200
H	0.32905600	-0.90323500	-1.84380100
H	0.66768100	1.70945400	-0.98003000
H	-2.65223800	2.18689200	1.59383500
C	-0.88964200	2.39956800	0.32382100
H	-0.55285500	3.41705300	0.44597000
N	-0.22080200	1.54508600	-0.51874700
C	3.00148200	0.20683400	-0.39346900
N	2.33537600	-0.45457300	0.56967900
O	2.48937200	0.89496300	-1.25911200
H	1.32274300	-0.39648200	0.54866100
H	4.09443600	0.07097800	-0.33398000
C	2.96551200	-1.28734600	1.57497600
H	2.74360200	-0.92239200	2.57890500
H	2.63051100	-2.32238600	1.48975400
H	4.04594700	-1.26035100	1.42951400

Ind...NDMF

C	-0.77017600	0.38695500	-0.71967400
C	-1.70860100	0.62332300	0.31364500
C	-2.53799200	-0.43117800	0.73046700
C	-2.41504500	-1.66450500	0.11844600
C	-1.48519900	-1.87230500	-0.92075200
C	-0.65742100	-0.85404200	-1.35643400

C	-1.55747500	1.99869700	0.70099600
H	-3.26737700	-0.27624100	1.51739600
H	-3.05117200	-2.48437700	0.42977100
H	-1.42742800	-2.84540700	-1.39420800
H	0.04192000	-1.00065000	-2.17157100
H	0.77887000	1.61410100	-1.45892300
H	-2.12152400	2.53114200	1.44986000
C	-0.55994400	2.51827000	-0.07503100
H	-0.13673000	3.51058800	-0.08095200
N	-0.09045100	1.55994900	-0.94228900
C	2.34999500	-0.55642900	-0.61258600
N	1.98412200	-0.60217500	0.68333000
O	2.62004900	0.45145800	-1.24499700
H	2.39037700	-1.55726400	-1.07263300
C	1.40867900	-1.80270300	1.25777400
H	1.87639100	-2.02031800	2.22100500
H	0.32984900	-1.67087400	1.39896000
H	1.56943000	-2.64671500	0.58670100
C	1.83411300	0.61504500	1.45971000
H	2.33213900	0.49350300	2.42482900
H	2.28964000	1.43909100	0.91467700
H	0.77392700	0.83057100	1.62839800

Ind...AM

C	-0.92358700	0.18378500	-0.43101700
C	-2.12208600	0.52471700	0.24244400
C	-3.04005400	-0.49355600	0.54489600
C	-2.74300800	-1.79445900	0.18407800
C	-1.54361900	-2.11056900	-0.48483300
C	-0.62093800	-1.13102200	-0.80550500
C	-2.08102100	1.94274800	0.46071000
H	-3.96824300	-0.26092200	1.05442000
H	-3.44411900	-2.58811200	0.41296500
H	-1.34546600	-3.13937300	-0.76108300
H	0.29827500	-1.35906800	-1.33366500
H	0.75054400	1.34874400	-0.96182000
H	-2.83093700	2.55064900	0.94065100
C	-0.89896000	2.38771200	-0.06264600
H	-0.49135500	3.38602100	-0.09208200
N	-0.20072800	1.33807300	-0.60825200
C	2.91541600	-0.12715500	0.11550100
N	2.08733100	-0.52136200	1.11091400
H	1.08638600	-0.43033200	0.99115400
H	2.43260100	-1.00133400	1.92362600
C	4.38730900	-0.40307200	0.31930900
H	4.94562700	0.49489400	0.05839800
H	4.63190600	-0.70755600	1.33657900
H	4.68409800	-1.19321100	-0.37250900

O 2.50846900 0.41348100 -0.90161300

Ind···NMA

C -1.20080800 0.30341800 -0.46249100
C -2.35111300 0.43304100 0.35374100
C -3.18750800 -0.68162200 0.52432600
C -2.85873800 -1.86991600 -0.10083700
C -1.70827700 -1.97608600 -0.90782800
C -0.86728700 -0.89551200 -1.10447800
C -2.36077700 1.78447800 0.83689900
H -4.07822500 -0.60972500 1.13814100
H -3.49712700 -2.73637100 0.02411600
H -1.48476700 -2.91957300 -1.39152600
H 0.01189400 -0.96015600 -1.73601000
H 0.36391900 1.65261200 -0.88364800
H -3.09493500 2.24175600 1.48048800
C -1.25209000 2.39537900 0.31990800
H -0.89826100 3.40588700 0.45168600
N -0.55357300 1.51480000 -0.46952300
C 2.71613000 0.20361400 -0.30406700
N 2.00834000 -0.47979700 0.62515900
H 1.00213600 -0.37874300 0.57481000
C 4.21793100 0.03992400 -0.26094200
H 4.65622000 0.72773700 -0.97888700
H 4.61126700 0.24210000 0.73714200
H 4.49293400 -0.98351100 -0.52739400
O 2.17138000 0.90829300 -1.14573500
C 2.56471200 -1.32471900 1.66605500
H 3.08179800 -0.74206500 2.43325800
H 1.74679800 -1.86432300 2.13959200
H 3.25889100 -2.05898800 1.25294300

Ind···NDMA

C -1.04429800 0.16199600 -0.74750200
C -2.11618700 0.15597600 0.17673400
C -2.59493800 -1.07682400 0.65049300
C -2.00562700 -2.24377700 0.20101200
C -0.94904300 -2.21395900 -0.73219000
C -0.46006900 -1.01665100 -1.22200500
C -2.45998100 1.53055000 0.41513800
H -3.41718300 -1.11090000 1.35619400
H -2.36764500 -3.20036800 0.55843200
H -0.52337200 -3.14772600 -1.08159100
H 0.33317100 -0.98311600 -1.96000400
H 0.11194400 1.75773600 -1.47993900
H -3.24343200 1.90574600 1.05381400

C	-1.60467100	2.28577000	-0.33740100
H	-1.52599200	3.35840500	-0.42221100
N	-0.76238400	1.47035900	-1.05582300
C	2.27135600	0.22698700	-0.31851800
N	1.83106900	0.21315500	0.96691700
C	2.96952600	-1.02093600	-0.82533200
H	3.28030500	-0.82658800	-1.84890600
H	3.84778200	-1.25022000	-0.21835300
H	2.30385500	-1.88568200	-0.80355300
O	2.14695500	1.20523500	-1.04851400
C	1.65884400	-1.00678400	1.73882000
H	1.80627800	-0.77782500	2.79598500
H	0.64691200	-1.40759300	1.60140600
H	2.38520200	-1.76319800	1.45327600
C	1.13684200	1.37045300	1.50956900
H	1.31877000	2.22980100	0.86998100
H	0.05944900	1.18300900	1.56960700
H	1.51699400	1.57522300	2.51342400

5MI···AM

C	-0.50464100	0.56217100	-0.47269900
C	-1.61627100	1.10551200	0.21076300
C	-2.73284900	0.28570300	0.45001400
C	-2.72685800	-1.03100200	0.02575300
C	-1.59500500	-1.54180700	-0.65265500
C	-0.48214900	-0.76631500	-0.91481600
C	-1.28705200	2.46967900	0.50965600
H	-3.59939500	0.68470800	0.96752200
H	-1.61063200	-2.57505900	-0.98437700
H	0.37617900	-1.16026300	-1.44783200
H	1.38613200	1.38020400	-0.92435000
H	-1.90334700	3.19317900	1.01868000
C	-0.02882700	2.68845300	0.01883700
H	0.57651800	3.58080500	0.04885300
N	0.44599200	1.54907400	-0.58190200
C	3.16545700	-0.54646200	0.13619200
N	2.23944800	-0.78798800	1.09339800
H	1.28439800	-0.48408900	0.95091300
H	2.45050800	-1.34961900	1.89963100
C	4.53952500	-1.13065900	0.37118900
H	5.28221900	-0.36688500	0.14525200
H	4.68367600	-1.49747100	1.38711800
H	4.68340900	-1.95414700	-0.33046000
O	2.91578400	0.09617800	-0.87225000
C	-3.91112300	-1.93421400	0.26575500
H	-4.33652500	-2.28249400	-0.67905700
H	-3.62279500	-2.81786800	0.84093900
H	-4.69593900	-1.41437400	0.81676300

5CI...AM

C	-0.11447600	0.75479100	-0.45101600
C	-1.19874000	1.40833600	0.18342900
C	-2.39935200	0.70716100	0.37827400
C	-2.46249700	-0.59889200	-0.05645300
C	-1.38456700	-1.24409000	-0.68800500
C	-0.19650700	-0.56901000	-0.89602400
C	-0.75492800	2.73615600	0.49302500
H	-3.25460500	1.16967700	0.85452400
H	-1.50168000	-2.26879000	-1.01549600
H	0.64234600	-1.04171300	-1.39391100
H	1.85747700	1.38721800	-0.83547600
H	-1.32066100	3.51744300	0.97392600
C	0.53797300	2.82901200	0.05590400
H	1.22350700	3.66015100	0.10898600
N	0.92817900	1.64540300	-0.51841100
C	3.39980400	-0.78395800	0.14553100
N	2.48338700	-0.93374200	1.13052100
H	1.57904900	-0.48942000	1.03948600
H	2.63487500	-1.56154200	1.90077200
C	4.68059100	-1.57084300	0.29564400
H	5.51800800	-0.91347000	0.06649800
H	4.80817900	-2.00000300	1.28901500
H	4.67483400	-2.37406600	-0.44329500
O	3.20830500	-0.06426800	-0.82323900
Cl	-3.94426700	-1.50382000	0.17613200

5NI...AM

C	0.14270800	0.82955600	-0.43987400
C	-0.93681800	1.55944600	0.12427900
C	-2.16854100	0.92277800	0.29828700
C	-2.26181100	-0.39901300	-0.08958300
C	-1.19804800	-1.12388600	-0.65392000
C	0.02205400	-0.50928200	-0.83905500
C	-0.44416700	2.87851000	0.39886300
H	-3.02821500	1.42542100	0.72083700
H	-1.36076500	-2.15293300	-0.94140900
H	0.85828400	-1.03209100	-1.28789700
H	2.14724500	1.35395800	-0.77926900
H	-0.99222700	3.70279700	0.82498400
C	0.86534700	2.89310400	0.01214200
H	1.58809800	3.69235300	0.05753200
N	1.22142500	1.66511200	-0.49665600
C	3.61685600	-0.87700000	0.17613100
N	2.70849800	-1.04154900	1.16601600

H	1.82196400	-0.55844900	1.11194100
H	2.85283700	-1.69827000	1.91336400
C	4.87748200	-1.70176400	0.27525200
H	5.73145800	-1.04555100	0.11218200
H	4.98333200	-2.21496000	1.23039300
H	4.86565500	-2.43859200	-0.52950800
O	3.43184000	-0.11184400	-0.75906500
N	-3.54854900	-1.08985300	0.09640300
O	-4.47214500	-0.45434500	0.56138300
O	-3.61315100	-2.25935500	-0.22339600

11.2. Cartesian co-ordinate of optimized structures of the series of N–H···O hydrogen-bonded complexes (12–15):

Ind···THF

C	2.23974500	0.59764400	1.03483600
O	2.16160300	0.93293200	-0.35889600
C	2.98764700	0.05258200	-1.12865600
C	3.40021600	-1.06981100	-0.17857000
C	3.43865000	-0.33626500	1.16480400
H	2.34200800	1.52268800	1.60357900
H	1.30959300	0.09822400	1.32918400
H	2.41591500	-0.29417200	-1.99220600
H	3.85905900	0.61077600	-1.48566700
H	2.63894100	-1.85386800	-0.15565700
H	4.35243100	-1.52097400	-0.45696300
H	3.35651700	-1.00112400	2.02419800
H	4.36275100	0.24011900	1.25562200
C	-1.18473900	0.16544200	-0.26899700
C	-2.53357100	0.31837600	0.13249600
C	-3.30920700	-0.83109800	0.35045300
C	-2.73388300	-2.07470800	0.16877300
C	-1.39013800	-2.20359600	-0.23509200
C	-0.60076100	-1.09082600	-0.46059600
C	-2.77781800	1.73023300	0.22175200
H	-4.34527000	-0.74281100	0.65720000
H	-3.32330900	-2.96853500	0.33428800
H	-0.97148100	-3.19312200	-0.37626200
H	0.42965300	-1.17989500	-0.78547600
H	0.32998000	1.58565400	-0.62786700
H	-3.69971000	2.21646800	0.49736100
C	-1.60896200	2.35406500	-0.11374000
H	-1.38017300	3.40705400	-0.16447400
N	-0.64754300	1.41969100	-0.41578300

Ind···THP

O	-1.79990400	0.39838800	0.44429900
C	-2.59193700	-0.55305600	1.13866000
H	-2.28801900	-1.56428500	0.83579400
H	-2.36125000	-0.43935700	2.19789000
C	-4.08170400	-0.31958600	0.84787600
H	-4.50755000	0.36751300	1.58170300
H	-4.61582400	-1.26939800	0.94303200
C	-4.24810700	0.25123100	-0.57162500
H	-4.15539500	1.34028900	-0.54242000
H	-5.24027300	0.02280100	-0.96396700
C	-3.15372200	-0.31396600	-1.47684100

H	-3.28257300	0.00549000	-2.51257300
H	-3.20714400	-1.40716200	-1.47264900
C	-1.78550200	0.16038300	-0.96680300
H	-1.51577800	1.11755100	-1.41709400
H	-0.99542100	-0.56384100	-1.20064100
C	1.61606100	0.13273800	0.30722400
C	2.91086600	0.49710400	-0.13316500
C	3.83588500	-0.51690700	-0.42806100
C	3.45476100	-1.83711600	-0.28086100
C	2.16095400	-2.17675600	0.16261400
C	1.22795100	-1.20191100	0.46389300
C	2.94512800	1.93197000	-0.16750100
H	4.83496900	-0.26576400	-0.76583100
H	4.16015000	-2.62815300	-0.50553000
H	1.89608300	-3.22161600	0.27380900
H	0.23461500	-1.45338800	0.81820000
H	-0.07118200	1.30285600	0.77920300
H	3.77549700	2.55781500	-0.45237600
C	1.71363800	2.36528300	0.23684000
H	1.33820700	3.37096500	0.34381200
N	0.91064200	1.28915900	0.53025000

7AI...THF

C	2.45030000	0.25987600	-1.21372400
O	2.21529500	1.14537300	-0.10462700
C	2.54711400	0.48478500	1.12216300
C	3.54016400	-0.59989400	0.72838100
C	2.96638600	-1.05192700	-0.61833900
H	1.51368000	0.12287400	-1.75970400
H	3.18594000	0.73634600	-1.86706200
H	2.95180600	1.23356100	1.80367100
H	1.63991100	0.04426000	1.55140700
H	4.53722700	-0.17010700	0.60187900
H	3.59485500	-1.40309500	1.46330700
H	3.70275500	-1.53486700	-1.26081600
H	2.12776900	-1.73028800	-0.45580400
C	-1.11604000	0.14877800	-0.01181900
C	-2.52968700	0.27531700	0.02961500
C	-3.26298700	-0.91221800	0.07125000
C	-2.55740700	-2.10487200	0.06861800
C	-1.15389500	-2.08969600	0.02516800
C	-2.81446300	1.67990400	0.01451500
H	-4.34665900	-0.90420400	0.10435400
H	-3.07363500	-3.05568100	0.09980000
H	-0.60618800	-3.02732700	0.02314300
H	0.42619500	1.58300400	-0.08094000
H	-3.78257100	2.15327000	0.03563200
C	-1.60642300	2.31960700	-0.03371800

H	-1.39264800	3.37656500	-0.05929200
N	-0.58006700	1.40625700	-0.04990200
N	-0.41695600	-0.98415100	-0.01513000

7AI...THP

O	-1.92874800	1.01610400	-0.14925200
C	-2.09841900	0.33961400	1.09562900
H	-1.45570900	-0.54737000	1.10749000
H	-1.74106600	1.02411300	1.86584700
C	-3.57316700	-0.02600100	1.30331400
H	-4.10418000	0.79342200	1.79203700
H	-3.62929700	-0.89295400	1.96803400
C	-4.22724700	-0.34567100	-0.05355800
H	-4.62928700	0.57189100	-0.49249900
H	-5.06393200	-1.03445300	0.07456400
C	-3.17560900	-0.92333200	-1.00014900
H	-3.61646400	-1.23736000	-1.94843600
H	-2.72046700	-1.81030500	-0.54868800
C	-2.10710000	0.14183500	-1.27145100
H	-2.41669000	0.79238800	-2.09202400
H	-1.14696800	-0.32343800	-1.51984200
C	1.54088700	0.10745500	-0.02497000
C	2.94153100	0.33448600	0.02488500
C	3.75677900	-0.79566100	0.11247500
C	3.13755500	-2.03472500	0.14314300
C	1.73707800	-2.12055400	0.08616200
C	3.12956300	1.75415200	-0.03370700
H	4.83665500	-0.70881100	0.15495100
H	3.71931800	-2.94496500	0.21049700
H	1.25679100	-3.09369200	0.10972200
H	-0.09187800	1.44656200	-0.15609200
H	4.06279600	2.29325200	-0.01863400
C	1.88166800	2.30691400	-0.11381900
H	1.59534800	3.34505600	-0.17538400
N	0.92030200	1.32444100	-0.10919100
N	0.92454200	-1.07204600	0.00272600

11.3. Cartesian co-ordinate of optimized structures of the series of N–H···N hydrogen-bonded complexes (16–19):

Ind···Im

C	3.59173100	0.41442400	-0.80896000
C	2.30669300	-0.21167700	0.78833000
C	3.50730100	-0.82113500	1.01470300
N	4.32141700	-0.41091000	-0.01545000
H	5.28284300	-0.67533400	-0.15779300
H	3.99493600	0.87683400	-1.69611500
H	1.39727400	-0.28062500	1.36567200
H	3.84765100	-1.48762300	1.78795800
N	2.37288300	0.55548000	-0.35201400
C	-1.21877200	0.14178400	-0.26303700
C	-2.52326900	0.49825700	0.15764600
C	-3.48939000	-0.51059000	0.29855500
C	-3.13856700	-1.81907100	0.02514100
C	-1.83446100	-2.15098000	-0.39338100
C	-0.86056300	-1.18113100	-0.54485800
C	-2.51863800	1.92040500	0.35016200
H	-4.49590200	-0.26448700	0.61773100
H	-3.87571600	-2.60616900	0.13051300
H	-1.59277400	-3.18609600	-0.60421300
H	0.14209200	-1.42843400	-0.87424300
H	-3.34309300	2.53846900	0.66750300
C	-1.25631100	2.35285500	0.05205100
H	-0.84703200	3.35075600	0.07626100
N	-0.46974000	1.29106900	-0.32219400
H	0.52328400	1.31438600	-0.54378600

Ind···Py

C	3.26650700	0.67909500	-0.99259400
C	4.38819500	-0.01517800	-0.55443700
C	4.28205200	-0.78652300	0.59647200
C	3.06283600	-0.83264200	1.25990400
C	1.99882800	-0.10225400	0.74244300
N	2.09170900	0.64157700	-0.36214500
H	5.13449700	-1.34258800	0.96858700
H	3.31055500	1.29064600	-1.88789900
H	5.31748500	0.05059200	-1.10561400
H	2.93064400	-1.42079700	2.15882500
H	1.02610500	-0.11544600	1.22731100
C	-2.79173500	0.45228100	0.19694900
C	-1.49504300	0.15704300	-0.28899800
C	-1.11462700	-1.13569700	-0.66539800
C	-2.05870700	-2.13865200	-0.54269900

C	-3.35477400	-1.86765900	-0.06083400
C	-3.72755100	-0.58835100	0.30602800
C	-2.81422300	1.85935900	0.48030900
H	-0.11965900	-1.33630000	-1.04625000
H	-1.79965800	-3.15172300	-0.82682600
H	-4.06852200	-2.67885700	0.01906200
H	-4.72786200	-0.38935900	0.67363500
H	-3.64199600	2.43450600	0.86286100
H	0.21061200	1.38724400	-0.54096900
C	-1.57415300	2.34292200	0.16971500
H	-1.18838700	3.34764800	0.24461500
N	-0.77591400	1.32727400	-0.29906800

7AI...Im

C	2.39680100	-0.71897100	0.00034300
C	3.72054100	0.97217900	-0.00080100
C	4.52462600	-0.13121400	-0.00013000
N	3.66369400	-1.20454600	0.00062500
H	3.92230800	-2.17774100	0.00130600
H	1.50675900	-1.33500100	0.00060800
H	4.01404700	2.00908200	-0.00141700
H	5.59434900	-0.24861400	-0.00016300
N	2.39941700	0.59357700	-0.00046500
C	-1.27368900	0.09435900	0.00005200
C	-2.62256200	0.54332700	-0.00008100
C	-3.61295300	-0.44011100	-0.00022900
C	-3.20598200	-1.76469500	-0.00028500
C	-1.83735000	-2.07629900	-0.00014900
C	-2.57701700	1.97480200	0.00012400
H	-4.66526900	-0.17877700	-0.00028200
H	-3.93026800	-2.56903200	-0.00040200
H	-1.52392600	-3.11567600	-0.00019400
H	-3.41076300	2.65787800	0.00009200
C	-1.25241100	2.31725600	0.00039200
H	-0.79986400	3.29648500	0.00056500
N	-0.46256600	1.19445400	0.00048200
H	0.56343200	1.16393700	-0.00012300
N	-0.86209200	-1.17296100	0.00001500

7AI...Py

C	3.31209200	1.22169200	0.00021300
C	4.54615100	0.58339700	-0.00030300
C	4.57137800	-0.80621500	-0.00044800
C	3.36645100	-1.49563200	-0.00008300
C	2.17995200	-0.76880100	0.00041700
N	2.15001500	0.56697800	0.00058800

H	5.51432400	-1.34044500	-0.00085600
H	3.25269100	2.30539100	0.00036300
H	5.45920000	1.16484000	-0.00061500
H	3.33656800	-2.57767500	-0.00019300
H	1.21156900	-1.26365400	0.00066800
C	-2.93753800	0.56336300	-0.00017800
C	-1.60391100	0.07406500	-0.00004400
C	-2.22743300	-2.07792200	0.00010800
C	-3.58697600	-1.72674300	-0.00004400
C	-3.95628300	-0.39139800	-0.00016100
C	-2.84908000	1.99332900	-0.00013400
H	-1.94308100	-3.12548500	0.00018000
H	-4.33403700	-2.50999200	-0.00004000
H	-5.00068100	-0.10016500	-0.00024100
H	-3.66195800	2.70115700	-0.00023700
H	0.26344200	1.09022200	0.00016200
C	-1.51539000	2.29671200	-0.00003100
H	-1.03473400	3.26249300	0.00003100
N	-0.75951700	1.14987900	0.00001100
N	-1.22760900	-1.20282200	0.00010200

**11.4. Cartesian co-ordinate of optimized structures of the series of O–H···O=C
hydrogen-bonded complexes (20–25):**

Phe···BP

O	0.64912700	-0.02131000	2.16649700
C	0.84521900	0.45507300	1.06079200
C	2.15934000	0.24082000	0.38340600
C	2.89541200	-0.89675300	0.72324800
C	2.68447200	1.15874900	-0.52849800
C	4.13180500	-1.12801400	0.13795800
H	2.48307800	-1.58538000	1.45115300
C	3.93341800	0.93565900	-1.09746600
H	2.12680300	2.05424500	-0.77585200
C	4.65173300	-0.21045300	-0.77248000
H	4.69485800	-2.01746700	0.39371200
H	4.34572400	1.65624800	-1.79331800
H	5.62068600	-0.38703800	-1.22455500
C	-0.22962200	1.22596200	0.36968100
C	-0.40380800	1.15411700	-1.01471500
C	-1.14549200	1.93356800	1.15094000
C	-1.48351000	1.79343600	-1.61046700
H	0.27443100	0.56007700	-1.61592600
C	-2.21112200	2.58802000	0.54981300
H	-1.01438200	1.95342800	2.22635700
C	-2.38061300	2.51689500	-0.83088200
H	-1.63296300	1.71289500	-2.68037100
H	-2.91592900	3.14369300	1.15642400
H	-3.22054000	3.01779700	-1.29822900
C	-0.88167500	-2.09023400	0.32016400
C	-1.96784400	-1.37084300	0.82367800
C	-3.02822400	-1.03802300	-0.01692300
C	-2.98724700	-1.40118400	-1.35677200
C	-1.89348200	-2.09183000	-1.87334700
C	-0.84503200	-2.43739300	-1.02573800
H	-0.07262000	-2.36820300	0.98684400
H	-3.85867000	-0.47745500	0.39494600
H	-3.81233100	-1.13110000	-2.00617500
H	-1.86361700	-2.36622700	-2.92064800
H	0.00713500	-2.98676500	-1.40983600
O	-2.03485700	-0.97902700	2.12283500
H	-1.13818900	-0.80148300	2.44645300

Phe···AP

O	0.43112900	-2.54584900	0.77127800
C	0.66485900	-1.97057100	-0.27465700
C	1.29153300	-0.61436600	-0.27463900

C	1.20157900	0.22988800	-1.38263400
C	1.92248100	-0.16768000	0.88899600
C	1.72529400	1.51583200	-1.32168900
H	0.69605300	-0.09850500	-2.28301900
C	2.45771800	1.11036800	0.94241700
H	1.97360500	-0.83039700	1.74419400
C	2.35386500	1.95484500	-0.16133400
H	1.63547500	2.17634500	-2.17560100
H	2.94886000	1.45373600	1.84494700
H	2.76351900	2.95729300	-0.11552300
C	-2.08360700	-0.62778700	0.19826300
C	-1.39756500	0.09983600	1.17165400
C	-1.20803300	1.47147200	1.01012300
C	-1.68019900	2.10305800	-0.13193100
C	-2.34270100	1.37982300	-1.12203600
C	-2.54592100	0.01493300	-0.94623100
H	-2.24528800	-1.69104600	0.34288500
H	-0.66720900	2.01279400	1.77682100
H	-1.51822300	3.16763600	-0.25633200
H	-2.70503000	1.87669900	-2.01349800
H	-3.07853700	-0.55615100	-1.69885100
O	-0.89570300	-0.48434800	2.29142700
H	-0.63278700	-1.39348000	2.08721100
C	0.29928200	-2.59964400	-1.59603100
H	-0.53576100	-2.04489500	-2.03409900
H	1.13455400	-2.55828600	-2.29732900
H	-0.00415700	-3.63020900	-1.42507700

Phe···FM

H	1.25434700	-0.42425200	-1.22123000
C	3.00732500	0.45688700	0.42399700
N	2.55169200	-0.57267500	1.16090900
H	1.84178400	-1.18536500	0.77491800
H	2.86352800	-0.70499600	2.10761100
O	2.64973300	0.70968000	-0.71291500
H	3.75582900	1.07545400	0.94088100
C	-0.53561800	-0.47192500	-0.51833000
C	-1.58468100	-1.27742800	-0.07793700
C	-0.64347200	0.91732400	-0.45405300
C	-2.73763400	-0.69063200	0.42628400
H	-1.47990700	-2.35350500	-0.14679700
C	-1.80434300	1.49073500	0.05471500
H	0.17755000	1.53405800	-0.80310900
C	-2.85561200	0.69525100	0.49739300
H	-3.55159700	-1.32180000	0.76353600
H	-1.88484000	2.57058700	0.10042600
H	-3.75715200	1.14838000	0.89011800
O	0.58062000	-1.09106900	-0.99272600

Phe···AM

C	-0.92396000	-0.36836800	-0.88471800
C	-1.88778500	-1.36713200	-0.76999500
C	-3.01626700	-1.17922400	0.01928200
C	-3.17586800	0.02730800	0.69923300
C	-2.22097800	1.02900200	0.60036800
C	-1.08636400	0.83619400	-0.19230300
H	-3.76440600	-1.95765400	0.10068300
H	-4.05356100	0.18932700	1.31431500
H	-2.32986500	1.97074800	1.12429700
C	2.61395600	-0.14721000	0.10236100
O	2.20788000	0.58035800	-0.79380700
N	1.79509200	-0.66158600	1.04594800
H	-0.05142700	-0.50548700	-1.51438000
H	-1.75415700	-2.29543800	-1.31356800
O	-0.18192800	1.83806300	-0.25499900
H	0.65400800	1.50808400	-0.63450400
C	4.07512900	-0.51352500	0.19957800
H	4.65518700	0.40801600	0.24820300
H	4.30834500	-1.13842500	1.06094600
H	4.35718300	-1.03512300	-0.71555800
H	2.13886200	-1.27473000	1.76423800
H	0.79941300	-0.48784700	0.99131000

Phe···NMA

C	-1.29167100	-1.06006800	0.01201800
C	-2.28570600	-1.26513300	0.96355200
C	-3.32157200	-0.35044600	1.12007000
C	-3.35708000	0.78163600	0.30938100
C	-2.37114400	1.00089000	-0.64315100
C	-1.33505600	0.07906500	-0.79378800
H	-4.09355400	-0.51851800	1.86050700
H	-4.16150700	1.50006200	0.41718300
H	-2.38808600	1.87303100	-1.28563600
C	2.37582200	-0.40227500	-0.18984700
O	1.81670100	-1.09481000	-1.03728200
H	-0.48607300	-1.77429900	-0.11839000
H	-2.24910400	-2.15356600	1.58352100
O	-0.38766300	0.34160800	-1.73154700
H	0.31860800	-0.33515200	-1.69177000
N	1.96039200	0.85113500	0.09569200
H	1.17025800	1.18341200	-0.44553100
C	2.55438600	1.73264700	1.08425300
H	3.53998100	2.08978500	0.77380300
H	1.90194700	2.59443400	1.20963900

H	2.64612600	1.23698200	2.05227300
C	3.55393600	-0.92516900	0.59539600
H	4.39230500	-0.22683600	0.56766000
H	3.27177400	-1.06911700	1.64127600
H	3.85078800	-1.87943100	0.16895000

Phe···NDMA

C	1.70016100	-0.85172200	-0.46233300
C	2.74275600	-0.78928200	-1.38140600
C	3.88138600	-0.03588900	-1.11655900
C	3.96948900	0.65960600	0.08756900
C	2.93593800	0.60950200	1.01267000
C	1.79388100	-0.14584900	0.74037800
H	4.69054800	0.00650600	-1.83484800
H	4.85281600	1.24756100	0.30937400
H	2.99091800	1.14400800	1.95329700
C	-2.50306500	-0.61762900	0.07116900
O	-1.46448300	-1.15426500	0.45241300
H	0.81500200	-1.44711600	-0.65862200
H	2.66286200	-1.34197300	-2.31064000
O	0.81063600	-0.16453800	1.66863600
H	0.02130700	-0.60587700	1.30468000
N	-2.53114200	0.68640000	-0.28528200
C	-3.73675800	1.43615100	-0.59147900
H	-3.92104500	2.19107700	0.17893300
H	-3.62567900	1.94282800	-1.55312800
H	-4.60152300	0.78155200	-0.64592200
C	-3.78015900	-1.42491400	-0.02225000
H	-4.52349600	-1.06365400	0.69138600
H	-4.21317500	-1.37985000	-1.02271800
H	-3.52897700	-2.45427900	0.21853000
C	-1.29326500	1.45462500	-0.18684900
H	-0.46535500	0.88694700	-0.61092600
H	-1.41672100	2.37967300	-0.74893100
H	-1.05089900	1.69064000	0.85265600

11.5. Cartesian co-ordinate of optimized structures of the series of O–H···O hydrogen-bonded complexes (26–27):

Phe···THF

H	0.27433300	-1.67942600	-0.37878700
C	-1.43606500	-0.83317900	-0.16830600
C	-2.74009700	-0.98139100	0.30790500
C	-0.99453400	0.42497100	-0.58546700
C	-3.58340400	0.11855200	0.37277000
H	-3.06607100	-1.96521800	0.62250000
C	-1.84820100	1.52125600	-0.51038100
H	0.01066300	0.53262700	-0.97722900
C	-3.14515300	1.37829100	-0.03123400
H	-4.59366600	-0.00864700	0.74438100
H	-1.49505900	2.49252700	-0.83826300
H	-3.80726900	2.23319500	0.02308200
O	-0.65090600	-1.93349700	-0.21238600
C	2.77902400	-0.25084000	-1.01831100
O	1.91248100	-0.95234200	-0.11756600
C	1.88226000	-0.29717200	1.16015200
C	2.43453800	1.09951300	0.90609700
C	3.47731300	0.81947300	-0.18014000
H	3.46671900	-0.96788500	-1.46844000
H	2.17067200	0.19732100	-1.81172100
H	0.85149600	-0.30579100	1.51953400
H	2.51233500	-0.85682700	1.85859600
H	1.64415600	1.75086500	0.52342700
H	2.85484200	1.55282000	1.80352600
H	3.74178800	1.69829600	-0.76773800
H	4.38836900	0.41600300	0.26825200

Phe···THP

H	-0.06463200	-1.02664600	-1.01405200
C	-1.85725500	-0.63231800	-0.45073700
C	-3.09517500	-1.16765100	-0.09069800
C	-1.63180300	0.73937800	-0.31282500
C	-4.09048500	-0.33843800	0.40630800
H	-3.25119500	-2.23297200	-0.20894500
C	-2.63737200	1.55912400	0.19031500
H	-0.67458000	1.15432000	-0.60848000
C	-3.87031700	1.02964400	0.55325700
H	-5.04808000	-0.76486900	0.68216100
H	-2.45306000	2.62254500	0.29224500
H	-4.65017500	1.67218000	0.94216100
O	-0.92035500	-1.48233900	-0.93260400
O	1.47771800	-0.21277500	-0.53580600

C	1.49515300	-0.09166800	0.88374300
H	1.33247500	0.95991500	1.15319900
H	0.64238500	-0.66360300	1.25135900
C	2.82793400	-0.61228800	1.43791700
H	2.74907500	-1.67488500	1.67431300
H	3.05399100	-0.08657100	2.36995200
C	3.94567800	-0.38115700	0.40561800
H	3.98205600	-1.22333700	-0.29051500
H	4.91803200	-0.32708500	0.89744500
C	3.65627100	0.89832000	-0.37951200
H	4.46741700	1.14064900	-1.06856100
H	3.56664600	1.73857500	0.31597800
C	2.35416900	0.71515000	-1.17303200
H	2.55665400	0.29177500	-2.15801800
H	1.83330000	1.67235100	-1.30508000

11.6. Cartesian co-ordinate of optimized structures of the series of O–H···N hydrogen-bonded complexes (28–29):

Phe···Im

H	0.36508500	-1.40499700	-0.32770400
C	-1.44182000	-0.78662900	-0.08755000
C	-2.66488000	-1.04078100	0.53830400
C	-1.23315200	0.44640200	-0.71334600
C	-3.65749400	-0.07140600	0.54459000
H	-2.81039500	-2.00387100	1.01225500
C	-2.23546200	1.41179200	-0.69426000
H	-0.29523800	0.63133900	-1.22447700
C	-3.45105500	1.16387100	-0.06673900
H	-4.60215000	-0.28183100	1.03300500
H	-2.06382500	2.36270700	-1.18610500
H	-4.22868600	1.91732400	-0.05864400
O	-0.50907600	-1.76288600	-0.06971500
C	1.98321900	0.47244900	0.63082300
C	3.27851900	-0.59458300	-0.70591600
C	4.07644100	0.28598600	-0.03344800
N	3.23357100	0.96144900	0.81847600
H	3.49437400	1.68858800	1.46490700
H	1.11875800	0.82762600	1.17213100
H	3.56027100	-1.30773100	-1.46275200
H	5.13223800	0.48850700	-0.08041400
N	1.97732700	-0.46675900	-0.28408100

Phe···Py

H	-0.04578500	-1.44268500	0.12048100
C	1.75227100	-0.76151700	-0.02910500
C	3.00114100	-0.93242400	-0.63066100
C	1.50404800	0.38589500	0.72916100
C	3.98283700	0.03621000	-0.47910500
H	3.17543100	-1.83032300	-1.21091600
C	2.49648300	1.35136400	0.86961900
H	0.54182600	0.50869000	1.21347400
C	3.73912900	1.18657500	0.26884300
H	4.94817700	-0.10796100	-0.95069600
H	2.29359500	2.23659900	1.46162100
H	4.50832800	1.93992800	0.38350000
O	0.82962500	-1.73359000	-0.20642300
C	-2.84117000	-0.82837900	0.87634300
C	-4.02118700	-0.13937000	0.62219300
C	-4.02302100	0.82561300	-0.37729800
C	-2.84922000	1.06392900	-1.08103000
C	-1.71944600	0.32431800	-0.75335700

N	-1.71048600	-0.60354300	0.20624600
H	-4.92447800	1.38258100	-0.60403700
H	-2.79800500	-1.59060700	1.64711100
H	-4.91236400	-0.35904900	1.19579500
H	-2.80328900	1.80529700	-1.86814400
H	-0.77822400	0.47776700	-1.27414800